QUANTIFICATION AND MODELING OF INORGANIC CARBON PROCESSING IN SCLERACTINIAN CORAL

by

ANNA LOUISA TANSIK

(Under the Direction of Brian M. Hopkinson)

ABSTRACT

Scleractinian corals build extensive reef frameworks that house extraordinary biodiversity and provide numerous ecosystem services to local human populations. Corals depend upon endosymbiotic dinoflagellates to provide them energy via photosynthesis, which supports both tissue and skeletal growth. Unfortunately, corals, and consequently reefs, are under threat from local and global stressors, including climate change. Increased anthropogenic CO_2 emissions causing CO_2 to invade the surface ocean, lowering pH levels and CO_3^{2-} concentrations; this is ocean acidification (OA). Changes to the dissolved inorganic carbon (DIC) system have the potential to alter both photosynthesis (CO_2 dependent) and calcification (CO_3^{2-} dependent). Scleractinian corals are faced with the possibility of impacts to both of these vital processes, yet studies have shown no clear picture of what is likely to occur as pH continues to decline over the course of this century. Much of how corals process DIC is still unquantified, making it difficult to understand the scale of potential changes and what the drivers might be. In order to address these knowledge gaps, membrane inlet mass spectrometry methods, which have been used to describe carbon concentrating mechanisms and photosynthetic DIC kinetics in phytoplankton, were adapted for use with corals. Three different species of Caribbean coral were

found to have high levels of carbonic anhydrase (CA) activity on the coral surface, within the coral tissues and in their symbionts. This enzyme is a key component of carbon concentrating mechanisms, and the surface CA provided CO_2 to support half of net photosynthesis. Taxanomic variation was found at the coral level with regard to DIC saturation for photosynthesis, but all symbionts had a high affinity for carbon, suggestive of host controlled DIC delivery. This information more completely quantified photosynthesis with regard to DIC, and allowed a model of DIC flow through a coral to be developed. Running the model under projected OA conditions showed no change to photosynthesis, but slight reductions in both calcification and calcifying fluid pH. Investigating the drivers of these changes indicated that increased fluxes of CO_2 into the calcifying fluid led to the declines, but biological modification of the calcifying fluid mitigated the effect.

INDEX WORDS: Coral, inorganic carbon, photosynthesis, carbonic anhydrase, Membrane Inlet Mass Spectrometry, modeling, ocean acidification

QUANTIFICATION AND MODELING OF INORGANIC CARBON PROCESSING IN SCLERACTINIAN CORAL

by

ANNA LOUISA TANSIK

B.S., Duke University, 2004

M.App.Sc, James Cook University, Australia, 2006

A Dissertation Submitted to the Graduate Faculty of The University of Georgia in Partial Fulfillment of the Requirements for the Degree

DOCTOR OF PHILOSOPHY

ATHENS, GEORGIA

2017

QUANTIFICATION AND MODELING OF INORGANIC CARBON PROCESSING IN SCLERACTINIAN CORAL

by

ANNA LOUISA TANSIK

Major Professor:	Brian Hopkinson
Committee:	William Fitt
	Christof Meile
	James Porter
	Wei-Jun Cai

Electronic Version Approved:

Suzanne Barbour
Dean of the Graduate School
The University of Georgia
August 2017

DEDICATION

"And when I behold the sea, I find that it speaketh to me of Thy majesty, and of the potency of Thy might, and of Thy sovereignty and Thy grandeur." -Bahá'u'lláh

To my ever supportive parents. Finally.

ACKNOWLEDGEMENTS

My gratitude goes to everyone who has helped me through the entire process of my PhD: my advisor; committee members; other faculty, staff and graduate students in Marine Sciences; my family and friends. My deepest thanks go to my advisor, Brian Hopkinson, for his unending support, guidance, patience, and willingness to take the chance on a student who had been out of school for so long and a project that had little more than potential when started. My time in the lab has greatly reinforced my love for academic research and desire to continue on. I also thank my committee members Bill Fitt, Christof Meile, Jim Porter and Wei-Jun Cai for all the advice, support and positivity through the years. I could not have asked for better people accompanying me through my project. My appreciation also goes to Chen Shen, Dan Baker and Dan Owen, my wonderful lab mates who have kept me company and helped me retain my good humor in the lab and the field. Finally, my love and gratitude goes to my family and friends who have stood behind me through all the ups and downs, and listened to me babble in jargon and acronyms about science that they may or may not understand.

TABLE OF CONTENTS

Page

ACKNOWLEDGEMENTS v

LIST OF TABLES ix

LIST OF FIGURES x

CHAPTER

1 INTRODUCTION AND LITERATURE REVIEW 1

Reefs, corals and climate change 1

Ocean acidification and its impacts on coral 2

Inorganic carbon processing by coral 4

Goals and chapters of this dissertation 10

References 12

2 EXTERNAL CARBONIC ANHYDRASE IN THREE CARIBBEAN CORALS: QUANTIFICATION OF ACTIVTY AND ROLE IN CO_2 UPTAKE 17

Abstract 18

Introduction 19

Materials and methods 21

Results 25

Discussion 30

Acknowledgements 36

References 37

3 INORGANIC CARBON IS SCARCE FOR SYMBIONTS IN SCLERACTINIAN CORAL 47

Abstract 48

Introduction 49

Methods and materials 51

Results 56

Discussion 58

Conclusions 66

Acknowledgements 66

References 67

4 MODELING THE EFFECTS OF OCEAN ACIDIFICATION ON INORGANIC CARBON FLOW IN SCLERACTINIAN CORAL 76

Abstract 77

Introduction 78

Methods 81

Results 83

Discussion 86

Acknowledgements 91

References 92

5 CONCLUSIONS 107

Inorganic carbon and coral photosynthesis 107

Applications of the model 108

Ocean acidification and the future of this work.....109

References.....110

APPENDICES

A EXTERNAL CARBONIC ANHYDRASE IN THREE CARIBBEAN CORALS: QUANTIFICATION OF ACTIVTY AND ROLE IN CO_2 UPTAKE ELECTRONIC SUPPLEMENTARY MATERIALS 111

Supplementary Materials 112

References.....114

B INORGANIC CARBON FLUX MODEL SUPPLEMENTARY TABLES 117

LIST OF TABLES

Page

Table 2.1: Model notation.....41

Table 4.1: Parameters of the model 98

Table B1: Model flux equations 118

Table B2: Model sensitivity analysis.....121

LIST OF FIGURES

Page

Figure 1.1: Inorganic carbon (DIC) fluxes through a scleractinian coral 16

Figure 2.1: Carbon fluxes and photosynthesis-related CA 42

Figure 2.2: An example of the ^{18}O-exchange data analyzed to determine eCA activities and model fits to the data.....43

Figure 2.3: eCA activities measured in three species of Caribbean corals 44

Figure 2.4: Example of the inhibition of O_2 evolution by DBAZ 45

Figure 2.5: The effect of DBAZ on net photosynthesis. 46

Figure 3.1: Whole coral photosynthetic parameters and external carbonic anhydrase activity.....72

Figure 3.2: Freshly isolated symbiont photosynthetic parameters and internal carbonic anhydrase activity.....73

Figure 3.3: Comparison of whole coral and freshly isolated symbiont half-saturation constants (K_ms)… 74

Figure 3.4: Overview of quantified DIC uptake and processing of in the two reef coral species studied… 75

Figure 4.1: Overview of the five box model.....100

Figure 4.2: Effect of varying calcifying fluid CA activity.....101

Figure 4.3: Effect of varying proton pump efficiency 102

Figure 4.4: Steady state fluxes in the five box model under normal seawater conditions.....103

Figure 4.5: Effect of varying external seawater pH and DIC 104

Figure 4.6: Changes to the steady state fluxes in the five box model from normal seawater conditions to end-century seawater conditions 105

Figure 4.7: Impact of varying external seawater pH and DIC on CO_2 and HCO_3^- fluxes to the calcifying fluid 106

Figure A1: O_2 traces showing that photosynthesis in the three coral species was not inhibited by DMSO, the solvent in which DBAZ was dissolved. 115

Figure A2: Model fits allowing various combinations of CO_2 and HCO_3^- flux through the surface layer….....116

CHAPTER 1

INTRODUCTION AND LITERATURE REVIEW

Reefs, corals and climate change

Stony corals of the order Scleractinia are reef builders in the warm, clear, oligotrophic waters of the tropical oceans. By secreting calcium carbonate, they create elaborate and rugose structures that house thousands of other species in what are otherwise nutrient deserts, and provide numerous benefits to humans living on shore nearby (Albert et al. 2015; Ferrario et al. 2014; Hughes et al. 2017). Scleractinian corals would not be able to calcify nearly as quickly without their photosynthetic endosymbionts, dinoflagellates of the genus *Symbiodinium* (Davy et al. 2012). In exchange for protection and nutrients, including dissolved inorganic carbon (DIC), *Symbiodinium* provide the corals most of their energy in the form of fixed carbon photosynthates (Falkowski et al. 1984). The entire system, from the symbiosis at the organismal level to the whole reef ecosystem, balances carefully at its optimum; almost at the upper end of a coral's temperature tolerance (Brown 1997), recycling nutrients and relying on grazers to keep algae in check (Arthur et al. 2006; Pandolfi et al. 2005), accretion of the reef balanced by bioerosion (Enochs et al. 2015). It does not take much to push coral reefs toward an undesirable state, and humans are adept at altering environments at multiple scales. Anthropogenic impacts can be seen at local levels, for example in terms of water quality and fishing, and globally with climate change (Hughes et al. 2017). While these factors interact with each other in various ways, it is important to understand how each affects corals in order to gain a better idea of what can be done

at a local level to mitigate those global factors which are unavoidable, or at least not be taken by surprise as the oceans continue to change in response to human activities.

Ocean acidification and its impacts on coral

Ocean acidification (OA) is a global impact, driven by the burning of fossil fuels and land use changes by humans since the beginning of the Industrial Revolution (IPCC 2014). This has added a number of gases to the atmosphere which cause the retention of heat, feeding back and warming the planet; CO_2 is the most abundant of them (IPCC 2014). As the gases of the atmosphere and ocean equilibrate, more CO_2 is being added to the surface waters (IPCC 2014). This weak acid drives down the pH by reacting with molecules of water and releasing protons. As DIC exists in a pH-dependent equilibrium of three species ($CO_2 \leftrightarrow HCO_3^- \leftrightarrow CO_3^{2-}$), reducing the pH drives speciation to the left, toward CO_2 and away from CO_3^{2-} (Allison et al. 2014; Feely et al. 2004). The latter is required for calcification by a many organisms; decreased concentrations of CO_3^{2-} combined with lower pH have the potential to lead to reduced calcification or shell and skeletal deformities (Cohen and Holcomb 2009; de Putron et al. 2010; Feely et al. 2004). Dissolution is even a possibility if the saturation state of aragonite or calcite drops low enough, a result of CO_3^{2-} buffering the system by reacting with the free protons to form HCO_3^- (Feely et al. 2004). Projections of the future ocean carbonate system suggest that saturation states will continue to decline, even to the point where dissolution is kinetically favored in some areas, over this century (IPCC 2014). This will limit where marine calcifiers will be able to thrive.

However, CO_3^{2-} is not the only DIC species necessary for biological processes. Photosynthetic carbon fixation needs CO_2 in order to produce the sugars, carbohydrates and lipids organisms use as energy sources (Davy et al. 2012; Falkowski et al. 1984). Under current

conditions, marine autotrophs have access to little CO_2 in the environment, and the enzyme that catalyzes carbon fixation (Ribulose-1,5-bisphosphate carboxylase/oxygenase [RubisCO]) has a low affinity for CO_2 (Gattuso et al. 1999; Mackey et al. 2015). As a result, many use complex and energetically costly carbon concentrating mechanisms in order to support high rates of photosynthesis (Hopkinson et al. 2011; Mackey et al. 2015; Wu et al. 2010). These mechanisms involve the transport and use of HCO_3^- in support photosynthesis, compartmentalization of carbon fixation to allow for greater regulation, and the use of the enzyme carbonic anhydrase (CA) to catalyze the hydration-dehydration reaction of CO_2 and HCO_3^- (Hopkinson et al. 2011; Mackey et al. 2015; Wu et al. 2010). CAs can raise CO_2 concentrations in local areas, or convert it HCO_3^- to reduce diffusion out of them (Hopkinson et al. 2011; Mackey et al. 2015). With more CO_2 in the environment, marine autotrophs could fix greater amounts of carbon, while downregulating these carbon concentrating mechanisms (Shi et al. 2017; Wu et al. 2010), leading to energetic savings and increased production.

Scleractinian corals exist in a precarious position with relation to OA. They require both CO_2 and CO_3^- for processes vital to their long-term survival. While having more CO_2 for their symbionts to fix would be a benefit, it comes at the price of potentially reduced rates of calcification. To date, the evidence for any particular response by corals to OA is unclear. Impacts on calcification have been examined far more than those on photosynthesis, but tell an ambiguous story. As is most logically expected, declines in calcification rate have been seen in some studies (Huang et al. 2014; Langdon and Atkinson 2005; Okazaki et al. 2013). However, there have been conditions where corals have shown a positive response to certain OA conditions (Castillo et al. 2014; Huang et al. 2014). Different coral taxa also show variable responses (Huang et al. 2014). Capping it off, in places were waters are naturally acidified by CO_2 vents or

seeps, or due to enclosure and minimal water exchange, corals will grow at rates which are essentially the same as their counterparts in non-acidified waters (Kelly and Hofmann 2013; Prada et al. 2017). Even then, in some places communities are diverse, while in others there are few taxa present (Barkley et al. 2015; Crook et al. 2012).

The response of photosynthesis to OA is just as hazy. Again, researchers have seen decreases in production (Anthony et al. 2008), no change (Hoadley et al. 2015), and increases (Langdon and Atkinson 2005). Different taxa show different results (Anthony et al. 2008; Hoadley et al. 2015). Most of the studies looking at OA impacts on photosynthesis are complicated by additional variables, such as increased temperatures or nutrient levels (Anthony et al. 2008; Hoadley et al. 2015; Langdon and Atkinson 2005). While this is reasonable considering that environmental perturbations are not taking place in isolation from each other, it does not assist with understanding the basic physiological changes and makes it difficult to answer the question of how the different factors are interacting with each other; are they additive or synergistic, do they mitigate each other? The lack of a clear understanding of coral DIC physiology and the drivers of change in the system is perhaps most troubling. Without knowing how the system functions, how will we know how bad the situation really is or what can be done to lessen the impact? A better, more quantitative description of DIC processing in corals is required.

Inorganic carbon processing by coral

With two biological processes requiring two different species of DIC, the pathways and components required to ensure CO_2 and CO_3^{2-} are available create a complex processing system through the coral (Fig. 1.1). The two processes are connected, as photosynthesis enhances calcification, however the two are not believed to be in direct competition for DIC (Davy et al.

2012); the physical separation between the site of calcification and the location of the symbionts prevents this. The distance between the two processes also allows for carbon to be concentrated for each (al-Moghrabi et al. 1996; Allison et al. 2014).

Calcification

Corals strive to keep the pH of their calcifying fluid notably basic through extensive biological mediation (Allison et al. 2014; McCulloch et al. 2017). An elevated pH ensures that the CO_3^{2-} concentration remains high and acid-base reactions will be favorable (Allison et al. 2014; Cohen and Holcomb 2009; Feely et al. 2004). Larger concentrations of CO_3^{2-} cause the aragonite saturation state to remain well above 1.0, making it is easier to precipitate strong, well-organized $CaCO_3$ crystals (Allison et al. 2014; Cohen and Holcomb 2009). This biological mediation is accomplished, it is proposed, predominately through the export of protons from the calcifying space to maintain a basic environment (Cohen and Holcomb 2009; Furla et al. 2000). Inhibitor studies have suggested that protons are pumped out in exchange with calcium using a transporter that requires ATP (Furla et al. 2000).

While all this energy investment does result in an elevated pH, it is unknown just how elevated it is. The calcifying fluid is difficult to study without invasive techniques which compromise the status quo of the space, such as lifting the tissue off the skeleton in order to put measuring devices into the space before replacing the tissue (Al-Horani et al. 2003). Regardless, a variety of measurements have been attempted using fluorescent dyes, boron isotope ratios, and microelectrodes (Cai et al. 2016; Comeau et al. 2017; Holcomb et al. 2014). These methods have returned a range of pH values from near 7.8 to over 10.0 (Cai et al. 2016; Comeau et al. 2017; Holcomb et al. 2014). Considering the shortcomings of the various techniques, the reality is likely to be somewhere in the middle. It may also depend on which part of the coral is being

examined. Work by Holcomb et al. (2014) found a gradient in the calcifying fluid pH, with lower values near the growing edge of their nubbin and higher values toward the center of the colony.

There are other matters still up for debate in terms of DIC processing for calcification. A central one is the exact source of DIC for calcification. Some researchers believe that seawater is transported directly to the calcifying space via paracellular pathways or through the tissues in vessicles (Cohen and Holcomb 2009; Gagnon et al. 2012). In support of this idea, skeletal isotopic signatures have been seen to more closely align with seawater signatures than metabolic ones, and fluorescent dye tracers have shown how quickly seawater can move into the calcifying space (Cohen and Holcomb 2009; Gagnon et al. 2012). However, others consider metabolic DIC to be the primary—though not only—source for calcification, specifically CO_2 which diffuses in from the calicoblastic tissue layer in response to the large concentration gradient (Allison et al. 2014; Furla et al. 2000). Skeletal isotopic signatures have also been used to lend support to this idea, as well as pulse-chase radiotracer studies (Allison et al. 2014; Furla et al. 2000). As with the calcifying fluid pH, the reality is likely to be somewhere in the middle; a combination of the two sources. It is unlikely that seawater will not move through the paracellular pathways and other available openings into the calcifying space, just as it is unlikely that CO_2 will not diffuse in based on the concentration gradient. Regardless of the source of the DIC, it will be subject to modification within the calcifying fluid.

Along with the acid-base chemistry that drives the DIC equilibrium toward CO_3^{2-}, CO_2 will be subject to hydration by CA, converting it more rapidly to HCO_3^- (Bertucci et al. 2013; Moya et al. 2008). The presence of CA in the calcifying fluid has been proposed to deliver DIC for calcification and/or address acidosis by converting carbonic acid to HCO_3^-, though its activity rate has not been measured and can only be generally assumed based upon gene expression

(Moya et al. 2008). Further modification to any DIC in the calcifying fluid may be caused by the organic matrix which connects the tissue and the skeleton, and has been proposed to play an extensive role in facilitating calcification (Clode and Marshall 2002; Clode and Marshall 2003; Von Euw et al. 2017). This remains rather controversial; many consider that seawater chemistry plays a more central role to determining calcifying fluid characteristics and calcification rates than biological processes (Cohen and Holcomb 2009; Comeau et al. 2017), though a recent observational study contradicts the laboratory experiments (McCulloch et al. 2017). In spite of these unknowns surrounding biological facilitation, calcification can still be described fairly well based on pH, CO_3^{2-} concentration and Ca^{2+} concentration.

Photosynthesis

Photosynthesis, as opposed to calcification, does not have a well-established and direct link to the concentration of a DIC species, and so it is known in almost exclusively descriptive terms. A few studies have examined the relationship of coral photosynthesis to total DIC concentration or to HCO_3^- concentrations (Buxton et al. 2009; Goiran et al. 1996; Herfort et al. 2008). The shortcoming of this is that the coral is not the one fixing carbon; the *Symbiodinium* are, and only Goiran et al. (1996) examined the symbionts themselves. Work has been done on cultured strains to understand how they acquire and process carbon (Brading et al. 2013; Oakley et al. 2014), but cultured *Symbiodinium* are a poor model for in hospite symbionts (Buxton et al. 2009; Goiran et al. 1996). Having defined DIC kinetics for photosynthesis in both the host and the symbiont would go a long way to illustrating how carbon is concentrated by the coral.

Descriptive and semi-quantitative studies have shown that corals have all the aspects of an active carbon concentrating process (al-Moghrabi et al. 1996; Bertucci et al. 2013; Weis et al. 1989). A CA has been molecularly identified and localized to the tissues of *Stylophora pistillata*

(Bertucci et al. 2011). This supports work done by Weis et al. (1989) on this same coral, where pH titrations indicated CA activity in the animal tissues. Additional evidence of the role CA plays in DIC uptake for photosynthesis came when production declined by more than half following the inhibition of CA in *S. pistillata* (Weis et al. 1989). CA was also assumed in *Galaxea fascicularis* when two different inhibitors reduced photosynthesis, both in the coral and its freshly isolated symbionts (al-Moghrabi et al. 1996). Declines in oxygen production in the presence of both the membrane permeable and less membrane permeable inhibitors suggest that CA is present both in the tissues and on the surface of the coral (al-Moghrabi et al. 1996). The reduction observed in the symbionts implies an active carbon concentrating mechanism is employed in hospite (al-Moghrabi et al. 1996).

Additional work with inhibitors showed that HCO_3^- is transported across membranes in the light to support photosynthesis (al-Moghrabi et al. 1996). H^+-ATPases were likewise blocked with a similar impact (al-Moghrabi et al. 1996). The suggestion was that they served to locally acidify the surface of the coral in order to facilitate HCO_3^- uptake (al-Moghrabi et al. 1996) However, proton pumps are also present other places in the coral; it is possible these were also impacted. Fluorescent dyes demonstrated their presence on the symbiosome membrane (Barott et al. 2015). These served to acidify the area near the symbionts to a low pH and ensure a high concentration of CO_2 for use by the symbionts (Barott et al. 2015).

Taken all together, these studies paint a picture of an active carbon concentrating process. Including the information about the half saturation constant for symbiont DIC (Goiran et al. 1996), it can be assumed that this process serves to supply DIC to the *Symbiodinium* as carbon is scarce in their vicinity. While a good and convincing story, it does not allow for a quantitative understanding of the impacts OA will have on photosynthesis.

Modeling

Even without completely quantified information, well parameterized numerical models can give additional insight into the processes going on in a coral and the potential impacts of OA. Two previous models have sought to do this, exploring the impact of OA on calcification (Hohn and Merico 2012; Nakamura et al. 2013). While both were box models (Hohn and Merico 2012; Nakamura et al. 2013), each took a different approach to modeling DIC in a coral. Hohn and Merico (2012) designed a model with fully detailed inorganic carbon chemistry, and included the coral tissue as a compartment, but did not include photosynthesis as a dynamic process. On the other hand, Nakamura et al. (2013) considered all the DIC species together and included gross photosynthesis, but did not model DIC in the tissues of the coral. In spite of the differences, both managed to simulate calcification well (Hohn and Merico 2012; Nakamura et al. 2013). Decreases in this output resulted from OA conditions, as expected based on experimental literature (Hohn and Merico 2012; Nakamura et al. 2013). The Nakamura et al. (2013) model allowed for simulations of the photosynthetic response, where an increase was the result of OA. Hohn and Merico (2012) built their model in such a way as to allow for an investigation into possible drivers of the observed changes in calcification, finding increased CO_2 fluxes through their model.

In general, both models are able to reproduce observations. However, there are missing pieces—photosynthesis, DIC speciation, tissue compartments—and a very large number of assumed or estimated parameters in each (Hohn and Merico 2012; Nakamura et al. 2013). This indicates that there is still a great deal of room for improvement in how DIC flow is modeled in corals. Large strides could be made if better data was available for quantifying and defining DIC-associated biological processes.

Goals and chapters of this dissertation

The overall goal of this dissertation is to gain a clearer understanding of DIC cycling in topical scleractinian corals. My specific focus is to quantify DIC uptake, processing and saturation with regard to photosynthesis, and to use this information to develop a detailed numerical model of DIC fluxes which incorporates more experimentally quantified parameters than previous models have. In order to do this, methods which have been used to characterize phytoplankton carbon concentrating mechanisms and photosynthetic parameters were applied for the first time to corals. In the chapters that follow, I describe various components of the carbon concentrating process in three Caribbean corals (*Orbicella faveolata, Porites astreoides,* and *Siderastrea radians*), as well as the relationship between DIC and photosynthesis in the corals and their symbionts. Finally, I employ the new model to explore the impacts of OA, and the drivers of any changes.

The photosynthetic carbon concentrating process of corals is complex. Chapter two focuses on quantifying the components which are associated with the surface of the coral, at the bottom of the diffusive boundary layer. Using membrane inlet mass spectrometry (MIMS), I applied ^{18}O-exchange methods previously applied to human and phytoplankton systems (Hopkinson et al. 2011; Silverman and Tu 1976) to determining external CA (eCA) activity of the three coral species. Employing inhibitors, the impact on net photosynthesis of CO_2 production at the surface of the coral by eCA was explored. This allowed for the calculation of photosynthetic partitioning between CO_2 and HCO_3^-, as well as the membrane permeability of CO_2. In addition to quantifying these components for the first time and demonstrating the

importance of eCA for photosynthetic production, the successful application of these techniques showed that the carbon concentrating process in corals can be fully characterized.

In the third chapter, the relationship between photosynthesis and DIC concentration was evaluated for the corals as well as for their symbionts. I again used MIMS and stable isotopes methods in order to conduct photosynthesis vs DIC assays (Buxton et al. 2009; Goiran et al. 1996; Herfort et al. 2008). Conducting this assay on the freshly isolated symbionts, still reflective of their in hospite state, effectively quadrupled the amount of available data, as only one coral taxa was studied by Goiran et al. (1996). The resulting Michaelis-Menten curves gave half saturation constants (K_ms) and maximum rates of photosynthesis. Comparisons were made between taxa, both coral and symbiont, as well as between corals and their freshly isolated symbionts. Additional data regarding coral eCA and symbiont internal CA activity rates gave a additional details to frame the Michaelis-Menten kinetics. The differences seen between the corals and the symbionts allowed for the hypothesis to be put forward of host control in DIC delivery. These assays also completed the necessary data to characterize DIC processing in corals with regard to photosynthesis.

With the data in hand, a new model describing DIC fluxes through a scleractinian coral was created. Chapter four details this five box model, based mostly on *O. faveolata*, and its successful implementation. I used the model to assess the impacts on gross photosynthesis, calcification and calcifying fluid pH of mid- and end-century OA projections for seawater pH and DIC concentration (IPCC 2014). The chapter explores the implications for corals of changes to photosynthesis and calcification, as well as the potential drivers of these OA related changes in the model. With the detailed parameterization of this model, many possible scenarios involving acclimation and varying physiology can be evaluated in the future.

References

Al-Horani FA, Al-Moghrabi SM, de Beer D (2003) Microsensor study of photosynthesis and calcification in the scleractinian coral, Galaxea fascicularis: active internal carbon cycle. Journal of Experimental Marine Biology and Ecology 288:1-15

al-Moghrabi SM, Goiran C, Allemand D, Speziale N, Jaubert J (1996) Inorganic carbon uptake for photosynthesis by the symbiotic coral-dinoflagellate association II. Mechanisms for bicarbonate uptake. Journal of Experimental Marine Biology and Ecology 199:227-248

Albert JA, Olds AD, Albert S, Cruz-Trinidad A, Schwarz AM (2015) Reaping the reef: Provisioning services from coral reefs in Solomon Islands. Mar Pol 62:244-251

Allison N, Cohen I, Finch AA, Erez J, Tudhope AW, Edinburgh Ion Microprobe F (2014) Corals concentrate dissolved inorganic carbon to facilitate calcification. Nat Commun 5:6

Anthony KRN, Kline DI, Diaz-Pullido G, Dove S, Hoegh-Guldberg O (2008) Ocean acidification causes bleaching and productivity loss in coral reef builders. Proc Natl Acad Sci U S A 105:17442-17446

Arthur R, Done TJ, Marsh H, Harriott V (2006) Local processes strongly influence post-bleaching benthic recovery in the Lakshadweep Islands. Coral Reefs 25:427-440

Barkley HC, Cohen AL, Golbuu Y, Starczak VR, DeCarlo TM, Shamberger KEF (2015) Changes in coral reef communities across a natural gradient in seawater pH. Science Advances 1:e1500328

Barott KL, Venn AA, Perez SO, Tambutte S, Tresguerres M (2015) Coral host cells acidify symbiotic algal microenvironment to promote photosynthesis. Proc Natl Acad Sci U S A 112:607-612

Bertucci A, Tambutte S, Supuran CT, Allemand D, Zoccola D (2011) A new coral carbonic anhydrase in Stylophora pistillata. Mar Biotechnol (NY) 13:992-1002

Bertucci A, Moya A, Tambutté S, Allemand D, Supuran CT, Zoccola D (2013) Carbonic anhydrases in anthozoan corals—A review. Bioorganic & Medicinal Chemistry 21:1437-1450

Brading P, Warner ME, Smith DJ, Suggett DJ (2013) Contrasting modes of inorganic carbon acquisition amongst Symbiodinium (Dinophyceae) phylotypes. New Phytol 200:432-442

Brown BE (1997) Coral bleaching: causes and consequences. Coral Reefs 16:S129-S138

Buxton L, Badger M, Ralph P (2009) Effects of Moderate Heat Stress and Dissolved Inorganic Carbon Concentration on Photosynthesis and Respiration of Symbiodinium Sp. (Dinophyceae) in Culture and in Symbiosis(1). J Phycol 45:357-365

Cai WJ, Ma YN, Hopkinson BM, Grottoli AG, Warner ME, Ding Q, Hu XP, Yuan XC, Schoepf V, Xu H, Han CH, Melman TF, Hoadley KD, Pettay DT, Matsui Y, Baumann JH, Levas S, Ying Y, Wang YC (2016) Microelectrode characterization of coral daytime interior pH and carbonate chemistry. Nat Commun 7:8

Castillo KD, Ries JB, Bruno JF, Westfield IT (2014) The reef-building coral Siderastrea siderea exhibits parabolic responses to ocean acidification and warming. Proc R Soc B-Biol Sci 281:9

Clode PL, Marshall AT (2002) Low temperature FESEM of the calcifying interface of a scleractinian coral. Tissue Cell 34:187-198

Clode PL, Marshall AT (2003) Calcium associated with a fibrillar organic matrix in the scleractinian coral Galaxea fascicularis. Protoplasma 220:153-161

Cohen AL, Holcomb M (2009) Why Corals Care About Ocean Acidification: Uncovering the Mechanism. Oceanography 22:118-127

Comeau S, Tambutte E, Carpenter RC, Edmunds PJ, Evensen NR, Allemand D, Ferrier-Pages C, Tambutte S, Venn AA (2017) Coral calcifying fluid pH is modulated by seawater carbonate chemistry not solely seawater pH. Proc R Soc B-Biol Sci 284:10

Crook ED, Potts D, Rebolledo-Vieyra M, Hernandez L, Paytan A (2012) Calcifying coral abundance near low-pH springs: implications for future ocean acidification. Coral Reefs 31:239-245

Davy SK, Allemand D, Weis VM (2012) Cell Biology of Cnidarian-Dinoflagellate Symbiosis. Microbiol Mol Biol Rev 76:229-261

de Putron SJ, McCorkle DC, Cohen AL, Dillon AB (2010) The impact of seawater saturation state and bicarbonate ion concentration on calcification by new recruits of two Atlantic corals. Coral Reefs 30:321-328

Enochs IC, Manzello DP, Carlton RD, Graham DM, Ruzicka R, Colella MA (2015) Ocean acidification enhances the bioerosion of a common coral reef sponge: implications for the persistence of the Florida Reef Tract. Bull Mar Sci 91:271-290

Falkowski PG, Dubinsky Z, Muscatine L, Porter JW (1984) LIGHT AND THE BIOENERGETICS OF A SYMBIOTIC CORAL. Bioscience 34:705-709

Feely RA, Sabine CL, Lee K, Berelson W, Kleypas J, Fabry VJ, Millero FJ (2004) Impact of anthropogenic CO2 on the CaCO3 system in the oceans. Science 305:362-366

Ferrario F, Beck MW, Storlazzi CD, Micheli F, Shepard CC, Airoldi L (2014) The effectiveness of coral reefs for coastal hazard risk reduction and adaptation. Nat Commun 5:9

Furla P, Galgani I, Durand I, Allemand D (2000) Sources and mechanisms of inorganic carbon transport for coral calcification and photosynthesis. J Exp Biol 203:3445-3457

Gagnon AC, Adkins JF, Erez J (2012) Seawater transport during coral biomineralization. Earth Planet Sci Lett 329:150-161

Gattuso J-P, Allemand D, Frankignoulle M (1999) Photosynthesis and Calcification at Cellular, Organismal and Community Levels in Coral Reefs: A Review of Interactions and Control by Carbonate Chemistry. American Zoologist 39:160-183

Goiran C, Al-Moghrabi SM, Allemand D, Jaubert J (1996) Inorganic carbon uptake for photosynthesis by the symbiotic coral/dinoflagellate association I. Photosynthetic performances of symbionts and dependence on sea water bicarbonate. Journal of Experimental Marine Biology and Ecology 199:207-225

Herfort L, Thake B, Taubner I (2008) Bicarbonate Stimulation of Calcification and Photosynthesis in Two Hermatypic Corals(1). J Phycol 44:91-98

Hoadley KD, Pettay DT, Grottoli AG, Cai WJ, Melman TF, Schoepf V, Hu XP, Li Q, Xu H, Wang YC, Matsui Y, Baumann JH, Warner ME (2015) Physiological response to elevated temperature and pCO(2) varies across four Pacific coral species: Understanding the unique host plus symbiont response. Sci Rep 5:15

Hohn S, Merico A (2012) Modelling coral polyp calcification in relation to ocean acidification. Biogeosciences 9:4441-4454

Holcomb M, Venn AA, Tambutte E, Tambutte S, Allemand D, Trotter J, McCulloch M (2014) Coral calcifying fluid pH dictates response to ocean acidification. Sci Rep 4:4

Hopkinson BM, Dupont CL, Allen AE, Morel FMM (2011) Efficiency of the CO_2-concentrating mechanism of diatoms. PNAS 108:3830-3837

Huang H, Yuan XC, Cai WJ, Zhang CL, Li XB, Liu S (2014) Positive and negative responses of coral calcification to elevated pCO(2): case studies of two coral species and the implications of their responses. Marine Ecology Progress Series 502:145-156

Hughes TP, Barnes ML, Bellwood DR, Cinner JE, Cumming GS, Jackson JBC, Kleypas J, van de Leemput IA, Lough JM, Morrison TH, Palumbi SR, van Nes EH, Scheffer M (2017) Coral reefs in the Anthropocene. Nature 546:82-90

IPCC (2014) Climate Change 2014: Synthesis Report. Contribution of Working Groups I, II and III to the Fifth Assessment Report of the Intergovernmental Panel on Climate Change. In: Core Writing Team RKPaLAM (ed). IPCC, Geneva, Switzerland 151 pp.

Kelly MW, Hofmann GE (2013) Adaptation and the physiology of ocean acidification. Funct Ecol 27:980-990

Langdon C, Atkinson MJ (2005) Effect of elevated pCO(2) on photosynthesis and calcification of corals and interactions with seasonal change in temperature/irradiance and nutrient enrichment. J Geophys Res-Oceans 110:16

Mackey KRM, Morris JJ, Morel FMM, Kranz SA (2015) Response of Photosynthesis to Ocean Acidification. Oceanography 28:74-91

McCulloch MT, D'Olivo JP, Falter J, Holcomb M, Trotter JA (2017) Coral calcification in a changing World and the interactive dynamics of pH and DIC upregulation. Nat Commun 8:8

Moya A, Tambutte S, Bertucci A, Tambutte E, Lotto S, Vullo D, Supuran CT, Allemand D, Zoccola D (2008) Carbonic anhydrase in the scleractinian coral Stylophora pistillata: characterization, localization, and role in biomineralization. J Biol Chem 283:25475-25484

Nakamura T, Nadaoka K, Watanabe A (2013) A coral polyp model of photosynthesis, respiration and calcification incorporating a transcellular ion transport mechanism. Coral Reefs 32:779-794

Oakley CA, Schmidt GW, Hopkinson BM (2014) Thermal responses of Symbiodinium photosynthetic carbon assimilation. Coral Reefs 33:501-512

Okazaki RR, Swart PK, Langdon C (2013) Stress-tolerant corals of Florida Bay are vulnerable to ocean acidification. Coral Reefs 32:671-683

Pandolfi JM, Jackson JBC, Baron N, Bradbury RH, Guzman HM, Hughes TP, Kappel CV, Micheli F, Ogden JC, Possingham HP, Sala E (2005) Are U.S. coral reefs on the slippery slope to slime? Science 307:1725-1726

Prada F, Caroselli E, Mengoli S, Brizi L, Fantazzini P, Capaccioni B, Pasquini L, Fabricius KE, Dubinsky Z, Falini G, Goffredo S (2017) Ocean warming and acidification synergistically increase coral mortality. Sci Rep 7:10

Shi Q, Xiahou WQ, Wu HY (2017) Photosynthetic responses of the marine diatom Thalassiosira pseudonana to CO2-induced seawater acidification. Hydrobiologia 788:361-369

Silverman DN, Tu CK (1976) CARBONIC-ANHYDRASE CATALYZED HYDRATION STUDIED BY C-13 AND O-18 LABELING OF CARBON-DIOXIDE. J Am Chem Soc 98:978-984

Von Euw S, Zhang QH, Manichev V, Murali N, Gross J, Feldman LC, Gustafsson T, Flach C, Mendelsohn R, Falkowski PG (2017) Biological control of aragonite formation in stony corals. Science 356:933-+

Weis VM, Smith GJ, Muscatine L (1989) A "CO_2 supply" mechanism in zooxanthellate cnidarians: role of carbonic anhydrase. Marine Biology 100:195-202

Wu Y, Gao K, Riebesell U (2010) CO2-induced seawater acidification affects physiological performance of the marine diatom Phaeodactylum tricornutum. Biogeosciences 7:2915-2923

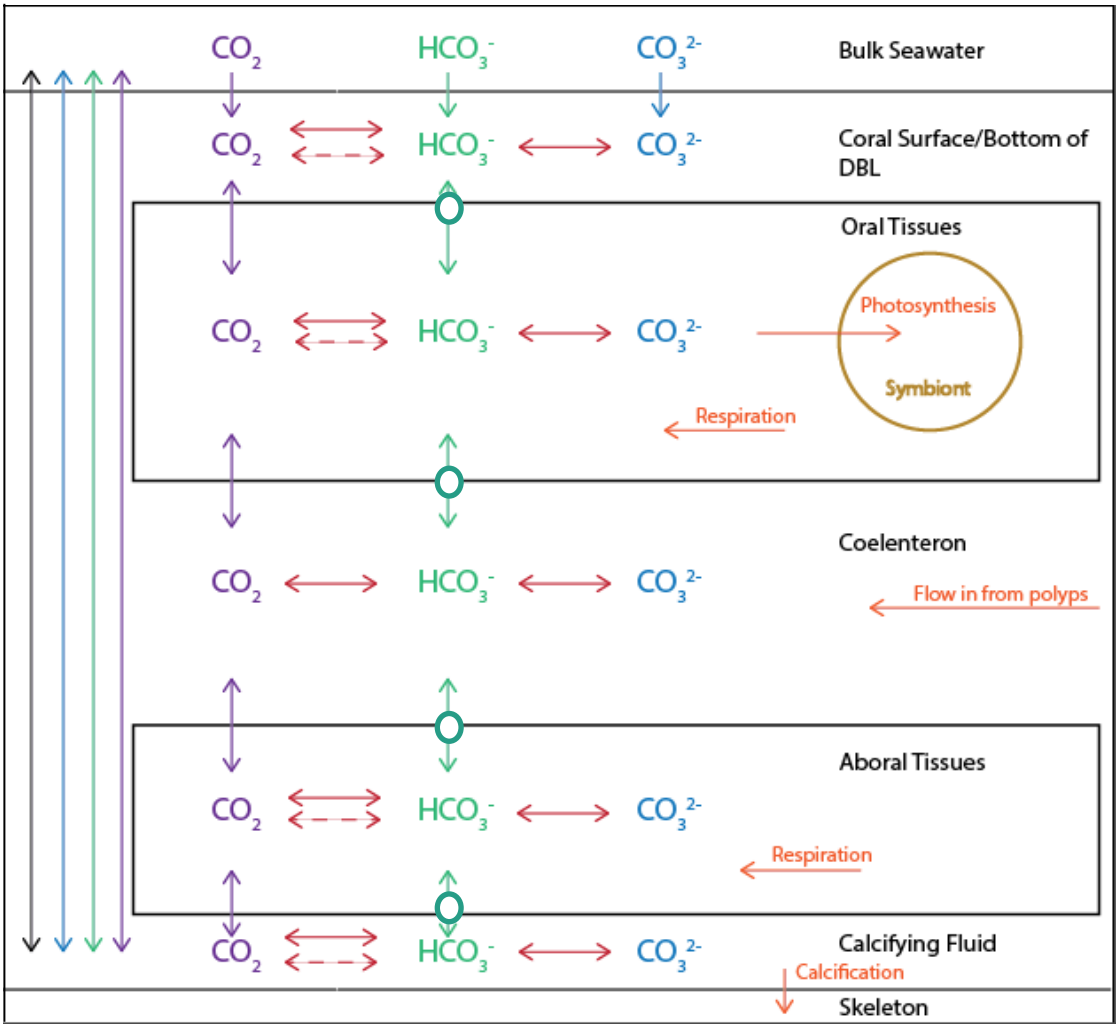

Figure 1.1: Inorganic carbon (DIC) fluxes through a scleractinian coral. CO_2 diffuses through membranes. HCO_3^- must be actively transported (circles along the tissue membranes). All DIC species can reach the calcifying fluid via paracellular pathways. Ca^{2+} and H^+ are hypothesized to be exchanged as well (black arrow). Sources of additional DIC are respiration by the coral and its symbionts (CO_2), as well as transport into the coelenteron from other polyps. Photosynthesis and calcification are sinks of CO_2 and CO_3^{2-}, respectively. Carbonic anhydrase catalyzed exchange occurs at the coral surface, within the tissues and in the calcifying fluid (dashed red arrows). pH dependent acid-base reactions (solid red arrows) equilibrate the DIC species through the coral.

CHAPTER 2

EXTERNAL CARBONIC ANHYDRASE IN THREE CARIBBEAN CORALS: QUANTIFICATION OF ACTIVTY AND ROLE IN CO_2 UPTAKE[1]

[1] Tansik, A. L., W. K. Fitt, and B. M. Hopkinson. 2015. External carbonic anhydrase in three Caribbean corals: quantification of activity and role in CO2 uptake. *Coral Reefs* 34:703-713. doi: 10.1007/s00338-015-1289-8 Reprinted here with permission of the publisher.

Abstract

Scleractinian corals have complicated inorganic carbon (C_i) transport pathways to support both photosynthesis, by their symbiotic dinoflagellates, and calcification. The first step in C_i acquisition, uptake into the coral, is critical as the diffusive boundary layer limits the supply of CO_2 to the surface and HCO_3^- uptake is energy intensive. An external carbonic anhydrase (eCA) on the oral surface of corals is thought to facilitate CO_2 uptake by converting HCO_3^- into CO_2, helping to overcome the limitation imposed by the boundary layer. However, this enzyme has not yet been identified or detected in corals, nor has its activity been quantified. We have developed a method to quantify eCA activity using a reaction-diffusion model to analyze data on ^{18}O removal from labeled C_i. Applying this technique to three species of Caribbean corals (*Orbicella faveolata*, *Porites astreoides*, and *Siderastrea radians*) showed that all species have eCA and that the potential rates of CO_2 generation by eCA greatly exceed photosynthetic rates. This demonstrates that eCA activity is sufficient to support its hypothesized role in CO_2 supply. Inhibition of eCA severely reduces net photosynthesis in all species (on average by 46 ± 27%), implying that CO_2 generated by eCA is a major carbon source for photosynthesis. Because of the high permeability of membranes to CO_2, CO_2 uptake is likely driven by a concentration gradient across the cytoplasmic membrane. The ubiquity of eCA in corals from diverse genera and environments suggests that it is fundamental for photosynthetic CO_2 supply.

Introduction

Scleractinian corals require inorganic carbon (C_i) for photosynthesis and calcification. While the pathways of C_i supply have not been fully determined, it is clear that the supply routes are complicated and interconnected (Gattuso et al. 1999; Furla et al. 2000b; Cohen and McConnaughey 2003; Bertucci et al. 2013). There is a highly active internal carbon cycle in which carbon is fixed by the symbiotic dinoflagellates of the genus *Symbiodinium*, known as zooxanthellae, then respired by the coral host, and recycled (Muscatine et al. 1984; Furla et al. 2000b; Fig. 2.1a). Internal recycling of C_i would at best allow photosynthetic rates to match respiratory rates if the recycling was completely efficient. To support net photosynthesis and calcification, C_i must be imported from seawater where CO_2 and HCO_3^- are the most readily accessible forms.

Corals import CO_2 as shown by microelectrode measurements of CO_2 drawdown in the diffusive boundary layer (DBL; de Beer et al. 2000). However, potential CO_2 uptake rates by CO_2 diffusion through the boundary layer are low since the DBL surrounding the coral is relatively thick and the concentration of CO_2 in seawater is low (~10 μM). The thickness of the DBL will vary with fluid flow characteristics, becoming thinner under faster turbulent flows and thicker under sluggish laminar flows; but under environmentally relevant flow conditions the boundary layer is an important constraint on mass transfer (Patterson 1992). To overcome this constraint, corals likely have an external carbonic anhydrase (eCA) on the surface of the coral to generate CO_2 from HCO_3^- for uptake (Furla et al. 2000a; Bertucci et al 2013). HCO_3^- can also be taken up directly through active transporters (Al Moghrabi et al. 1996). Newly imported C_i is routed both to the zooxanthellae, which reside primarily in the oral endoderm, and to the

calcifying space below the aboral ectoderm, but recycled respiratory CO_2 makes up much of the C_i used in gross photosynthesis and calcification (Furla et al. 2000b). Direct seawater transport into the calcifying fluid may also contribute C_i for calcification (Cohen and McConnaughey 2003; Gagnon et al. 2012). Transport of C_i into and within coral tissue is facilitated by HCO_3^- pumps (Al Moghrabi et al. 1996; Furla et al. 2000b) and carbonic anhydrases (CAs) (Weis et al. 1989).

Although the reactions catalyzed by CAs are relatively simple, i.e., the hydration of CO_2 and dehydration of HCO_3^-, CAs play diverse roles in C_i processing in the coral holobiont. CA is present in the calcifying space of *Stylphora pistillata*, presumably to convert respiratory CO_2 into HCO_3^- for use in calcification (Moya et al. 2008). Zooxanthellae also contain CA that is involved in CO_2 supply to RubisCO as part of its CO_2 concentrating mechanism (Isa and Yamazato 1984; Leggat et al. 1999). In zooxanthellae, chloroplastic CA serves to dehydrate HCO_3^- producing CO_2 around RubisCO, while cytoplasmic CA is involved in CO_2 uptake and prevention of CO_2 leakage (Badger and Price 1994). CA is also present throughout coral tissue, serving to recapture respired CO_2 as HCO_3^- for use in calcification and photosynthesis, or assisting in pH homeostasis (Weis et al. 1989; Bertucci et al. 2011).

eCA on the surface of the coral animal is also thought to be important for CO_2 supply. Extensive work on photosynthetic C_i supply in the zooxanthellate sea anemone *Anemonia viridis* has shown that the primary C_i uptake pathway is likely a CO_2 uptake mechanism based on H^+ extrusion to convert HCO_3^- to carbonic acid followed by eCA-catalyzed conversion of carbonic acid to CO_2 (Benazet-Tambutte et al. 1996a; Furla et al. 2000a). A similar system is believed to function in corals based primarily on the fact that acetazolamide, a CA inhibitor, which generally does not pass through membranes, inhibits photosynthesis in several corals, implying that eCA

supplies CO_2 for photosynthesis (Weis et al. 1989; Al-Moghrabi et al. 1996). However, eCA has not yet been identified on the oral surface of corals, nor has its activity been quantified.

Here we developed a method to quantify eCA activity in corals based on the removal of an ^{18}O label from C_i. The method was then applied to three species of Caribbean corals from diverse genera that occupy distinct environmental niches: the reef-building species *Orbicella* (previously *Montastraea*) *faveolata*, a resilient reef "filler" species *Porites astreoides*, and a stress-tolerant species *Siderastrea radians*.

Materials and Methods

Coral collection and maintenance

Fragments of *O. faveolata* and *P. asteroides* were collected from Little Grecian reef at a depth of 2-3 m and fragments of *S. radians* were collected from Florida Bay at a depth of ~1 m, Key Largo, Florida, USA. These taxa are from different phylogenetic groups of corals and have different ecological and environmental niches, stress-tolerance being one aspect of this. For instance, the genus *Orbicella* includes the major reef-building corals in the Caribbean, which have been bleaching and decreasing in percent cover with El Niño Southern Oscillations. Little Grecian reef is an offshore site in the northern Florida Keys exposed to clear, warm, low-nutrient waters of the Gulf Stream. In contrast, the waters of Florida Bay are generally more turbid and nutrient-rich, and temperatures fluctuate more seasonally. Each coral fragment was collected from a different coral colony. Exposed coral skeleton was covered with modeling clay, and colonies were maintained in closed circulation tanks.

One set of experiments was conducted on fragments that had been recently collected (< 2 weeks, having been allowed to rest at least 2 d after collection) from the Florida Keys, and are referred to as the field experiments. Another set of experiments was performed on corals that

were collected from the Florida Keys and then maintained in a laboratory tank at the University of Georgia for more than 6 months, which are referred to as lab experiments.

The laboratory tank was under a 12:12 light:dark regime that supplied ~200 μmol photons m^{-2} s^{-1} to the colonies, with the temperature maintained at 26° C and a salinity of 35.5 ppt. Inorganic carbon conditions in the tank were monitored by measuring pH (Zhang and Byrne 1996) and alkalinity to ensure the system was kept near oceanic conditions (pH 8.0 – 8.3; alkalinity 2.0 – 2.4 mM). These conditions are meant to provide a healthy, stable environment for the corals, but were not meant to precisely replicate field conditions. The field tank was exposed to the natural light regime, with shading added at midday to keep the maximum irradiance below 600 μmol photons m^{-2} s^{-1}. Temperature in the tank was maintained close to the ambient reef value of 23 °C (December 2012) or 26 °C (August 2013) with salinity at 35 ppt. All field colonies were given at least two days to recover from collection and handling before testing. Coral surface area was determined using the aluminum foil method (Marsh 1970). This method is most accurate for corals with massive morphologies such as those studied here, but is known to typically overestimate surface area by ~20% (Hoegh-Guldberg 1988; Veal et al. 2010). Such inaccuracies would not have major effects on the results obtained here.

Membrane Inlet Mass Spectrometry (MIMS)

^{18}O-isotope exchange and O_2 production experiments were conducted in a water-jacketed chamber interfaced with a MIMS system. The chamber was constructed from clear acrylic and the internal volume was adjustable (30-50 mL) so that a small volume of assay solution could be used with each coral and headspace could be eliminated. The chamber was placed on a magnetic stir plate and the assay solution stirred constantly (1500 rpm) with a small magnetic stir bar throughout the run. A coral fragment was set on a perforated stand over the stir bar and assay

solution was added to just cover the coral, at which point the top was screwed down to eliminate headspace. The assay solution was C_i-free artificial seawater (made following the recipe of Morel al. 1979), buffered with 20 mM Bicine and adjusted to a final pH of 8.0. Additions to the system were made using a syringe through a 1-mm hole drilled through the lid of the chamber.

To measure dissolved gases in the assay solution, water was continuously drawn out of the chamber using a peristaltic pump at a rate of 560 μL min^{-1} and passed through a 25-mm length of gas-permeable, silicone tubing under vacuum (the flow though inlet). Gases diffused through the tubing, through a dry-ice ethanol water trap (-75 °C), and then into a mass spectrometer (Pfeiffer PrismaPlus QMS 220) where they were quantified. The solution was then returned to the chamber. The mass spectrometer was outfitted with a yttrium-oxide coated iridium filament run at 0.5 mA emission current. The ion focusing electrodes were tuned for optimum performance by measuring atmospheric air, and a secondary electron multiplier was used to amplify ion currents.

Measurement of eCA activity

Background readings were taken with the MIMS for 5 min and then 250 μM $^{13}C^{18}O$-labeled C_i was added to the chamber. The $^{13}C^{18}O$-labeled C_i (primarily bicarbonate at the stock and assay pH) was synthesized by adding 1 M ^{13}C-bicarbonate (Sigma-Aldrich) to 97% ^{18}O-water (Cambridge Isotope Laboratories) and heating at 92 °C for > 6 h, which was then stored at -20 °C until use. The background rate of ^{18}O-removal was monitored for 15 min. A coral fragment was then placed in the chamber and covered to maintain darkness, monitoring ^{18}O-exchange for 10 min. At this point, experiments diverged. To study the origin of the ^{18}O-exchange signal 100 μM of the eCA inhibitor dextran-bound acetazolamide (DBAZ) was added to the chamber, and ^{18}O-exchange was monitored for a further 10 min to assess the response of

the colony to the inhibitor. In other cases, the effect of DBAZ on photosynthesis was assessed as described below. All fragments were ultimately subjected to both experiments, but a resting period of at least 2 d was allowed between experiments. After completion of the assay, coral colonies were then moved to a lit, aerated recovery container for 45 min prior to being returned to the holding tank. eCA activity was determined by numerical analysis of the ^{18}O removal rates as described in the Results. Neither this assay nor the photosynthesis measurement (see below) appeared to induce major coral stress as indicated by the lack of visible signs of stress (mesenterial filament extrusion, polyp retraction), the maintenance of high rates of photosynthesis throughout the assay (as is most clearly indicated in the control experiments shown in Appendix A, Fig. A1), and the lack of effects of the assay on long-term coral survival.

Photosynthesis

After measurement of ^{18}O-exchange as described above, a light source was turned on to provide 500 μmol photons m^{-2} s^{-1} to the colony. At the same time, an additional 2-mM unlabeled $NaHCO_3^-$ was added to the system to bring the C_i to 2.2 mM, similar to seawater concentrations. Photosynthetic O_2 production was measured for 15 min before addition of 100 μM DBAZ to the chamber. The light was left on for 10 min to determine the effect of the inhibitor on O_2 production. Control experiments showed that the DMSO in which DBAZ was dissolved had no effect on photosynthesis (Appendix Fig. A1). The effect of eCA inhibition by DBAZ on photosynthesis was quantified by measuring the rate of O_2 production for 5 min before and 5 min after DBAZ addition. The chamber was returned to darkness for 5 min before coral colonies were transferred to a lit, aerated recovery container for 45 min and then returned to the holding tank.

CO_2 reaction and diffusion model

A one-dimensional, reaction-diffusion model of the DBL was developed to estimate the maximal flux of CO_2 that can reach the coral surface from the bulk solution in the absence of eCA. This maximal flux represents the maximal potential CO_2 uptake rate in the absence of eCA and occurs when the CO_2 concentration at the coral surface is depleted to zero. The numerical model treats reaction and diffusion of inorganic carbon species (CO_2, HCO_3^-, CO_3^{2-}) and other important components determining seawater pH (H^+, OH^-, $B(OH)_3$, $B(OH)_4^-$) within the DBL. The model domain (the DBL, broken into 100 sublayers in the model) extends from the cell surface out 200 μm to an outer boundary representing the bulk solution. Chemical concentrations are held constant in the bulk solution (seawater with salinity = 35, pH = 8.0, and C_i = 2.2 mM, matching our experimental conditions), but allowed to vary due to uptake at the cell surface and reaction-diffusion within the boundary layer. Only CO_2 hydration/dehydration reactions are treated kinetically since the timescales of the other acid/base reactions are much faster than the timescale for diffusive transport through the boundary layer. Equilibrium constants for these reactions were obtained from Dickson and Goyet (1994) and Lueker et al. (2000). The differential algebraic equation system was formulated following Hofmann et al. (2008) and Chilakapati et al. (1998), and solved in Matlab varying the CO_2 uptake rate until the CO_2 concentration at the coral surface was fully depleted.

Results

Analysis of ^{18}O-exchange

The three species of corals we assayed (*O. faveolata, S. radians, P. asteroides*) accelerate the removal of ^{18}O label from C_i, a signature of CA activity (Silverman 1982; Fig 2.2.). To assess the origin of this signal, a polymeric CA inhibitor (molecular weight 7000 Da) that cannot

enter cells, DBAZ, was applied during ^{18}O-exchange assays. Application of DBAZ reduced the ^{18}O-exchange rate, showing that extracellular CA (eCA) activity is responsible for a substantial portion of the ^{18}O-removal signal (Fig. 2.2a).

We quantified eCA activity by fitting a reaction-diffusion model to the ^{18}O-exchange data, closely following an approach used to measure eCA activity in microalgae (Hopkinson et al. 2013; Fig. 2.1b). The ^{18}O-exchange data consists of three phases (Fig. 2.2a). In the first phase, prior to the addition of the coral, spontaneous hydration of CO_2 and dehydration of HCO_3^- is responsible for a slow rate of ^{18}O removal. In the second phase, after addition of the coral to the MIMS chamber, CA activity both on the coral surface and within the coral accelerate C_i hydration and dehydration reactions leading to a faster rate of ^{18}O loss. Finally in the third phase, after application of the eCA inhibitor DBAZ, the ^{18}O loss rate slows as only internal CA (iCA) remains active. The uncatalyzed, spontaneous rates of CO_2 hydration and dehydration and the effective iCA activity can be determined from the first and third phases respectively. Knowing the rate of spontaneous hydration/dehydration and iCA activty, the eCA activity can then be determined by analysis of ^{18}O exchange in the second phase. The coral is maintained in the darkness throughout the assay to avoid complicating the C_i dynamics with photosynthetic uptake.

The reaction-diffusion model used to determine eCA activity treats ^{18}O-CO_2 and ^{18}O-HCO_3^- isotopologues in the bulk solution, in the surface boundary layer, and within the coral tissue (Fig. 2.1b). Fluxes between the compartments are controlled by passive processes (diffusion through the boundary layer and across the outermembrane), and the uncatalyzed and catalyzed CO_2 hydration/HCO_3^- dehydration reactions, responsible for ^{18}O removal, are treated as first order reactions. This system is diagrammed in Fig. 1b and described by the following system of differential equations:

$$\frac{d\mathbf{c_e}}{dt} = -k_{ef}\mathbf{c_e} + k_{er}\mathbf{Hb_e} + \frac{D_c A}{L_{DBL} V_e}(\mathbf{c_s} - \mathbf{c_e}) \quad (1)$$

$$\frac{d\mathbf{b_e}}{dt} = k_{ef}\mathbf{Gc_e} - k_{er}\mathbf{b_e} + \frac{D_b A}{L_{DBL} V_e}(\mathbf{b_s} - \mathbf{b_e}) \quad (2)$$

$$\frac{d\mathbf{c_s}}{dt} = \frac{1}{L_{DBL}}\left[-k_{sf}\mathbf{c_s} + k_{sr}\mathbf{Hb_s} + \frac{D_c}{L_{DBL}}(\mathbf{c_e} - \mathbf{c_s}) + P_c(\mathbf{c_i} - \mathbf{c_s})\right] \quad (3)$$

$$\frac{d\mathbf{b_s}}{dt} = \frac{1}{L_{DBL}}\left[k_{sf}\mathbf{Gc_s} - k_{sr}\mathbf{b_s} + \frac{D_b}{L_{DBL}}(\mathbf{b_e} - \mathbf{b_s}) + P_b(\mathbf{b_i} - \mathbf{b_s})\right] \quad (4)$$

$$\frac{d\mathbf{c_i}}{dt} = -k_{if}\mathbf{c_i} + k_{ir}\mathbf{Hb_i} + \frac{P_c A}{V_i}(\mathbf{c_s} - \mathbf{c_i}) \quad (5)$$

$$\frac{d\mathbf{b_i}}{dt} = k_{if}\mathbf{Gc_i} - k_{ir}\mathbf{b_i} + \frac{P_b A}{V_i}(\mathbf{b_s} - \mathbf{b_i}) \quad (6)$$

where the parameters and variables are defined in Table 1. CO_2 and HCO_3^- fluxes into the coral (controlled by P_c, P_b) and CA activity within the coral (k_{if}, k_{ir}) are constrained by least squares fitting of the data collected after inhibition of eCA, whereas eCA activity (k_{sf}, k_{sr}) is determined from fitting the data prior to DBAZ addition. For a more intuitive measure of eCA activity, k_{sf}, reported in cm s^{-1}, could be converted to a first order rate constant by dividing by the boundary layer thickness. However, since this thickness was not directly measured here eCA activity was kept in cm s^{-1}. CO_2 and HCO_3^- flux through the coral membrane cannot be rigorously distinguished, but both processes are included to fit the ^{18}O-exchange data after inhibition of eCA since CO_2 flux alone cannot always explain the rate of ^{18}O depletion. (Appendix A AI.I; Appendix Fig. A2). While this issue limits our ability to infer membrane permeabilities and absolute iCA activity from the data, as long as the net effect of iCA on ^{18}O removal is accounted for, this limitation does not affect the determination of eCA activity (Appendix A AI.I).

The most important parameter in the model that could not be measured directly is the thickness of the DBL (L_{DBL}). L_{DBL} was set to 200 μm, on the low end of measured values (Kuhl

et al. 1995; de Beer et al. 2000), which in turn means eCA activities are minimal estimates. In the eCA assay, the ^{18}O label is removed by eCA on the coral surface (primarily) and by iCA within the coral (secondarily). The two main factors affecting the rate of ^{18}O removal are thus 1) the flux of C_i to the surface of the coral and 2) the rate of CA activity, with higher C_i flux to the surface and higher CA activity leading to more rapid ^{18}O removal. A thicker L_{DBL} results in lower fluxes of C_i to the coral surface and so results in higher inferred eCA activity in order to account for the observed rate of ^{18}O removal. A sensitivity analysis was conducted to assess the effects of uncertainty in L_{DBL} on inferred eCA activities. L_{DBL} varied by 50% from the base value (minimum 100 μm, maximum 300 μm), which led to 70% changes on average in the inferred eCA activity (increasing L_{DBL} to 300 μm, average 80% change, range 0-190%; decreasing L_{DBL} to 100 μm, average 60% change, range 0-90%). While this uncertainty is certainly substantial it does not affect the major conclusions of this work as argued in the Discussion. Further details of the model are discussed in Appendix A (Appendix A AI.II).

eCA activity

eCA activity was measured on specimens of corals that were either recently collected from reefs in the Florida Keys (field) or that had been maintained in a laboratory aquarium for > 6 months (lab). Two considerations motivated this approach: 1) coral collection requires fragmenting a small sample from a coral colony, which, despite allowing at least 2 d for recovery, could lead to prolonged stress that alters physiology, and 2) many techniques used to study C_i processing are better suited to the lab and so we wanted to assess whether corals kept under laboratory conditions maintained broadly similar C_i-processing physiology.

eCA activity was detected in all taxa in both specimens recently collected from the field and those maintained in the laboratory (Fig. 2.3). There were no significant differences (t-test;

p>0.05) between eCA activity in the field and lab for any species. The eCA activity of *O. faveolata* was high with the exception of one outlier from the field with nearly undetectable eCA activity. Excluding that outlier and pooling the remaining lab and field data, *O. faveolata* had significantly higher eCA activity (t-test; $p < 0.05$) than either *S. radians* or *P. astreoides*. The eCA activities of *S. radians* and *P. astreoides* were not significantly different from each other.

Inhibition of photosynthesis

The addition of the eCA inhibitor DBAZ had an immediate negative impact on the rate of net photosynthesis in nearly all experiments, as measured by the net O_2 production from the colonies (Fig. 2.4). As this study investigates C_i uptake, we focus on net photosynthesis because the coral must import C_i to sustain photosynthesis above the rate of respiration (i.e., net photosynthesis). Across all taxa and conditions, the effects of DBAZ on net photosynthesis ranged widely from complete inhibition of net photosynthesis to essentially no effect. DBAZ significantly reduced net photosynthesis in all taxa and conditions, except in laboratory specimens of *S. radians* (Fig. 2.5a). Averaged across taxa, DBAZ had a similar effect on net photosynthesis in both the lab (48 ± 27% of net photosynthesis remaining after DBAZ addition) and field (43 ± 26%). *Orbicella faveolata* fragments recently collected from the field were less affected by DBAZ than those maintained in the lab, but there were no significant differences between field and lab specimens of the other species (Fig. 2.5b).

Maximal CO_2 uptake rate in the absence of eCA

In the absence of eCA, CO_2 is delivered to the coral surface by diffusion through and reaction within the boundary layer. The maximal CO_2 influx in the absence of eCA occurs when the coral is able to completely deplete CO_2 at the surface. This maximal CO_2 flux was determined using a reaction-diffusion model to be 6.4×10^{-8} mol cm^{-2} hr^{-1} under our experimental

conditions (2.2 mM DIC; pH 8.0; 200 μm DBL). If corals were able to achieve this maximal CO_2 uptake rate, CO_2 could supply only 11 – 23 % (average 16 %) of the total C_i uptake rate required to support the net photosynthetic rates measured in this study.

Discussion

eCA is thought to play in important role in C_i supply for photosynthesis by catalyzing the conversion of HCO_3^- to CO_2 at the coral surface for subsequent uptake. This model is based primarily on the fact that an eCA inhibitor, acetazolamide, inhibits photosynthesis in several scleractinian corals (Weis et al. 1989; Al-Moghrabi et al. 1996), and by analogy with the system identified in the sea anemone *Anemonia viridis* (Benazet-Tambutte et al. 1996a; Furla et al. 2000a). However, eCA has yet to be detected on the oral surface of scleractinian corals by either molecular or chemical approaches, nor has the activity of eCA been quantified. We have developed a method to quantify eCA activity in corals and applied this method to three species of Caribbean corals from diverse genera. In all species, eCA was present and its activity was sufficient to support its proposed role in CO_2 supply. Furthermore eCA is important for photosynthetic CO_2 supply in these species as indicated by reduced rates of photosynthesis in the presence of an eCA inhibitor.

Quantification of eCA activity

Although CO_2 concentrations in seawater are approximately two orders of magnitude lower than HCO_3^-, CO_2 is often the preferred substrate for photosynthetic organisms since CO_2 is ultimately required by RubisCO and its ability to traverse membranes passively reduces the energetic costs of uptake (Kaplan and Reinhold 1999; Rost et al. 2003). In corals, the thickness of the DBL and the naturally slow rate of HCO_3^- dehydration severely limit the potential for CO_2 uptake. Under our experimental conditions, the maximal CO_2 supply due to diffusion across and

production within the boundary layer can only support 11 – 23 % (average 16 %) of the measured net photosynthetic rates. In contrast, HCO_3^- concentrations in seawater are more than 100 fold higher than CO_2 concentrations and so the rate of HCO_3^- diffusion through the DBL is high compared to the rate of photosynthesis and will not limit HCO_3^- uptake. Although the DBL limits CO_2 flux from bulk seawater, our measurements of ^{18}O-exchange show that scleractinian corals from several different families possess an eCA capable of generating CO_2 at the coral surface. Because of uncertainty in the thickness of the DBL and nearly complete ^{18}O depletion at the coral surface, we conservatively estimated lower-bounds on eCA activity by using a thin DBL estimate (200 μm; Fig. 3). These eCA activities are high in that they are capable of generating more than enough CO_2 to support net photosynthesis. The maximum rate of CO_2 production at the surface of the colony (calculated as $k_{sr}[HCO_3^-]$) ranges from 5.0×10^{-6} – 3×10^{-4} mol cm^{-2} hr^{-1}, or 10 - 800 times greater than the net photosynthetic rate. Actual net CO_2 production rates would be much lower, matching organismal uptake rates up to the maximal CO_2 production rate.

A sensitivity analysis of the effect of uncertainty in the DBL thickness on inferred eCA activity showed that a 50% change in DBL thickness (100 to 300 μm range) results in, on average, a 70% change in eCA activity. Although this is certainly substantial, it does not affect the primary conclusions that eCA is present and that the eCA activity is sufficient to support CO_2 uptake for photosynthesis. Even if the DBL were very thin (100 μm), resulting in ~70% lower inferred eCA activity, the potential CO_2 generation rates would still be higher than net photosynthetic rates, and thus capable of supplying ample CO_2 for photosynthesis.

The only previous comparable measurements of eCA activity were conducted on marine diatoms (Hopkinson et al. 2013). The eCA activity in diatoms, when normalized to surface area

for comparison with the coral data, is at the lower end of the range observed in corals (*Thalassiosira pseudonana*: 0.1 ± 0.01 cm s^{-1}; *Thalassiosira weissflogii*: 0.2 ± 0.03 cm s^{-1}), consistent with boundary layer resistance being a greater constraint on C_i acquisition in larger organisms such as corals (Raven and Hurd 2012).

The eCA detected via ^{18}O-exchange is most likely on the oral surface of the coral adjacent to seawater or perhaps in the mucus layer. Its activity is inhibited by DBAZ, which is too large to enter cells or pass through the septate junctions that connect cells in the oral layer (Benazet-Tambutte et al. 1996b; Furla et al. 1998). The only alternative location would be within the coelenteron, but exchange of fluid and ions in the coelenteron is slow enough that CA within the coelentron is not likely to significantly affect the rate of ^{18}O removal. The fluid in the coelenteron is exchanged with a turnover time of approximately 5 min (Tambutte et al. 1996; Furla et al. 2000b). If we assume that the coelenteron makes up 30% of the total coral volume (an upper bound based on analysis of fragmented colonies and histological sections in the literature; Galloway et al 2007) then the rate of C_i flux into the coelenteron is at most 20% the rate of diffusive C_i flux to the coral surface (for *O. faveolata* 20%, *P. astreoides* 9%, *S. radians* 3%, using measurements of effective tissue thickness of 1.9 mm, 0.8 mm, and 0.3 mm, respectively, to calculate coelenteron fluid fluxes). Alternatively, C_i can enter the coelenteron by diffusion through cell junctions, but the permeability of cnidarian epithelial tissue to C_i is low (2.5×10^{-5} cm s^{-1}; Furla et al. 1998) compared with the diffusional flux of C_i through the DBL (mass transfer coefficient = $D_c/DBL = 1 \times 10^{-3}$ cm s^{-1}) such that flux of ^{18}O-labled C_i into the coelenteron by this pathway would be only ~2.5% of the C_i flux to the coral surface. The C_i fluxes into the coelenteron are small relative to C_i fluxes to the coral surface, except in the case of *O. faveolata*, and so in general, eCA within the coelenteron is not likely to contribute

significantly to the observed ^{18}O removal. Consequently, the eCA detected in the assay is most likely on the outer oral layer of the coral.

While some coral CAs have been identified and characterized, none have yet been localized to the coral surface. Numerous CAs have been identified in a single coral transcriptome and several are phylogenetically grouped with secreted and membrane-associated CAs, one or more of which may be responsible for the observed eCA activity (Moya et al. 2012). However, the two CAs that have been extensively characterized in a scleractinian coral (*Stylophora pistillata*) were localized to the calcifying space (Moya et al. 2008) and within the cytoplasm of coral cells (Bertucci et al. 2011).

Role of eCA in CO_2 uptake and potential CO_2 uptake pathways

To support net photosynthesis corals must import C_i and the two main pathways available to them are direct uptake of HCO_3^- and eCA catalyzed dehydration of HCO_3^- to CO_2 followed by CO_2 uptake. The relative importance of these pathways can be determined by inhibiting eCA activity, thereby blocking the CO_2 uptake pathway. Inhibition of eCA activity using DBAZ reduced net photosynthetic rates by an average of 46 ± 27%, which indicates that eCA-facilitated CO_2 is a critical source of C_i for photosynthesis (Fig. 4, 5). Since the potential CO_2 uptake in the absence of eCA is small, the decline in photosynthesis after application of DBAZ serves as an estimate of the net CO_2 uptake rate for photosynthesis. With CO_2 uptake eliminated, the remaining carbon to support net photosynthesis must come from HCO_3^- uptake. There are a number of genes with homology to HCO_3^- transporters in the transcriptomes of *Acropora millepora* and *P. astreoides* offering a potential mechanism for HCO_3^- import (Moya et al. 2012; Kenkel et al. 2013). HCO_3^- uptake may be increased when eCA is inhibited so this is likely a lower estimate on the true net CO_2 uptake rate. Using this approach, CO_2 supplies ~50% of the

C_i for net photosynthesis with HCO_3^- comprising the remaining portion (as illustrated in Fig. 1a), although these fractions vary greatly among taxa and particular samples (Fig. 5b).

Marine microalgae have a broadly similar partitioning of C_i uptake between CO_2 and HCO_3^-, illustrating that the disproportionate use of CO_2 observed in corals is common in marine autotrophs (Burkhardt et al. 2001; Rost et al. 2003). Certain species of macroalgae, aquatic macrophytes, sea anemones, and other macroscopic photoautotrophs like zooxanthellate corals are also highly reliant on eCA generated CO_2 for photosynthesis (Axelsson et al. 1995; Mercado et al. 1998; Furla et al. 2000a; Uku et al. 2005). The clear importance of eCA for carbon supply in corals is in striking contrast to microalgae, where inhibition of eCA has relatively small effects on photosynthesis, and is another manifestation of the limitations imposed by the DBL (Atkinson and Bilger 1992; Lesser et al. 1994; Mass et al. 2010).

There were no consistent distinctions in preference for CO_2 or HCO_3^- uptake among the species tested, nor was eCA activity correlated with the fraction of total C_i uptake obtained from CO_2 (Fig. 5). The broadly similar fraction of CO_2 and HCO_3^- uptake among the coral species and the ubiquity of eCA suggest that carbon uptake pathways are similar throughout the scleractinian corals, but flexible depending on environmental conditions. Despite the similarity in the fraction of photosynthesis supported by CO_2 uptake across taxa, eCA activity was dramatically higher in *O. faveolata* relative to the other taxa. This additional eCA activity may help maintain CO_2 supply during bursts of demand or could relate to differences in the photosynthetic physiology or the CCM of the zooxanthellae (Brading et al. 2013).

CO_2 flux into the coral is likely driven by a concentration gradient across the outer coral membrane. This gradient could either be generated by CO_2 uptake by zooxanthellae in the oral endoderm or by CA-catalyzed conversion of CO_2 to HCO_3^- in the oral ectoderm and subsequent

export of HCO_3^- to the endodermal cells to support photosynthesis, a process similar to the CO_2 uptake mechanism described for zooxanthellate sea anemones (Allemand et al. 1998; Furla et al. 2000a). The proposed CO_2 uptake pathway requires that the coral membrane be highly permeable to CO_2, and though there are scattered reports of biological membranes showing some resistance to CO_2 diffusion (Tu et al. 1986; Sültemeyer and Rinast 1996), generally CO_2 permeabilities are high (Silverman et al. 1981; Hopkinson et al. 2011), on the order of 10^{-1} to 10^{-2} cm s^{-1}, consistent with the properties of synthetic lipid bilayers (Gutknecht et al. 1977). Taking the average rate of photosynthesis in our study (4.3 x10^{-7} mol cm^{-2} hr^{-1}) and assuming that half of this comes from CO_2 uptake and that the membrane permeability is 5 x10^{-2} cm s^{-1}, a concentration difference of 1.2 μM across the coral membrane would be required to support uptake. While this is a moderate portion of the ~10 μM CO_2 in seawater, it does not seem unreasonable given that some marine algae are able to drawdown CO_2 to <1 μM, internally (Hopkinson 2014). There is no precedent for an active, membrane-based CO_2 transporter, presumably because cell membranes are so permeable to CO_2 (Gutknecht et al. 1977).

Although the thickness of the DBL limits direct CO_2 uptake by corals, an extracellular carbonic anhydrase facilitates CO_2 uptake by generating CO_2 from HCO_3^- at the coral surface. We found that eCA is present in all three species of Caribbean corals examined and that the activity of this enzyme is sufficient to support its proposed role in CO_2 supply. Inhibition of eCA reduced photosynthesis, implying that CO_2 is an important source of C_i for photosynthesis in these corals. This work, in conjunction with previous research on corals and the sea anemone *Anemonia viridis*, suggests that CO_2 generated from HCO_3^- is an important source of C_i for photosynthesis in a wide variety of corals and cnidarians. Finally, the quantitative rates of eCA

activity obtained here are suitable for incorporation into numerical models of coral photosynthesis and C_i processing (e.g., Hohn and Merico 2012; Nakamura et al. 2013).

Acknowledgments

This study was supported by grants from the National Science Foundation (EF-1315944 to BMH and WKF, and EF-1041034 to BMH). Corals were collected from the Florida Keys National Marine Sanctuary (Permits: 2011-093 and 2014-015).

References

Allemand D, Furla P, Benazet-Tambutte S (1998) Mechanisms of carbon acquisition for endosymbiont photosynthesis in Anthozoa. Can J Bot 76:925-941

Al-Moghrabi S, Goiran C, Allemand D, Speziale N, Jaubert J (1996) Inorganic carbon uptake for photosynthesis by the symbiotic coral-dinoflagellate association II. Mechanisms for bicarbonate uptake. J Exp Mar Bio Ecol 199:227-248

Atkinson MJ, Bilger RW (1992) Effects of water velocity on phosphate uptake in coral reef flat communities. Limnol Oceanogr 37:273-279

Axelsson L, Ryberg H, Beer S (1995) Two modes of bicarbonate utilization in the marine green macroalga *Ulva lactuca*. Plant Cell Environ 18:439-445

Badger M, Price G (1994) The role of carbonic anhydrase in photosynthesis. Annu Rev Plant Physiol Plant Mol Biol 45:369-392

Benazet-Tambutte S, Allemand D, Jaubert J (1996a) Inorganic carbon supply to symbiont photosynthesis of the sea anemone, *Anemonia viridis*: role of the oral epithelial layers. Symbiosis 20:199-217

Benazet-Tambutte S, Allemand D, Jaubert J (1996b) Permeability of the oral epithelial layers in cnidarians. Mar Biol 126:43-53

Bertucci A, Tambutte S, Supuran CT, Allemand D, Zoccola D (2011) A new coral carbonic anhydrase in *Stylophora pistillata*. Mar Biotechnol 13:992-1002

Bertucci A, Moya A, Tambutte S, Allemand D, Supuran CT, Zoccola D (2013) Carbonic anhydrases in anthozoan corals - a review. Bioorg Med Chem 21:1437-1450

Brading P, Warner ME, Smith DJ, Sugget DJ (2013) Contrasting modes of inorganic carbon acquisition amongst *Symbiodinium* (Dinophyceae) phylotypes. New Phytol 200:432-442

Burkhardt S, Amoroso G, Riebesell U, Sültemeyer D (2001) CO_2 and HCO_3^- uptake in marine diatoms acclimated to different CO_2 concentrations. Limnol Oceanogr 46:1378-1391

Chilakapati A, Ginn T, Szecsody J (1998) An analysis of complex reaction networks in groundwater modeling. Water Resour Res 34:1767-1780

Cohen AL, McConnaughey TA (2003) Geochemical perspectives on coral mineralization. In: Dove PM, DeYoreo JJ, Weiner S (eds) Biomineralization. Mineralogical Society of America, Chantilly, pp151-187

de Beer D, Kuhl M, Stambler N, Vaki L (2000) A microsensor study of light enhanced Ca^{2+} uptake and photosynthesis in the reef-building hermatypic coral *Favia* sp. Mar Ecol Prog Ser 194:75-85

Dickson AG, Goyet C (1994) DOE handbook of methods for the analysis of the various parameters of the carbon dioxide system in sea water. Version 2., ORNL/CDIAC-74, Oak Ridge National Lab., Tennessee, USA

Furla P, Allemand D, Orsenigo MN (2000a) Involvement of H^+-ATPase and carbonic anhydrase in inorganic carbon uptake for endosymbiont photosynthesis. Am J Physiol Regul Integr Comp Physiol 278:R870-R881

Furla P, Benazet-Tambutte S, Jaubert J, Allemand D (1998) Diffusional permeability of dissolved inorganic carbon through the isolated oral epithelial layers of the sea anemone, *Anemonia viridis*. J Exp Mar Bio Ecol 221:71-88

Furla P, Galgani I, Durand I, Allemand D (2000b) Sources and mechanisms of inorganic carbon transport for coral calcification and photosynthesis. J Exp Biol 203:3445-3457

Gagnon AC, Adkins JF, Erez J (2012) Seawater transport during coral biomineralization. Earth Planet Sci Lett 329:150-161

Galloway SB, Work TM, Bochsler VS, Harley RA, Kramarsky-Winters E, McLaughlin SM, Meteyer CU, Morado JF, Nicholson JH, Parnell PG, Peters EC, Reynolds TL, Rotstein DS, Sileo L, Woodley CM (2007) Coral disease and health workshop: coral histopathology II. NOAA Technincal Memorandum NOS NCCOS 56 and NOAA Technical Memorandum CRCP5. National Oceanic and Atmospheric Administration, Silver Spring, MD. p 84

Gattuso JP, Allemand D, Frankignoulle M (1999) Photosynthesis and calcification at cellular, organismal and community levels in coral reefs: A review on interactions and control by carbonate chemistry. Am Zool 39:160-183

Gutknecht J, Bisson M, Tosteson F (1977) Diffusion of carbon dioxide through lipid bilayer membranes: effects of carbonic anhydrase, bicarbonate, and unstirred layers. J Gen Physiol 69:779-794

Hoegh-Guldberg O (1988) A method for determining surface area of corals. Coral Reefs 7:113-116

Hohn S, Merico A (2012) Modelling coral polyp calcification in relation to ocean acidification. Biogeosciences 9:4441-4454

Hofmann AF, Meysman FJR, Soetaert K, Middelburg JJ (2008) A step-by-step procedure for pH model construction in aquatic systems. Biogeosciences 5:227-251

Hopkinson BM (2014) A chloroplast pump model for the CO_2 concentrating mechanism in the diatom *Phaeodactylum tricornutum*. Photosynth Res 121:223-233

Hopkinson BM, Meile C, Shen C (2013) Quantification of extracellular carbonic anhydrase activity in two marine diatoms and investigation of its role. Plant Physiol 162:1142-1152

Hopkinson BM, Dupont CL, Allen AE, Morel FMM (2011) Efficiency of the CO_2-concentrating mechanism of diatoms. Proc Natl Acad Sci USA 108:3830-3837

Isa Y, Yamazato K (1984) The distribution of carbonic anhydrase in a staghorn coral, *Acropora hebes* (Dana). Galaxea 3:25-36

Kaplan A, Reinhold L (1999) CO_2 concentrating mechanisms in photosynthetic microorganisms. Ann Rev Plant Biol 50:539-570

Kenkel CD, Meyer E, Matz MV (2013) Gene expression under chronic heat stress in populations of the mustard hill coral (*Porites astreoides*) from different thermal environments. Mol Ecol 22:4322-4334

Kuhl M, Cohen Y, Dalsgaard T, Jorgensen BB, Revsbech NP (1995) Microenvironment and photosynthesis of zooxanthellae in scleractinian corals studied with microsensors for O_2, pH, and light. Mar Ecol Prog Ser 117:159-172

Leggat W, Badger M, Yellowlees D (1999) Evidence for an inorganic carbon-concentrating mechanism in the symbiotic dinoflagellate *Symbiodinium* sp. Plant Physiol 121:1247-1255

Lesser MP, Weis VM, Patterson MR, Jokiel PL (1994) Effects of morphology and water motion on carbon delivery and productivity in the reef coral *Pocillopora damincornis* (Linnaeus): Diffusion barriers, inorganic carbon limitation, and biochemical plasticity J Exp Mar Bio Ecol 178:153-179

Lueker TJ, Dickson AG, Keeling CD (2000) Ocean pCO_2 calculated from dissolved inorganic carbon, alkalinity, and equations for K_1 and K_2: validation based on laboratory measurements of CO_2 in gas and seawater at equilibrium. Mar Chem 70:105-119

Marsh JA (1970) Primary productivity of reef-building calcareous red algae. Ecology 51:255-263

Mass T, Genin A, Shavit U, Grinstein M, Tchernov D (2010) Flow enhances photosynthesis in marine benthic autotrophs by increasing the efflux of oxygen from the organism to the water. Proc Natl Acad Sci USA 107:2527-2531

Mercado JM, Gordillo FJL, Figueroa FL, Niell FX (1998) External carbonic anhydrase and affinity for inorganic carbon in intertidal macroalgae. J Exp Mar Bio Ecol 221:209-220

Morel FMM, Rueter JG, Anderson DM, Guillard RRL (1979) Aquil: A chemically defined phytoplankton culture medium for trace metal studies. J Phycol 15:135-141

Moya A, Tambutte S, Bertucci A, Tambutte E, Lotto S, Vullo D, Supuran CT, Allemand D, Zoccola D (2008) Carbonic anhydrase in the scleractinian coral *Stylophora pistillata* - Characterization, localization, and role in biomineralization. J Biol Chem 283:25475-25484

Moya A, Huisman L, Ball EE, Hayward DC, Grasso LC, Chua CM, Woo HN, Gattuso JP, Foret S, Miller DJ (2012) Whole transcriptome analysis of the coral *Acropora millepora* reveals complex responses to CO_2-driven acidification during the initiation of calcification. Mol Ecol 21:2440-2454

Muscatine L, Falkowski PG, Porter JW, Dubinsky Z (1984) Fate of photosynthetic fixed carbon in light-adapted and shade-adapted colonies of the symbiotic coral *Stylophora pistillata*. Proc R Soc Lond B Biol Sci 222:181-202

Nakamura T, Nadaoka K, Watanabe A (2013) A coral polyp model of photosynthesis, respiration and calcification incorporating a transcellular ion transport mechanism. Coral Reefs 32:779-794

Patterson MR (1992) A chemical engineering view of cnidarian symbioses. Amer Zool 32:566-582

Raven JA, Hurd CL (2012) Ecophysiology of photosynthesis in macroalgae. Photosynth Res 113:105-125

Rost B, Riebesell U, Burkhardt S, Sültemeyer D (2003) Carbon acquisition of bloom-forming marine phytoplankton. Limnol Oceanogr 48:55-67

Silverman D (1982) Carbonic anhydrase: oxygen-18 exchange catalyzed by an enzyme with rate-contributing proton-transfer steps. Methods Enzymol 87:732-752

Silverman D, Tu C, Roessler N (1981) Diffusion-limited exchange of ^{18}O between CO_2 and water in red cell suspensions. Respir Physiol 44:285-298

Sültemeyer D, Rinast K (1996) The CO_2 permeability of the plasma membrane of *Chlamydomonas reinhardtii*: mass-spectrometric ^{18}O-exchange measurements from $^{13}C^{18}O_2$ in suspensions of carbonic anhydrase-loaded plasma-membrane vesicles. Planta 200:358-368

Tambutte E, Allemand D, Mueller E, Jaubert J (1996) A compartmental approach to the mechanism of calcification in hermatypic corals. J Exp Biol 199:1029-1041

Tu C, Acevedo-Duncan M, Wynns G, Silverman D (1986) Oxygen-18 exchange as a measure of accessibility of CO_2 and HCO_3^- to carbonic anhydrase in *Chlorella vulgaris* (UTEX 263). Plant Physiol 80:997-1001

Uku J, Beer S, Bjork M (2005) Buffer sensitivity of photosynthetic carbon utilisation in eight tropical seagrasses. Mar Biol 147:1085-1090

Veal CJ, Holmes G, Nunez M, Hoegh-Guldberg O, Osborn J (2010) A comparative study of methods for surface area and three-dimensional shape measurement of coral skeletons. Limnol Oceanogr Methods 8: 241-253

Weis VM, Smith GJ, Muscatine L (1989) A CO_2 supply mechanism in zooxanthellate cnidarians: role of carbonic anhydrase. Mar Biol 100:195-202

Zhang HN, Byrne RH (1996) Spectrophotometric pH measurements of surface seawater at in-situ conditions: Absorbance and protonation behavior of thymol blue. Mar Chem 52:17-25

Table 2.1: Model notation

Symbol	Description	Units
$\mathbf{c_x}$, $\mathbf{b_x^a}$	^{18}O CO_2 and HCO_3^- concentrations	mol cm^{-3}
k_{xf}, k_{xr}	Hydration and dehydration rate constants	s^{-1} or cm s^{-1} (surface rates)
D_c, D_b	Diffusivity of CO_2 and HCO_3^-	cm^2 s^{-1}
P_c, P_b	Membrane permeability to CO_2 and HCO_3^-	cm s^{-1}
V_x	Compartment volume	cm^3
A	Coral surface area	cm^2
L_{DBL}	Diffusive boundary layer thickness	cm
G, **H**	Stoichiometric matrices describing hydration and dehydration reactions	–

[a] x: e = bulk solution, s surface, i intracellular

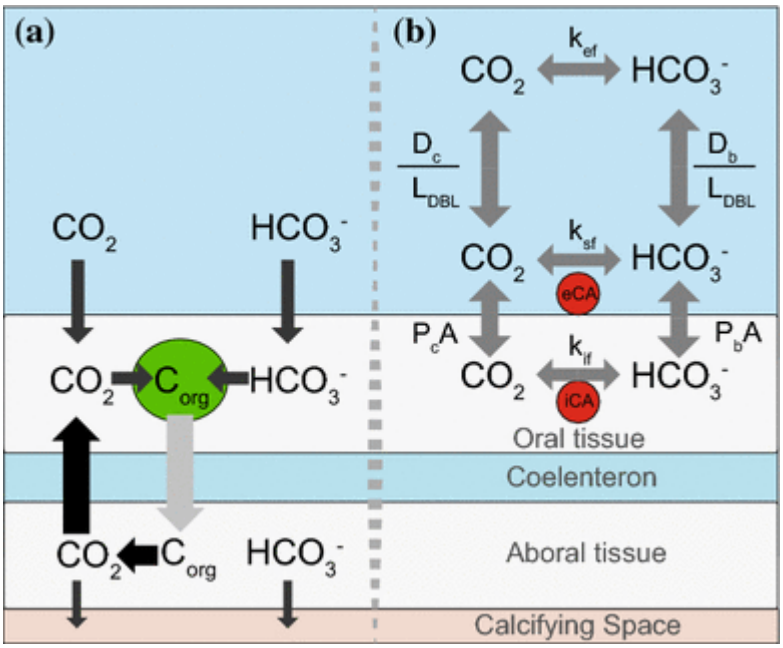

Figure 2.1: Carbon fluxes and photosynthesis-related CA (a) Diagram of major carbon fluxes in the coral holobiont. CO_2 and HCO_3^- are taken up from seawater to support net photosynthesis and calcification. Fixation of inorganic carbon by zooxanthellae (green oval), primarily in the oral tissue, creates organic carbon (C_{org}), much of which is exported to coral tissue where it is respired. A large portion of the respired CO_2 is refixed and some is used in calcification. The sizes of the arrows reflect approximate relative fluxes. (b) A diagram of the inorganic carbon transport and reactions processes considered in the model used to determine eCA activity. See Table 1 for parameter definitions.

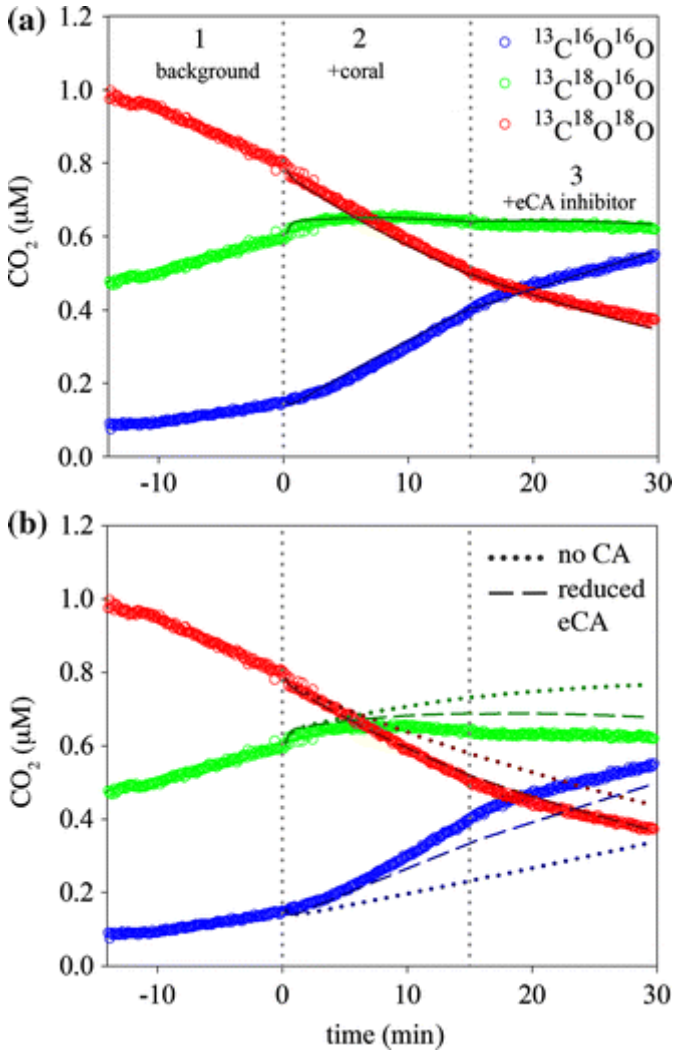

Figure 2.2: An example of the ^{18}O-exchange data analyzed to determine eCA activities and model fits to the data. Three $^{13}CO_2$ isotopologues are tracked and analyzed: $^{13}C^{16}O^{16}O$ (blue circles), $^{13}C^{18}O^{16}O$ (green circles), and $^{13}C^{18}O^{18}O$ (red circles). (a) The data consist of three phases: 1) no coral added, background rate of exchange; 2) coral (*S. radians*) added, exchange catalyzed by eCA and iCA; 3) eCA inhibitor (DBAZ) added, exchange catalyzed by iCA. The best fit (lines, k_{sf} = 1.75 cm s^{-1}) of the model to phases 2 and 3 is shown, as well as simulations of ^{18}O-CO_2 behavior (b) if eCA activity as 10 fold lower (dashed lines, k_{sf} = 0.175 cm s^{-1}) or if the coral had no CA (dotted lines).

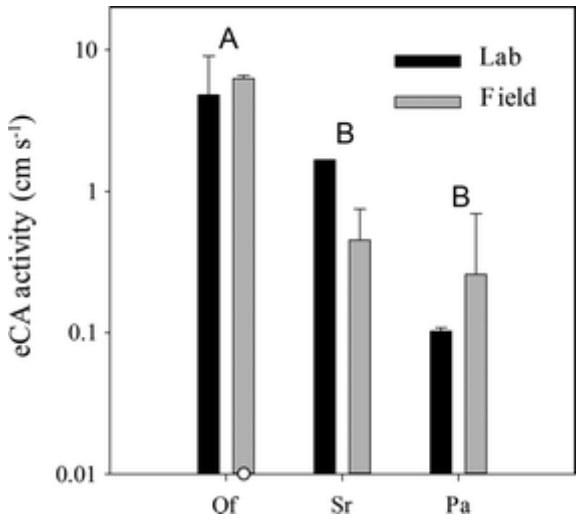

Figure 2.3: eCA activities measured in three species of Caribbean corals (Of: *Orbicella faveolata*, Sr: *Siderastrea radians*, Pa: *Porites astreoides*). Measurements were made on corals maintained in the lab for six months or more ('Lab') and on corals recently collected from the field ('Field'). Error bars represent ±1 SD, and one outlier from a field *O. faveolata* sample is represented by a point. Different letters indicate that species (pooling field and lab data) have significantly different eCA activities (t-test; $p < 0.05$).

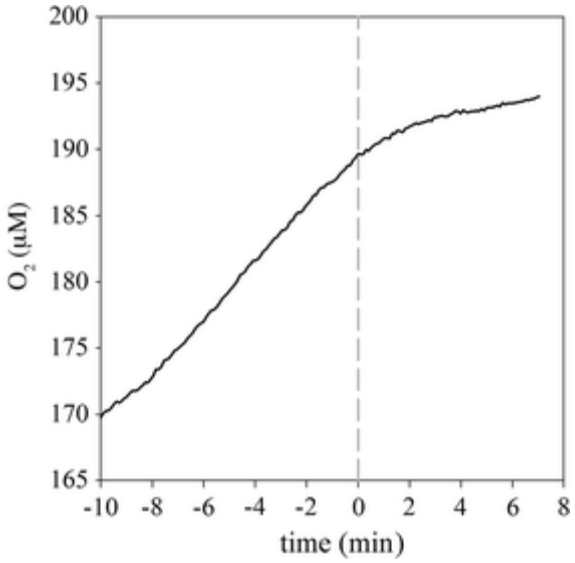

Figure 2.4: Example of the inhibition of O_2 evolution by DBAZ. The vertical line indicates the time at which 100 μM DBAZ was added to a photosynthesizing colony of *Orbicella faveolata*. Net photosynthetic rates were determined from the rate of O_2 production 5 min prior to DBAZ addition, and for 5 min after DBAZ addition, allowing ~1 min between the actual addition and calculation of the photosynthetic rate to allow for mixing of the DBAZ and for the chamber solution to reach the MIMS inlet.

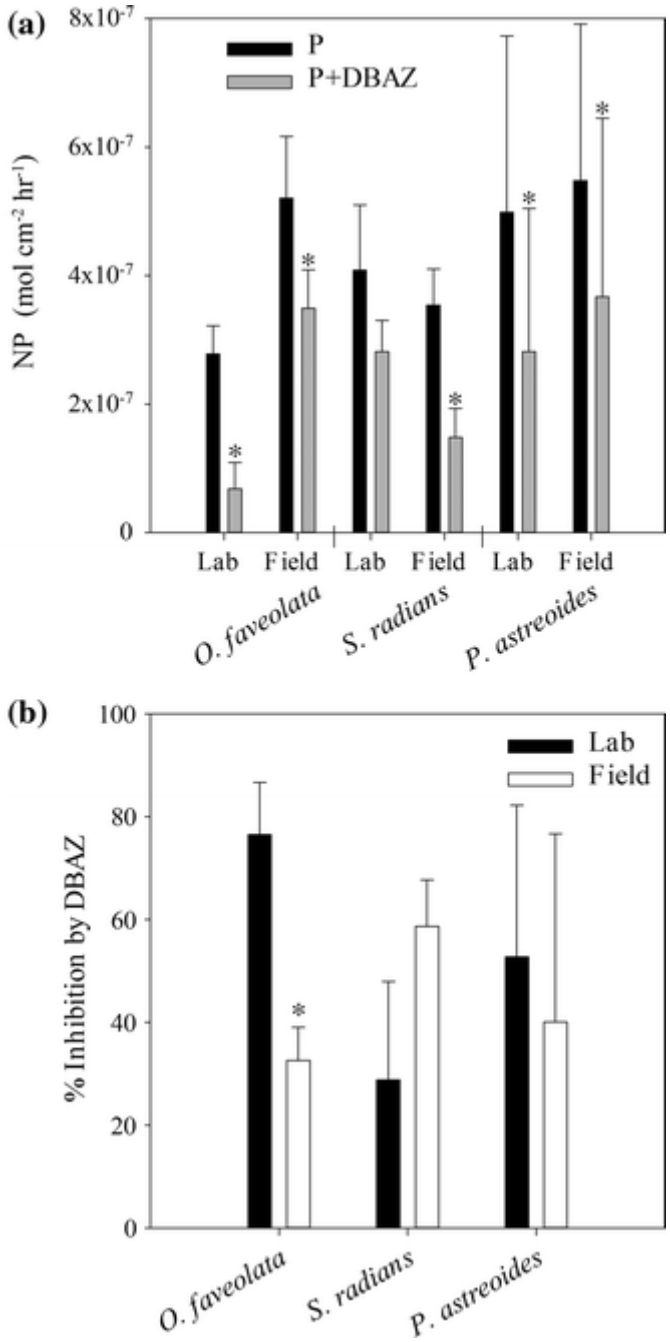

Figure 2.5: The effect of DBAZ on net photosynthesis. (a) Net photosynthetic rates based on O_2 production before (P) and after (P+DBAZ) the addition of DBAZ. Error bars represent ±1 SD and asterisks indicate a significant difference ($p < 0.05$) between rates with and without DBAZ as determined using a paired t-test (n = 3-5). (b) The percent inhibition of net photosynthesis by DBAZ as calculated from the data presented in panel *a*. This is also a minimal estimate of the percent of inorganic carbon for net photosynthesis that comes from external CO_2. Error bars represent ±1 SD and asterisks indicate a significant difference (t-test; $p < 0.05$) between field and lab specimens.

CHAPTER 3

INORGANIC CARBON IS SCARCE FOR SYMBIONTS IN SCLERACTINIAN CORAL[2]

[2] Tansik, A. L., W. K. Fitt, and B. M. Hopkinson. 2017. Inorganic carbon is scarce for symbionts in scleractinian corals. *Limnology and Oceanography*. doi: 10.1002/lno.10550. Reprinted here with permission of the publisher.

Abstract

Ocean acidification and changing sea surface temperatures stand to affect the interactions of corals and their *Symbiodinium* symbionts with regard to the inorganic carbon used for photosynthesis. However there have been few investigations on the availability of dissolved inorganic carbon (DIC) for algal symbionts in hospite. This study compared the DIC-associated photosynthetic kinetic parameters of three Caribbean corals and their freshly isolated symbionts, as well as components of the DIC concentrating systems of both corals and symbionts. Species level differences were found in the extent of inorganic carbon saturation among the coral taxa studied. Only *Orbicella faveolata* was photosynthesizing at maximum rates under current seawater conditions, while *Porites astreoides* and *Siderastrea radians* were at or below half DIC saturation. *O. faveolata* also had significantly more external carbonic anhydrase activity, indicating that this species could produce more CO_2 at the coral surface than *P. astreoides* or *S. radians*. In contrast and despite differences in *Symbiodinium* type, the symbionts of all the corals had a similar, very low DIC half saturation constant for photosynthesis and high levels of internal carbonic anhydrase activity, showing that they live in a carbon scarce environment and invest a great deal of energy in concentrating carbon at the site of photosynthesis. Considering the diffusional dynamics of the system and the relationship of host to symbiont kinetic parameters, the most likely cause of this scarcity is host regulation of DIC delivery to the symbionts.

Introduction

Scleractinian corals house symbiotic dinoflagellates of the genus *Symbiodinium* (zooxanthellae). These symbionts produce up to 90% of the coral's energy by transferring photosynthetic products to their hosts (Falkowski et al. 1984). In order to produce photosynthates, microalgae require inorganic carbon as a substrate for RuBisCO. With a low affinity type II RuBisCO, dinoflagellates require a higher concentration of CO_2 at the site of fixation than many other algae (Whitney et al. 1995). This is exacerbated for *Symbiodinium*, which live in the tissues of their hosts, and are therefore separated from the abundant dissolved inorganic carbon (DIC) in the external seawater. Corals have pathways to deliver DIC to their symbionts, and though the full details of DIC processing pathways have not been determined they include the ability to take up CO_2 and HCO_3^-, interconversion of CO_2 and HCO_3^- using carbonic anhydrases, and transport of DIC through various tissue layers (Weis 1989; Al-Moghrabi et al. 1996; Bertucci et al 2013; Tansik et al. 2015; Zoccola et al 2015). Similarly, *Symbiodinium* has a CO_2 concentrating mechanism (CCM) for the uptake and concentration of DIC employing carbonic anhydrases and active HCO_3^- transport (Al-Moghrabi et al. 1996; Leggat et al. 1999; Oakley et al. 2014).

Despite these adaptations, there is some disagreement over whether seawater DIC concentrations limit photosynthetic rates in corals. Several studies have indicated this kind of limitation (Muscatine et al. 1989; Herfort et al. 2008), while other studies showed DIC saturation of photosynthesis (Goiran et al. 1996; Buxton et al. 2009). The possibility that DIC limits photosynthetic rates is surprising given the adaptations of corals and *Symbiodinium* to acquire DIC, and the high concentrations of DIC in seawater compared to other potentially limiting nutrients. While DIC concentrations in seawater are high (~ 2 mM) and relatively constant, the

concentrations of other commonly limiting nutrients such as nitrogen and phosphorous are typically extremely low (< 1 μM) in the tropical, oligtrophic waters where corals are found (Szmant and Forrester 1996).

Since corals rely on their symbionts for a substantial portion of their nutritional needs, factors that control the rate of photosynthesis and biomass of *Symbiodinium* are critical to understanding the success of their coral hosts. Many different factors have been proposed to limit production and biomass of *Symbiodinium* in hospite. These include nitrogen (Muscatine et al. 1989; Dubinsky et al. 1990), carbon (Lesser et al. 1994; Goiran et al. 1996), phosphorous (Dubinsky et al. 1990; Jackson and Yellowlees 1990), light (Falkowski et al. 1984; Porter et al. 1984), temperature (Rowan 2004) and oxygen (Mass et al. 2010). Prevailing local environmental conditions will in part determine which factor is limiting; *Symbiodinium* in corals living at depth are far more likely to suffer from light limitation than those in shallow waters (Falkowski et al. 1984; Porter et al. 1984). Within the host, limitation of symbiont growth and production may occur via different mechanisms. In some cases, the symbionts may grow unrestricted by the host, until one of these nutrients becomes limiting (Hoadley et al. 2016). However, the coral host may also intentionally limit the availability of certain nutrients in order to control symbionts. For example, some have suggested that corals regulate the density of *Symbiodinium* within their tissues in part by controlling the availability of nitrogen (Falkowski et al. 1993). Controlling the flow of DIC to the *Symbiondinium* could prevent the sequestration of fixed carbon by the symbionts for their own growth, decoupling it from photosynthetic production and ensuring a steady, maximized transfer of photosynthates to the coral (Davy et al. 2012).

Given the potential for DIC availability to limit photosynthetic rates, we sought to characterize DIC availability by studying DIC acquisition simultaneously in coral holobionts and

freshly isolated symbionts. Such experiments have previously been done on coral holobionts of different taxa, with variable results (Goiran et al. 1996; Herfort et al. 2008; Buxton et al. 2009). Far rarer are studies that have looked at freshly isolated symbionts in relation to their hosts (Goiran et al. 1996). Information about the symbiosis needs to be garnered from these freshly isolated symbionts, as in hospite zooxanthellae behave and are morphologically and physiologically different than their cultured or free-living counterparts (Zahl and McLaughlin 1957; Goiran et al. 1996; Stochaj and Grossman 1997). This study serves to determine the kinetic parameters of photosynthesis related to external DIC concentrations and carbonic anhydrase activities for three species of scleractinian corals from the Caribbean to better characterize the availability of DIC to *Symbiodinium* in hospite and to assess the potential for DIC to limit photosynthetic rates. The taxa were chosen to cover a range of ecological niches: dominant reef-building species, reef-filler species and stress-tolerant, marginal habitat species.

Methods and materials

Coral collection and maintenance

Fragments of *Orbicella faveolata* and *Porites astreoides* were collected from Little Grecian Reef off Key Largo, Florida, USA. *O. faveolata* were collected from approximately 4 m depth, while *P. astreoides* were collected from 2 – 3 m. Small colonies of *Siderastrea radians* were collected at 1.5 - 2.5 m from Florida Bay in Key Largo, Florida, USA. Samples were taken in July 2013 and July 2014. All collections were done under permit (FKNMS-2011-093; FKNMS-2014-015), issued by the Florida Keys National Marine Sanctuary.

Specimens were maintained in a closed circulation, holding tank at the Key Largo Marine Research Laboratory. The natural seawater used in the holding tanks was collected from Little Grecian Reef. Exposed coral skeleton was covered by wax-based modeling clay before being

placed in the tank. Water temperature was held at 26° C, and salinity ranged from 35 – 38 ppt. The tank was exposed to the natural light regime; screening was added at midday to keep the maximum irradiance below 600 μmol photons m^{-2} s^{-1}. Colonies were allowed to recover for at least two days before testing. Fragment surface areas were measured using the aluminum foil method (Marsh 1970). Algal cell density was determined microscopically using a haemocytometer (Fitt et al. 2000). Algal cell ITS 2 type was identified using denaturing gradient gel electrophoresis according to LaJeunesse (2002). Each species was dominated by a single symbiont type; B1 in *O. faveolata*, A4a in *P. astreoides* and B5a in *S. radians*, consistent with the long term data set for these species (Thornhill et al. 2006a; Thornhill et al. 2006b).

Membrane Inlet Mass Spectrometry (MIMS)

All assays were conducted using a membrane inlet mass spectrophotometer (Pfeiffer PrismaPlus) to continuously and concurrently monitor all relevant dissolved gas species. The assay medium was DIC-free artificial seawater (ASW) buffered with 20mM Tris, and the pH adjusted to 8.03 ±0.03. All additions to testing chambers were made through a 1 mm injection port in the lid of the testing chamber.

Corals were placed in a clear acrylic, water jacketed chamber interfaced to the MIMS via a flow-through inlet. The internal volume of the chamber was adjustable from 35 – 50 ml in order to allow for a small assay volume and eliminate headspace, and the assay medium was continuously stirred at 1500 rpm. A fragment was added to the chamber, resting on a perforated stand with enough ASW to just cover the coral, and the lid screwed down to remove any headspace. The inlet functions by continuously removing water from the chamber at a rate of 560 μl min^{-1} using a peristaltic pump, passing it through a length of gas-permeable silicone tubing

under vacuum, and returning the ASW to the testing chamber. Dissolved gases diffuse across the silicone membrane and are measured by the mass spectrophototmeter.

Symbionts were isolated from coral fragments using an airbrush (Paasche, USA) and the assay medium. The blastate was homogenized and then centrifuged for 5 minutes at ~5,000 rpm. Symbiont pellets were resuspended in 1 ml ASW and centrifuged again for one minute. Samples were then resuspended in 1 ml ASW and 500 µl removed for symbiont identification. The remaining freshly isolated symbionts (FIS) were diluted with 500 µl ASW to 50% of the initial concentration. The diluted suspension was placed in a water jacketed chamber which interfaced directly to the MIMS. A Teflon membrane under vacuum at the base of the chamber allowed for dissolved gases to diffuse from the suspension for analysis in the mass spectrophotometer. The adjustable plunger in the lid of this chamber minimized headspace. A magnetic stir bar sitting just above the membrane kept the sample stirring at 400 rpm. All FIS assays were begun within 15 minutes of removal from the host.

Photosynthesis versus DIC assays (P vs. DIC)

Assays were conducted over two days, with whole coral fragments (whole coral) run the first day and their FIS run the next to minimize physiological changes associated with being in the holding tank. During the runs, O_2 production and $^{13}CO_2$ were monitored via the MIMS.

Both whole corals and FIS were exposed to a sequence of nine alternating light and dark periods. An initial light period preceded any DIC additions and photosynthesis was allowed to proceed, drawing down residual DIC in the assay buffer, until no net oxygen production was observed. For the whole corals, O_2 concentrations leveled off, indicating that any ongoing O_2 production was the result of internal carbon recycling, rather than new DIC fixation. FIS began to draw down O_2 in the chamber, showing that there was not enough DIC available to support net

photosynthesis. This initial light phase ensured that the subsequent additions of labeled DIC to the chamber gave an accurate reflection of the total DIC concentration in the chamber.

Light levels were saturating for whole coral photosynthesis without causing photoinhibition, as confirmed by photosynthesis vs irradiance curves (data not shown). All whole coral assays were conducted at 1000 μmol photons m^{-2} s^{-1} in Summer 2013. *O. faveolata* and *P. astreoides* assays were done at the same light level in Summer 2014. *S. radians* were collected from deeper (2.5 m) waters in July 2014. As a result, assays on this species were conducted at a lower irradiance of 600 μmol photons m^{-2} s^{-1} in Summer 2014. FIS assays both years were conducted at an average of 350 μmol photons m^{-2} s^{-1}. This light level was shown to be saturating without causing photoinhibition with trials at both higher and lower irradiance levels (data not shown).

Aliquots of $H^{13}CO_3^-$ were added to the chamber during the dark phases. The light was turned on only after the $^{13}CO_2$ signal had stabilized. Small additions were made early in the assay, and progressively increased in volume. This ensured a final concentration at or above current seawater DIC concentrations (~2 mM) across the eight additions. Adjustments in DIC additions for the whole corals were made between the two field seasons in order to ensure the full saturation of the curve.

Carbonic anhydrase assays

Determination of external carbonic anhydrase (eCA) activity was done with the same methods as Tansik et al. 2015. Briefly, the rate of ^{18}O exchange was measured on the MIMS by following labeled $^{13}CO_2$ species. The background hydration-dehydration rate of the CO_2-HCO_3^- equilibrium was determined by monitoring ^{18}O removal from the labeled CO_2 species in the assay medium for 15 minutes. Coral colonies were then placed in the chamber in the dark to

prevent any light-associated transport of DIC, and exchange rates recorded for 10 minutes. The membrane impermeable CA inhibitor dextran-bound acetazolamide (AZ) was added to the chamber to a total concentration of 100 μM and exchange rates recorded for another ten minutes. The corals were then placed in a lit, aerated recovery chamber for at least 45 minutes before being returned to the holding tank.

Internal CA activity was determined for FIS as described in Hopkinson et al. 2011. Coral tissue was separated from the skeleton using an airbrush. The resulting slurry was centrifuged to separate symbionts and the animal fraction. Isotope exchange assays were then run on the symbionts using MIMS. After determining the background exchange rate, either the animal tissue fraction or the FIS were added to the chamber and changes to the rate of ^{18}O exchange were monitored. AZ was added to the chamber at a concentration of 10 μM after 10 minutes in the homogenate assays to ensure that the measured changes came from CA activity. The inhibitor was added before the FIS in the other assay to prevent any contamination by any residual animal CAs. The measured response was therefore due to internal CA (iCA) activity in the symbionts.

Data Analysis

Analysis of the data was done using custom scripts in MATLAB (MathWorks). For the P vs. DIC assays, the photosynthetic and respiratory O_2 data were normalized to surface area for whole corals, and per cell for FIS. These data were then fitted with linear regressions for each light and dark phase to determine O_2 production (or consumption) rates. A Michaelis-Menten curve was fitted to the light phase O_2 production rates, and the half-saturation constant (K_m) and maximum net photosynthetic rate (P_{max}) for DIC determined from this fit. For the whole coral

assays, an offset had to be added to account for animal respiration. This allowed proper fitting of the Michaelis-Menten curve, and was removed from P_{max} to give net photosynthetic values.

Activity rates of CA were determined using reaction-diffusion models. For a full description of the model equations and development, refer to Hopkinson et al. 2011 (iCA of algal symbionts) and Tansik et al. 2015 (eCA of coral). MATLAB codes for both models are available for download on the Hopkinson Laboratory website, or by contacting the authors.

As there were no significant differences between the two years within a species (t-test, $p > 0.05$), results for each species were averaged across summers.

Results

Whole coral fragments

P vs. DIC assays on the three coral species tested showed them to have variable adaptation to the external DIC environment. With knowledge of the surrounding carbon environment, K_m for DIC can provide an index of whether an organism is carbon saturated for photosynthesis under ambient conditions. A low K_m value relative to ambient DIC concentrations indicates that an organism is DIC sufficient in its natural environment. Alternatively, a high K_m value suggests that photosynthesis is not naturally carbon saturated, and additional carbon would increase this rate. Of the three coral taxa tested, only *O. faveolata* had a K_m for DIC below that of average seawater concentrations (Fig. 3.1A). In comparison, the K_m values of *P. astreoides* and *S. radians* were significantly higher, above or at current oceanic DIC concentrations (Fig. 3.1A; t-test, $p < 0.05$).

The other kinetic variable obtained from the Michaelis-Menten fits is P_{max}, the maximum production rate. High net P_{max} values, as given by higher O_2 production, mean that the organism is most likely fixing more carbon, giving it elevated energy resources in comparison with those

that photosynthesize at lower rates. In this set of experiments, the trend in the P_{max} values mirrored the K_m values. *P. astreoides* had the highest rate of maximum photosynthesis across these two summers (Fig. 3.1B). This was significantly higher than the P_{max} of measured in *O. faveolata* (Fig. 3.1B, t-test, $p < 0.05$). While *S. radians* fell between the other two taxa, there were no significant differences between maximum rates of photosynthesis in it and either of the other species (Fig. 3.1B, t-test, $p > 0.05$).

eCA activity also differed significantly between the coral taxa. This enzyme is an integral part of a DIC processing system of the coral animal (Weis et al. 1989; Bertucci et al. 2013; Tansik et al. 2015). While all three taxa had high levels of eCA activity, *O. faveolata* had the greatest eCA activity of the three taxa (Fig. 3.1C). Such activity allows this taxa to produce the most CO_2 at the coral surface. This was significantly higher than either *P. astreoides* or *S. radians* (Fig. 3.1C, t-test, $p < 0.05$).

Freshly isolated symbionts

Without the knowledge of the external DIC environment the symbionts face in hospite, the K_m values from the P vs. DIC assays give an indication of what kind of carbon environment the FIS are adapted or acclimated to. Low half-saturation constants indicate that an organism has the capacity to maximize its photosynthesis with very little DIC, a characteristic of organisms living in a carbon scarce environment (Rost et al. 2003; Oakley et al. 2014). These assays showed that all the symbionts had low mean K_m values ($6.65 \times 10^{-5} – 2.35 \times 10^{-4}$ mol DIC) which were not significantly different from each other (Fig. 3.2A, t-test, $p > 0.05$), despite each coral hosting a different *Symbiodinium* type. These half-saturation constants were well below those of their respective coral hosts (Fig. 3.3). FIS from *S. radians* had the lowest K_m, two orders

of magnitude below that of the whole coral (Fig. 3.2A). Even the FIS of the carbon sufficient *O. faveolata* had a K_m less than a third that of the coral (Fig. 3.3A).

Despite similarities in the carbon affinity of the FIS, there was greater variability between the P_{max} rates of the symbionts. The values followed the same trend as those of the whole corals; *P. astreoides* symbionts had the highest maximum photosynthetic rate, followed by *S. radians* FIS, while symbionts from *O. faveolata* had the lowest P_{max} (Fig. 3.2B). High variability among the replicates meant that the P_{max} rate of *P. astreoides* FIS was not significantly different from either taxa, despite the difference in the mean value with *O. faveolata* FIS (Fig. 3.2B, t-test, $p > 0.05$). Symbiont P_{max} values were, however, significantly different between *S. radians* and *O. faveolata* (Fig. 2B, t-test, $p < 0.05$). All the FIS achieved maximal photosynthesis well below the DIC concentration of seawater (~2 mM).

Internal CAs are key components of algal carbon concentrating mechanisms (Badger 2003). All three FIS taxa tested here had high iCA activity rates (Fig. 3.2C). FIS from *P. astreoides* and *S. radians* had significantly higher iCA activity than the symbionts from *O. faveolata* (Fig. 3.2C, t-test, $p < 0.05$).

Discussion

Previous work assessing the potential for DIC limitation of photosynthesis in corals has resulted in conflicting findings, with some studies reporting evidence for DIC limitation (Muscatine et al. 1989; Herfort et al. 2008) and others finding that photosynthesis is saturated for DIC (Goiran et al. 1996; Buxton et al. 2009). The studies in which DIC limitation was tested directly used varying protocols and specimens collected from diverse locations leaving open the possibility that the differing results obtained were due to differences in the local environments or assay procedures, rather than differences in the physiology of the study species. Here, we tested

multiple coral species including two from the same environment (*O. faveolata, P. astreoides*) using a common assay protocol and also found differences in the effect of short-term increases in DIC on photosynthesis. In two species (*P. asteroides, S. radians*), photosynthetic rates increased substantially when DIC was increased above seawater concentrations, while in the other species (*O. faveolata*) photosynthetic rates were saturated at seawater DIC concentrations. Taken in combination with previous work, our results indicate that DIC limitation of photosynthesis is species-specific and may not be simply an environmental limitation.

DIC limitation of photosynthesis

Given the high concentration of DIC in seawater (~ 2 mM) compared to other potentially limiting nutrients (e.g. N, P), DIC limitation of photosynthetic rates seems surprising. On the other hand, though *Symbiodinium* density is typically N-limited in hospite, the algae transfer N-poor photosynthates to their host (Falkowski et al. 1984; Yellowlees et al. 2008; Burriesci et al. 2012; Kopp et al. 2015), giving DIC availability increased importance over other nutrients for maintaining high rates of photosynthesis. Additionally, algal cell densities are very high, being concentrated into the upper layer of coral tissue and sequestered within coral cells meaning there must be a high rate of DIC delivery to support photosynthesis. Delivery of inorganic carbon from seawater to RubisCO to support net photosynthesis can conceptually be broken down into several steps: 1) diffusion of DIC through the boundary layer to the coral surface, 2) uptake across the coral membrane, 3) transport to the algal cells, and 4) uptake and processing by the algal cells. Below we consider each of these steps and the likelihood that it limits photosynthetic rates.

The thick diffusive boundary layer (DBL) that surrounds corals is known to limit the flux of nutrients (Bilger and Atkinson 1992), O_2 (Mass et al. 2010), and inorganic carbon (Lesser et

al. 1994; Tansik et al. 2015) into and out of the coral animal in some situations. The DBL thickness is dependent on fluid flow characteristics and the animal shape, but in corals is typically between 0.2 – 1.0 mm (Kühl et al. 1995). DBLs in this range severely limit the flux of CO_2 from seawater to the coral such that maximal CO_2 fluxes are only a few percent of observed photosynthetic rates (Tansik et al. 2015). However, corals are also able to access HCO_3^- for photosynthesis (Goiran et al. 1996; Tansik et al 2015), which is present at much higher concentrations in seawater (~1.8 mM) than CO_2 (~ 10 μM). In the well-stirred chamber used in our experiments the DBL thickness should be on the lower end and maximal fluxes of HCO_3^- to the coral are approximately an order of magnitude higher than observed photosynthetic rates at any DIC concentration, showing that diffusional fluxes to the coral surface do not limit photosynthetic rates (Tansik et al. 2015).

Since diffusional fluxes of DIC do not limit photosynthetic rates under our experimental conditions, it is possible that the DIC uptake systems of either the corals or symbionts have a low affinity for DIC leading to the observed limitation. This possibility can be easily ruled out for the symbionts. *Symbiodinium* from all the coral species have a high affinity (low K_m) for DIC, with K_ms in the 100-300 μM range, consistent with previous work on cultured strains (Buxton et al. 2009; Oakley et al. 2014) and a single study on freshly isolated *Symbiodinium* (Goiran et al. 1996). As these K_m values are far lower than those of their hosts, the symbionts appear to have a much higher affinity than their hosts, maximizing their production in hospite with very little carbon. This data agrees with the only other comparison between intact coral colonies and their freshly isolated symbionts (Goiran et al. 1996). With a lower DIC affinity (higher K_m), the potential for the limitation to be coming from the host side is greater. Additionally, the high iCA activities seen in the FIS are indicative of active carbon concentrating mechanisms (Leggat et al.

1999; Brading et al. 2013; Fig. 3.4). In the cytoplasm they reduce CO_2 diffusion back out of the cell by accelerating CO_2 hydration to HCO_3^- while working to maintain the CO_2 concentration gradient across the membrane (Hopkinson et al. 2016), while the reverse reaction will concentrate CO_2 around RuBisCO, making fixation more efficient (Leggat et al. 1999; Yellowlees et al. 2008). Having an active carbon concentrating mechanism signals that the FIS are living in carbon poor environment where they are adapted to taking up all the DIC made available to them (Fig. 3.4). More evidence for this comes from the presence of a host derived H^+-ATPase on the symbiosome membrane, which acidifies the lumen and subsequently results in CO_2 being the dominant DIC species around the symbionts (Barott et al. 2015). The symbionts would therefore be surrounded by DIC readily available for photosynthesis, yet still have a low K_m and an active carbon concentrating mechanism, again suggesting that the corals are the source of limitation.

Our experiments do not independently assess the performance of the coral DIC uptake system, but the case of *O. faveolata* demonstrates that it is possible for a coral DIC uptake system to create an environment around the symbionts which will saturate photosynthetic rates well below seawater DIC concentrations (Fig. 3.4A). One element of this is the high eCA activity at the surface of the coral helping to overcome depletion of CO_2 at the surface by accelerating the dehydration of HCO_3^- to provide more CO_2 at the surface of the coral for subsequent uptake (Tansik et al. 2015; Fig. 3.4). This is further supported by the presence of SLC4 and SLC26-type HCO_3^- transporters that corals likely employ for HCO_3^- uptake (Zoccola et al. 2015; Fig. 3.4), which typically have K_ms < 200 μM (Knauf et al. 2002; Price et al. 2004). These transporters would, therefore, be fully saturated and providing a steady influx of HCO_3^- into the corals. The corals also have high iCA activity within their tissues, helping to maintain

the CO_2 gradient across the coral membrane, as well as providing CO_2 for symbiont photosynthesis (Hopkinson et al. 2015; Fig. 3.4). More generally, uptake systems of organisms adapted to oligotrophic environments are typically capable of working at very low substrate concentrations and taking up substances so rapidly that diffusion through the boundary layer limits uptake, as has been observed in some cases for corals (Patterson et al. 1992; Lesser et al. 1994). It would consequently be unusual for deficiencies in the uptake or supply pathway to limit downstream reactions (here photosynthesis) in a case when the substrate is highly abundant in the environment. However, it is possible that the two coral species showing DIC limitation of photosynthesis (*P. astreoides, S. radians*; Fig. 3.4B) simply do not have a sufficiently high affinity DIC uptake system to saturate the photosynthesis of concentrated symbionts at a distance from the surface of the coral.

An alternate hypothesis which explains the trends seen in all three studied taxa is that the coral hosts intentionally limit DIC supply to the symbionts in order to control photosynthesis. That is, the observed "DIC limitation" may not be an environmental limitation on photosynthetic rates but rather a host control on photosynthesis. Several lines of evidence support this hypothesis. First, in all corals tested the K_m of photosynthesis for DIC is much lower for *Symbiodinium* than for the holobiont, which implies that DIC availability to *Symbiodinium* in hospite is lower than in the surrounding seawater (Fig. 3.4). Second, the iCA activity of *Symbiodinium* is extremely high again indicating that DIC availability in hospite is low, requiring full mobilization of the algal CCM. Third, even with eCA activity sufficient to maintain CO_2 near equilibrium (~10 μM) at the surface of the coral (Tansik et al. 2015), calculations of CO_2 diffusion through the coenosarc and theca tissues (25 μm and 55 μm, respectively [Gattuso et al. 1999; Allemand et al. 2004; Marshall et al. 2007]) show a supply

averaging only 15.6% (range 6.82 – 27.5%) of what is needed to maintain maximum rates of photosynthesis. This means that the host must actively supply DIC to their symbionts to reach maximum photosynthesis, and provides the host an opportunity to regulate its delivery. Finally, despite the fact that the coral has sophisticated DIC delivery pathways, which in some species are capable of saturating symbiont photosynthesis, that the DIC availability to the symbiont in hospite is low argues that the limitation is intentionally imposed. Definitively determining whether the observed DIC limitation is intentionally imposed by the host or an unregulated environmental control on the coral will require further experimentation. For example experiments in which DIC supply (DIC concentration, pH, etc.) and demand (light intensity, temperature) are independently manipulated to determine how the host and algal DIC processing respond could help resolve the driver of the limitation.

Taxa specific DIC processing

The photosynthetic parameter values, in combination with the CA activity rates, paint an interesting picture with regard to carbon sufficiency among the studied taxa (Fig. 3.4). Adapted to increase carbon uptake, and with less DIC required to support its lower rate of net photosynthesis, *O. faveolata* will reach P_{max} at lower external DIC concentrations, making it more likely to be carbon saturated in its environment. The potential carbon limitation of *P. astreoides* and *S. radians*, on the other hand, could be caused by their lesser ability to produce CO_2 at the coral surface in combination with a greater carbon demand for support of higher maximum rates of net photosynthesis. This would mean that these corals likely require more DIC in the external environment to support their needs.

Much of the basis for photosynthetic production in corals is centered in the physiology of the *Symbiondinium*. The coral taxa studied here have different symbiont genotypes; past studies

have shown differences in the physiology among the various genotypes of *Symbiodinium* across a broad spectrum of parameters, including thermal tolerance, nitrate uptake, photosynthetic rate, photoacclimation, respiration, hydrogen peroxide and nitrous oxide production, eCA activity and growth rate (Rowan 2004; Robison and Warner 2006; Suggett et al. 2008; Hawkins and Davy 2012; Brading et al. 2013; Baker et al. 2013; Oakley et al. 2014; this study). This would imply that the observed differences between the coral taxa may stem from the carbon affinity of their symbionts. However, our results suggest otherwise, as the K_m values of all the *Symbiondinium* are similar and low, showing that they have the same high affinity for DIC in hospite. This supports the suggestion that the coral animal plays a substantial role in determining photosynthetic production, and that the studied species do so differently.

Such taxa specific differences have been seen before. Previous studies have shown carbon saturation at seawater concentrations in *Galaxea fasicularis* and *Pocillopora damicornis* (Goiran et al. 1996; Buxton et al. 2009). In contrast, Herfort et al. (2008) saw enhanced photosynthetic O_2 production in *Acropora* sp. and *Porites porites* with HCO_3^- additions above average DIC concentrations. However, seeing this variation within the same study and on corals collected from the same location (*O. faveolata* and *P. astreoides*; Fig. 4) is new, and raises questions about how DIC limitation might affect the role a species plays on the reef. The ability of *O. faveolata* to saturate photosynthesis in its symbionts could lead to greater productivity in this species, allowing for increased growth and calcification, as higher rates of photosynthesis have been linked to increased translocation of carbon from the symbionts under normal seawater conditions (Tremblay et al. 2012; Tremblay et al. 2014). This may help explain why this coral is a major reef builder in the Florida Keys, the Bahamas and the Caribbean Sea. In contrast, at ambient seawater conditions *P. astreoides* seemingly has more carbon limited production, which

may restrict its growth and extension rates, contributing to its role as a filler species that does little to add to the structure of the reef. Further examination of the productivity of these species is needed to fully understand how photosynthetic DIC saturation links to their overall carbon and energy budgets.

Implications in a changing ocean

The changing conditions of the ocean have the potential to impact, among many other processes in corals, DIC flow to *Symbiodinium*. Increasing concentrations of CO_2 in the ocean (ocean acidification; OA) have the potential to alter multiple parts of the inorganic carbon uptake and concentration systems in both host and symbiont. Diffusive fluxes of CO_2 from the seawater, driven by concentration gradients across the coral membrane, should increase. More CO_2 would, therefore, be reaching the symbionts without direct intervention of the host, reducing the need for eCA to produce CO_2 at the coral surface and HCO_3^- to be transported to support photosynthesis. With increased CO_2, the symbionts could also downregulate their CA expression, alter DIC uptake systems and/or lower their carbon affinity (Brading et al. 2013; Trimborn et al. 2013; Eberlein et al. 2014). In at least some taxa, OA related increases in CO_2 and HCO_3^- have the potential to increase observed photosynthetic rates and translocation to the benefit of the holobiont (Herfort et al. 2008; Tremblay et al. 2013; this study). The energy savings related to these changes in carbon uptake and concentration could then be redistributed elsewhere in the host and symbiont to support other physiological processes.

While increased CO_2 may benefit *Symbiodinium* or at least not cause direct harm, sea surface temperatures are projected to continue rising, leading to more instances of *Symbiodinium* being expelled from the coral (Warner et al. 1996; IPCC 2013; van Hooidonk et al. 2013). This would, of course, also reduce the investment in DIC uptake and concentration in corals as they

have to supply carbon to fewer symbionts, and potentially in *Symbiodinium* as there is less competition for the DIC that is available. In this case, however, the energetic savings are unlikely to have as beneficial a response, as photosynthetic production declines with the population of symbionts. While the work presented here does not address either OA or elevated sea surface temperatures, it provides an important point of comparison for future work to evaluate changes caused by them.

Conclusion

The relationship between corals and their algal symbionts is founded on the exchange of carbon, and the supply of DIC to the *Symbiodinium* provides a potential path for regulation of the symbiosis. In comparing the DIC parameters of photosynthesis for the coral and the FIS, we show that photosynthesis is often carbon limited in *Symbiodinium* in hospite. This limitation is consistent across the studied taxa, even though the corals themselves showed striking differences in their DIC saturation under normal seawater conditions. We propose that our results suggest inorganic carbon supply to the symbionts is generally host-controlled, and differences between taxa, colonies and/or habitats may lead to variable responses to changing seawater conditions. The results reported here for three coral taxa provide a strong point of comparison for evaluating how the symbiosis may alter with regard to DIC supply under climate change scenarios.

Acknowledgements

This study was funded by grants from the National Science Foundation (EF 1315944) and the Alfred P. Sloan Foundation. Corals were collected under permits in the Florida Keys National Marine Sanctuary (Permits 2011-093 and 2014-15).

References

Allemand, D., and others. 2004. Biomineralization in reef-building corals: from molecular mechanisms to environmental control. C. R. Palevol 3: 453-467.

Al-Moghrabi, S., C. Goiran, D. Allemand, N. Speziale, and J. Jaubert. 1996. Inorganic carbon uptake for photosynthesisby the symbiotic coral-dinoflagellate association II. Mechanisms for bicarbonate uptake. J. Exp. Mar. Biol. Ecol. 199: 227-248.

Badger, M. 2003. The roles of carbonic anhydrases in photosynthetic CO_2 concentrating mechanisms. Photosyn. Res. 77: 83- 94.

Baker, D. M., J. P. Andras, A. G. Jordán-Garza, and M. L. Fogel. 2013. Nitrate competition in a coral symbiosis varies with temperature among *Symbiodinium* clades. ISME J. 2013(7): 1248-1251.

Barott, K. L., A. A. Venn, S. O. Perez, S. Tambutté, and M. Tresguerres. 2015. Coral host cells acidify symbiotic algal microenvironment to promote photosynthesis. PNAS 112(2): 607-612.

Bertucci, A., A. Moya, S. Tambutte, D. Allemand, C. T. Supuran, and D. Zoccola. 2013. Carbonic anhydrases in anthozoan corals – a review. Bioorg. Med. Chem. 21: 1437-1450.

Bilger, R. W., and M. J. Atkinson. 1992. Anomalous mass transfer of phosphate on coral reef flats. Limnol. Oceanogr. 37(2): 264-272.

Brading, P., M. E. Warner, D. J. Smith, and D. J. Sugget. 2013. Contrasting modes of inorganic carbon acquisition amongst *Symbiodinium* (Dinophyceae) phylotypes. New Phytol. 200: 432-442.

Burriesci, M. S., T. K. Raab, and J. R. Pringle. 2012. Evidence that glucose is the major transferred metabolite in dinoflagellate-cnidarian symbiosis. J. Exp. Bio. 215: 3467-3477.

Buxton, L., M. Badger, and P. Ralph. 2009. Effects of moderate heat stress and dissolved inorganic carbon concentration on photosynthesis and respiration of *Symbiodinium* sp. (Dinophyceae) in culture and in symbiosis. J. Phycol. 45: 357-365.

Davy, S. K., D. Allemand and V. M. Weis. 2012. Cell Biology of Cnidarian-Dinoflagellate Symbiosis. Microbiol. Mol. Bio. Rev. 76(2): 229-261.

Dubinsky, Z., N. Stambler, M. Ben-Zion, L. R. McCloskey, L. Muscatine, and P. G. Falkowski. 1990. The effect of external nutrient resources on the optical properties and photosynthetic efficiency of *Stylophora pistillata*. Proc. R. Soc. B 239(1295): 231-246.

Eberlein, T., D. B. Van de Waal, and B. Rost. 2014. Differential effects of ocean acidification on carbon acquisition in two bloom-forming dinoflagellate species. Physiol. Plant. 151: 468-479.

Falkowski, P. G., Z. Dubinsky, L. Muscatine, and J. W. Porter. 1984. Light and the Bioenergetics of a Symbiotic Coral. BioScience 34(11): 705-709.

Falkowski, P. G., Z. Dubinsky, L. Muscatine, and L. McCloskey. 1993. Population control in symbiotic corals. BioScience 43(9): 606-611.

Fitt, W. K., F. K. McFarland, M. E. Warner, and G. C. Chilcoat. 2000. Seasonal patterns of tissue biomass and densities of symbiotic dinoflagellates in reef corals and relation to coral bleaching. Limnol. Oceanogr. 45: 677-685.

Gattuso, J. P., D. Allemand, and M. Frankignoulle. 1999. Photosynthesis and calcification at cellular, organismal and community levels in coral reefs: a reciew on interactions and control by carbonate chemistry. Amer. Zool. 39: 160-183.

Goiran, C., S. Al-Moghrabi, D. Allemand, and J. Jaubert. 1996. Inorganic carbon uptake by the symbiotic coral/dinoflagellate association I. Photosynthetic performances of symbionts and dependence on sea water bicarbonate. J. Exp. Mar. Biol. Ecol. 199: 207-225.

Hawkins, T. D., and S. K. Davy. 2012. Nitric oxide production and tolerance differ among *Symbiodinium* types exposed to heat stress. Plant Cell Physiol. 53(11): 1889-1898.

Herfort, L., B. Thake, and I. Taubner. 2008. Bicarbonate stimulation of calcification and photosynthesis in two hermatypic corals. J. Phycol. 44: 91-98.

Hoadley, K.D. , D. T. Pettay, D. Dodge, and M. E. Warner. 2016. Contrasting physiological plasticity in response to environmental stress within different cnidarians and their respective symbionts. Coral Reefs 35: 529-542.

Hopkinson, B. M., C. L. Dupont, A. E. Allen, and F. M. M. Morel. 2011. Efficiency of the CO_2-concentrating mechanism of diatoms. PNAS 108(10): 3830-3837.

Hopkinson B. M. C. L. Dupont, and Y. Matsuda. 2016. The physiology and genetics of CO_2 concentrating mechanisms in model diatoms. Curr Opin Plant Biol 31: 51-57.

Hopkinson, B. M., A. L. Tansik, and W. K. Fitt. 2015. Internal carbonic anhydrase activity in the tissue of scleractinian corals is sufficient to support proposed roles in photosynthesis and calcification. J. Exp. Biol. 218(13): 2039-2048.

IPCC. 2013: Summary for Policymakers. In: Climate Change 2013: The Physical Science Basis. Contribution of Working Group I to the Fifth Assessment Report of the Intergovernmental Panel on Climate Change [Stocker, T.F., D. Qin, G.-K. Plattner, M.

Tignor, S.K. Allen, J. Boschung, A. Nauels, Y. Xia, V. Bex and P.M. Midgley (eds.)]. Cambridge University Press, Cambridge, United Kingdom and New York, NY, USA

Jackson, A. E., and D. Yellowlees. 1990. Phosphate-uptake by zooxanthellae isolated from corals. Proc. R. Soc. B 242(1305): 201-204.

Kopp, C., I. Domart-Coulon, S. Escrig, B. M. Humbel, M. Hignette, and A. Meibom. 2015. Subcellular Investigation of Photosynthesis-Driven Carbon Assimilation in the Symbiotic Reef Coral *Pocillopora damicornis*. mBio doi:10.1128/mBio.02299-14.

Knauf, P. A., F. Y. Law, T. W. V. Leung, A. U. Gehret, and M. L. Perez. 2002. Substrate-dependent reversal of anion transport site orientation in the human red blood cell anion-exchange protein, AE1. PNAS 99:10861–10864.

Kühl, M., Y. Cohen, T. Dalsgaard, B. B. Jørgensen, and N. P. Revsbach. 1995. Microenvironment and photosynthesis of zooxanthellae in scleractinian corals studied with microsensors for O_2, pH and light. Mar. Ecol. Prog. Ser. 117: 159-172.

LaJeunesse, T. C. 2002. Diversity and community structure of symbiotic dinoflagellates from Caribbean reef corals. Mar. Biol. 141: 387-400.

Leggat, W., M. R. Badger, and D. Yellowlees. 1999. Evidence for an inorganic carbon-concentrating mechanism in the symbiotic dinoflagellate *Symbiodinium* sp. Plant Physiol. 121: 1247-1255.

Lesser, M. P., V. M. Weis, M. R. Patterson, and P. L. Jokiel. 1994. Effect of morphology and water motion on carbon delivery and productivity in the reef coral, *Pocillopora damicornis* (Linnaeus) – Diffusion barriers, inorganic carbon limitation, and biochemical plasticity. J. Exp. Mar. Biol. Ecol. 178(2): 153-179.

Marsh, J. A. 1970. Primary productivity of reef-building calcareous red algae. Ecology 51: 255-263.

Marshall, A. T., P. L. Clode, R. Russell, K. Prince, and R. Stern. 2007. Electron and ion microprobe analysis of calcium distribution and transport in coral tissues. J. Exp. Biol. 201: 2453-2463.

Mass, T., A. Genin, U. Shavit, M. Grinstein, and D. Tchernov. 2010. Flow enhances photosynthesis in marine benthic autotrophs by increasing the efflux of oxygen from the organism to the water. PNAS 107(6): 2527-2531.

Muscatine, L., P. G. Falkowski, Z. Dubinsky, P. A. Cook, and L. R. McCloskey. 1989. The effect of external nutrient resources on the population dynamics of zooxanthellae in a reef coral. Proc. R. Soc. B 236(1284): 311-324.

Oakley, C. A., G. W. Schmidt, and B. M. Hopkinson. 2014. Thermal responses of *Symbiodinium* photosynthetic carbon assimilation. Coral Reefs 33(2): 501-512.

Patterson M.R. 1992. A chemical engineering view of cnidarian symbioses. American Zoologist 32: 566-582.

Porter, J. W., L. Muscatine, Z. Dubinsky, and P. G. Falkowski. 1984. Primary production and photoadaptation in light- and shade-adapted colonies of the symbiotic coral, *Stylophora pistillata*. Proc. R. Soc. B 222(1227): 161-180.

Price G. D., F. J. Woodger, M. R. Badger, S. M. Howitt, and L. Tucker. 2004. Identification of a SulP-type bicarbonate transporter in marine cyanobacteria. PNAS 101: 18228–18233.

Rost, B., U. Riebesell, S. Burkhardt, and D. Sultemeyer. 2003. Carbon acquisition of bloom-forming marine phytoplankton. Limnol. Oceanogr. 48: 55-67.

Rowan, R. 2004. Coral bleaching – Thermal adaptation in reed coral symbionts. Nature 430(7001): 742.

Robison, J. D., and M. E. Warner. 2006. Differential impacts of photoacclimation and thermal stress on the photobiology of four different phylotypes of *Symbioninium* (Pyrrhophyta). J. Phycol. 42(3): 568-579.

Stochaj, W. R. and A. R. Grossman. 1997. Differences in the protein profiles of cultured and endosymbiotic *Symbiodinium* sp. (Pyrrophyta) from the anemone *Aiptasia pallida* (Anthozoa). J. Phycol. 33(1): 44-53.

Suggett, D. J., M. E. Warner, D. J. Smith, P. Davey, S. Hennige, and N. R. Baker. 2008. Photosynthesis and production of hydrogen peroxide by *Symbiodinium* (Pyrrhophyta) phylotypes with different thermal tolerances. J. Phycol. 44(4): 948-956.

Szmant, A. M., and A. Forrester. 1996. Water column and sediment nitrogen and phosphorus distribution patterns in the Florida Keys, USA. Coral Reefs 15(1): 21-41.

Tansik, A. L., W. K. Fitt, and B. M. Hopkinson. 2015. External carbonic anhydrase in three Caribbean corals: quantification of activity and role in CO_2 uptake. Coral Reefs 34:703-713. doi: 10.1007/s00338-015-1289-8

Thornhill, D. J., T. C. LaJeunesse, D. W. Kemp, W. K. Fitt, and G. W. Schmidt. 2006a. Multi-year, seasonal genotypic surveys of coral-algal symbioses reveal prevalent stability or post-bleaching reversion. Mar. Biol. 148(4): 711-722.

Thornhill, D. J., W. K. Fitt, and G. W. Schmidt. 2006b. Highly stable symbioses among western Atlantic brooding corals. Coral Reefs 25(4): 515-519.

Tremblay, P., C. Ferrier-Pagès, J. F. Maguer, C. Rottier, L. Legendre, and R. Grover. 2012. Controlling effects of irradiance and heterotrophy on carbon translocation in the temperate coral *Cladocora caespitosa*. PLoS ONE 7(9): e44672. doi: 10.1371/journal.pone.0044672

Tremblay, P., R. Grover, J.F. Maguer, L. Legendre, and C. Ferrier-Pagès. 2013. Photosynthate translocation increases in response to low seawater pH in a coral-dinoflagellate symbiosis. Biogeosciences 10: 3997-4007.

Tremblay, P., R. Grover, J. F. Maguer, M. Hoogenboom, and C. Ferrier-Pagès. 2014. Carbon translocation from symbiont to host depends on irradiance and food availability in the tropical coral *Stylophora pistillata*. Coral Reefs 33: 1-13.

Trimborn, S., T. Brenneis, E. Sweet, and B. Rost. 2013. Sensitivity of Antarctic phytoplankton species to ocean acidification: Growth, carbon acquisition, and species interaction. Limnol. Oceanogr. 58(3): 997-1007. doi: 10.4319/lo.2013.58.3.0997

van Hooidonk, R., J. A. Maynard, and S. Planes. 2013. Temporary refugia for coral reefs in a warming world. Nat. Clim. Change 3: 508-511. doi: 10.1038/nclimate1829

Warner, M. E., W. K. Fitt, and G. W. Schmidt. The effects of elevated temperature on the photosynthetic efficiency of zooxanthellae *in hospite* from four different species of reef coral: a novel approach. Plant, Cell Environ. 19: 291-299.

Weis, V. M., G. J. Smith, and L. Muscatine. 1989. A CO_2 supply mechanism in zooxanthellate cnidarians – Role of carbonic anhydrase. Mar. Biol. 100(2): 195-202.

Whitney, S. M., D. C. Shaw, and D. Yellowlees. 1995. Evidence that some dinoflagellates contain a Ribulose-1, 5-bisphosphate Carboxylase/Oxygenase related to that of the α-proteobacteria. Proc. R. Soc. B 259(1356): 271-275.

Yellowlees, D., T. Alwyn, V. Rees, and W. Leggat. 2008. Metabolic interactions between algal symbionts and invertebrate hosts. Plant, Cell Environ. 31: 679-694.

Zahl, P. A. and J. J. A. McLaughlin. 1957. Isolation and cultivation of zooxanthellae. Nature 180(4578): 199-200.

Zoccola, D., P. Ganot, A. Bertucci, and others. 2015. Bicarbonate transporters in corals point towards a key step in the evolution of cnidarian calcification. Sci. Rep. 5: 9983.

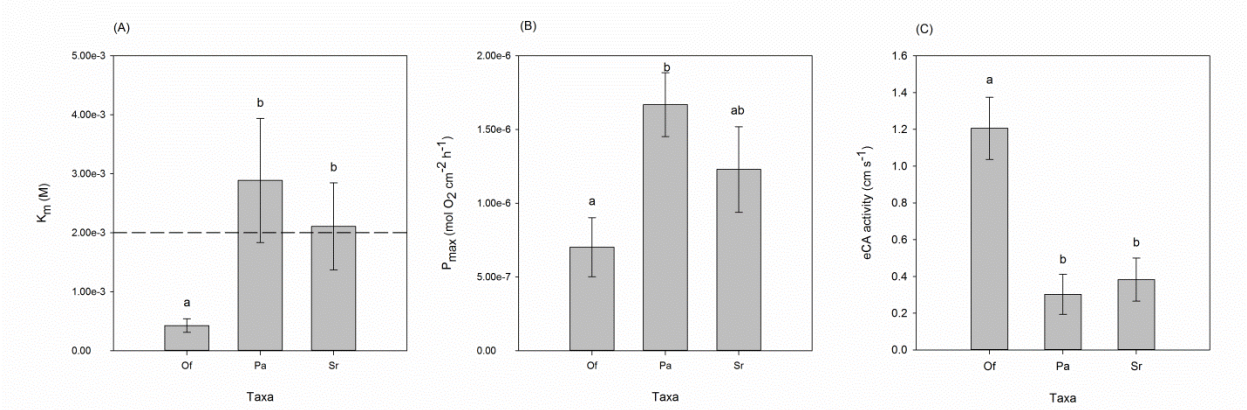

Figure 3.1: Whole coral photosynthetic parameters and external carbonic anhydrase activity. (A) Half-saturation constant (K_m) for DIC, (B) Maximum rate of photosynthesis (P_{max}), (C) external carbonic anhydrase (eCA) activity. Of: *Orbicella faveolata*, Pa: *Porites astreoides*, Sr: *Siderastrea radians*. Lowercase letters represent statistically significant groups and error bars represent the standard error of the mean. The dashed line is approximate ambient seawater concentration of DIC.

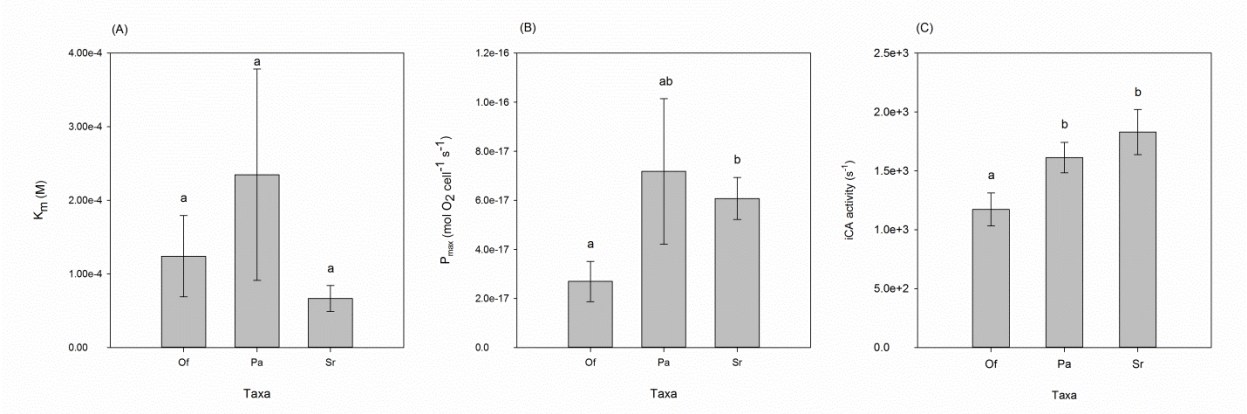

Figure 3.2: Freshly isolated symbiont photosynthetic parameters and internal carbonic anhydrase activity. (A) Half-saturation constant (K_m) for DIC, (B) Maximum rate of photosynthesis (P_{max}), (C) internal carbonic anhydrase (iCA) activity. Of: *Orbicella faveolata*, Pa: *Porites astreoides*, Sr: *Siderastrea radians*. Lowercase letters represent statistically significant groups and error bars represent the standard error of the mean.

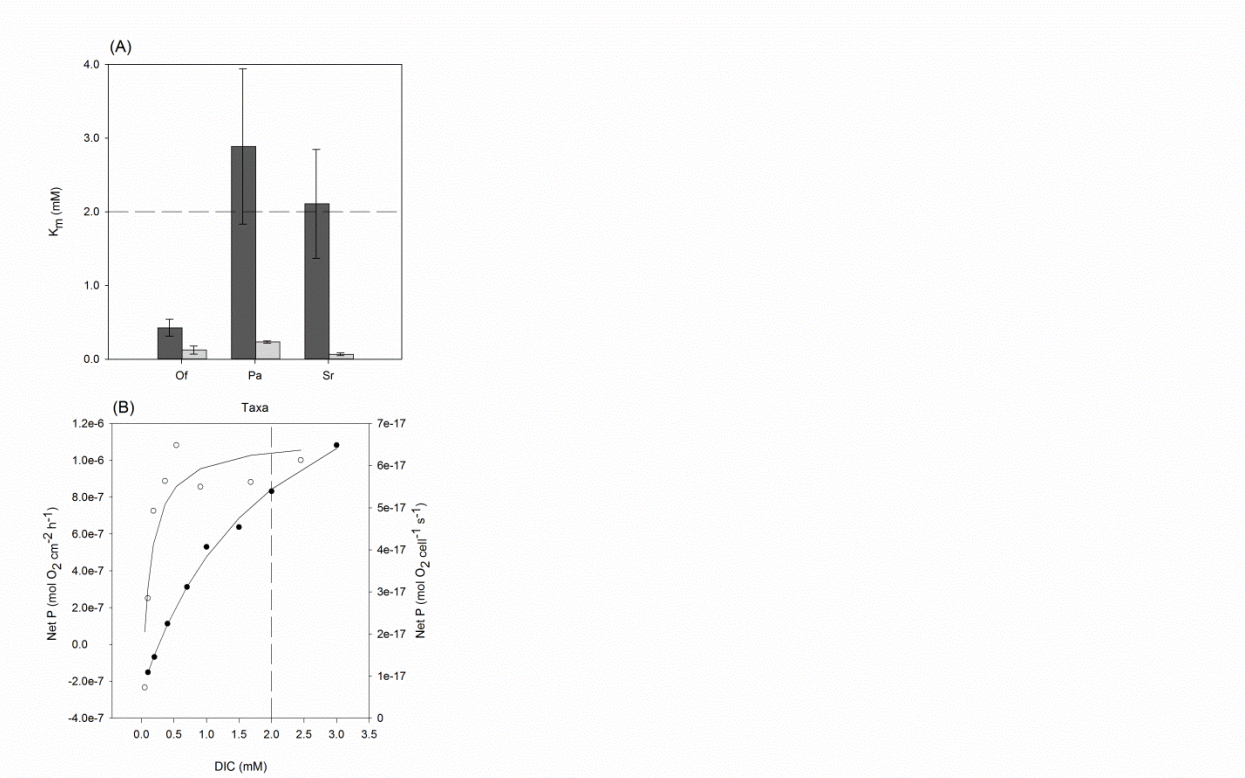

Figure 3.3: Comparison of whole coral and freshly isolated symbiont half-saturation constants (K_ms). (A) Averages of all taxa. Dark bars are whole corals, and light bars are freshly isolated symbionts. Of: *Orbicella faveolata*, Pa: *Porites astreoides*, Sr: *Siderastrea radians*. (B) Michaelis-Menton curves of a *S. radians* colony and its freshly isolated symbionts showing the difference in K_m. Closed circles are whole coral data. Open circles are freshly isolated symbiont data. The dashed lines are approximate ambient seawater concentration of DIC.

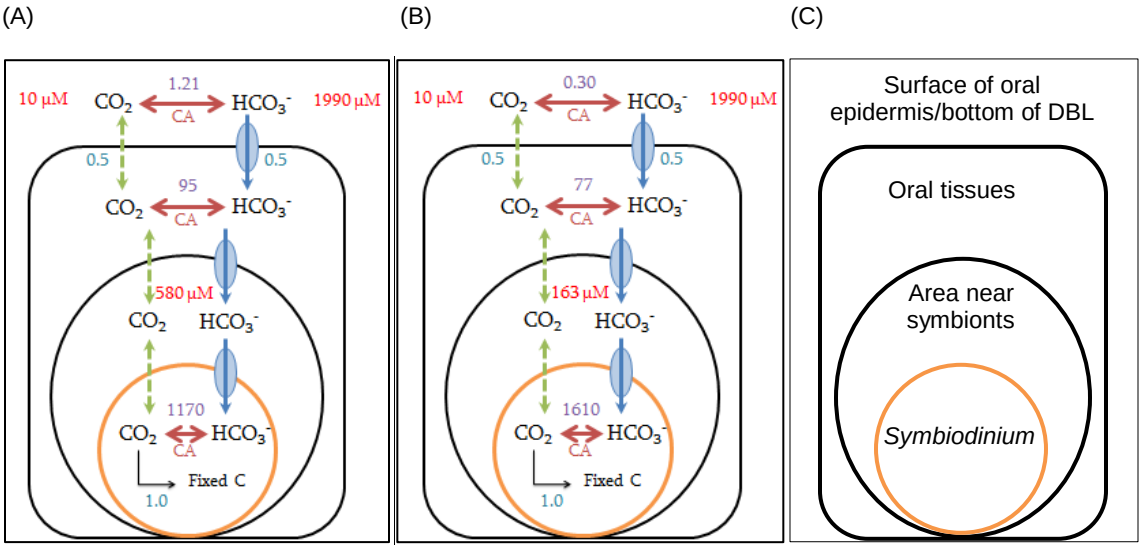

Fig. 3.4: Overview of quantified DIC uptake and processing of in the two reef coral species studied. This simplified schematic illustrates the elements which have been quantified in this and previous work to give a more complete picture as to investment and differences between the species. Included are: carbonic anhydrase (CA) activity, apparent DIC concentrations for coral host and symbiont under normal seawater conditions, and relative contribution to net photosynthesis of CO_2 and HCO_3^-. (A) *Orbicella faveolata.* (B) *Porites astreoides*. (C) The compartments from outer to innermost: surface of coral oral epidermis/bottom of diffusive boundary layer (DBL), coral oral tissues, area near the symbiont, symbiont. Red numbers are DIC concentration (µM) as calculated based on K_m values in this study. Purple numbers are CA activity rates (cm s^{-1} for external, s^{-1} for internal) from this study (coral eCA, symbiont iCA) and Hopkinson et al. 2015 (coral iCA). Blue numbers are the proportion of CO_2 and HCO_3^- that are used by the coral for each unit of fixed carbon (Tansik et al. 2015). Dashed lines are concentration gradient driven fluxes. Solid lines represent transport across membranes.

CHAPTER 4

MODELING THE EFFECTS OF OCEAN ACIDIFICATION ON INORGANIC CARBON FLOW IN SCLERACTINIAN CORAL[3]

[3] Tansik, A.L., B.M. Hopkinson, and C. Meile. To be submitted to *Nature Climate Change*.

Abstract

Ocean acidification (OA) is changing the dissolved inorganic carbon (DIC) system of seawater. For many marine organisms, including scleractinian corals, the biological processes of photosynthesis and/or calcification stand to be affected. Unfortunately, there is a great deal of ambiguity in the literature as to what kind of impact OA will have on corals. Some of these issues can be overcome by using models to evaluate the system; however, previous models have lacked key information about the processing of DIC by corals. Here, we present a process-based model of DIC flow in *Orbicella faveolata* which incorporates recent data quantifiying carbonic anhydrase activity and DIC-related photosynthetic parameters. The model performed well in reflecting gross photosynthesis and calcifying fluid pH, but only attains half of measured calcification rates, likely due to the parameterization of this process being based solely on precipitation/dissolution kinetics. Simulations of mid- and end-century scenarios for OA showed a negligible impact on gross photosynthesis, and only small decreases in calcification rate and calcifying fluid pH. High aragonite saturation states were maintained in the calcifying fluid in spite of the reduction in pH in this compartment under OA conditions. This resiliency of calcification was due to increased total DIC in the compartment, which supported an elevated aragonite saturation state and continued $CaCO_3$ precipitation. The pH in the calcifying fluid declined more than the calcification rate, and the model was used to examine possible drivers. Under OA conditions, the total flux of CO_2 to the calcifying fluid increased, while that of HCO_3^- declined, and CO_3^{2-} and protons continued to be exported. Changes in DIC fluxes are what caused the decline in pH.

Introduction

As the climate changes in response to the addition of CO_2 and other greenhouse gases to the atmosphere, the influence is felt across the globe (IPCC 2014). One of the main impacts on the ocean is associated with the equilibration of atmospheric CO_2 with the surface waters. Dissolved inorganic carbon (DIC) exists in a pH-dependent equilibrium of three species: $CO_2 \leftrightarrow HCO_3^- \leftrightarrow CO_3^{2-}$. Adding more CO_2 to the system leads to more free protons in the water and shifts this equilibrium to the left, reducing pH of the surface waters and the concentration of CO_3^{2-}, in a process known as ocean acidification (OA) (IPCC 2014). The effects of OA are felt by many organisms in the ocean, but especially those which are dependent on DIC for major biological processes (IPCC 2014). Photosynthesis requires CO_2, and it is common for marine autotrophs to concentrate this DIC species for fixation (Hopkinson et al. 2011; Mackey et al. 2015; Shi et al. 2017). With more CO_2 in the water, there is the potential for a benefit to those organisms (Mackey et al. 2015; Shi et al. 2017; Wu et al. 2010). At the other end of the spectrum, however, are those organisms which require CO_3^{2-} in order to create skeletons of aragonite or calcite. Reductions in the saturation state of both forms of $CaCO_3$ can lead to malformed shells or skeletons, or their dissolution (Cohen and Holcomb 2009; Feely et al. 2004; Kelly and Hofmann 2013).

Scleractinian corals face changes on both fronts. They host dinoflagellates of the genus *Symbiodinium* to provide photosynthetically fixed carbon (Falkowski et al. 1984) while secreting aragonite skeletons, forming colony structures and in some cases reefs (Cohen and Holcomb 2009; de Putron et al. 2010). Given the importance of coral reefs to marine biodiversity as well as to humans (Hughes et al. 2017), understanding how corals will be impacted by OA is imperative. To date, much of the attention of researchers has been given to calcification, as this

is the process which forms the reef structure so vital to biodiversity, shoreline protection and fisheries (Cohen and Holcomb 2009; de Putron et al. 2010; Hughes et al. 2017). Studies looking at OA impacts on photosynthesis often incorporate additional variables, usually temperature, which may be of greater impact (Anthony et al. 2008; Hoadley et al. 2015; Langdon and Atkinson 2005).

For both processes, however, there is ambiguity in the literature as to what kind of effect OA will have. Calcification has most often been seen to decrease (Castillo et al. 2014; Huang et al. 2014; Langdon and Atkinson 2005), but will occasionally remain the same (Barkley et al. 2017; Prada et al. 2017), or even increase (Castillo et al. 2014; Huang et al. 2014). Much of the variation seems to come from differences in experimental procedure; for example, how long a coral has been exposed to elevated CO_2 levels, if it is a natural CO_2 gradient or an imposed one, or what CO_2 concentration is being used. There are also taxonomic differences in response (Huang et al. 2014), and variation based on what part of the coral is being examined (Comeau et al. 2017). Photosynthesis is no clearer, as studies also examining other factors have also shown decreases (Anthony et al. 2008), no change (Hoadley et al. 2015), and increases (Langdon and Atkinson 2005) in a variety of measures of photosynthesis. Here, too, taxonomic differences appear (Anthony et al. 2008; Hoadley et al. 2015). Such ambiguity makes it difficult not only to understand what can be expected, but also the drivers behind the changes.

One way to clarify the effects of OA is to use models built on what is known about the processes and movement of DIC through a coral. Previous models have taken different approaches to address the question (Hohn and Merico 2012; Nakamura et al. 2013). Hohn and Merico (2012) focused their model on calcification, and included a detailed treatment of the inorganic carbon chemistry in the system, but little in the way of biological processes. Nakamura

et al. (2013), on the other hand, considered a wider range of biological processes, including photosynthesis, respiration and calcification, but ignored DIC speciation and did not model within the coral tissues. Both models showed important aspects of the DIC dynamics, and gave reasonable results in comparison to experimental results (Hohn and Merico 2012; Nakamura et al. 2013).

To date, the full quantification of parameters in models such as those previously described has been impossible due to a lack of information, as parts of the DIC system were either poorly quantified or completely unquantified. The enzyme carbonic anhydrase (CA) is essential for concentrating DIC for both photosynthesis and calcification by accelerating the hydration-dehydration reaction between CO_2 and HCO_3^-. While it has been known for many years that corals have CA within their tissues and in the calcifying fluid (al-Moghrabi et al. 1996; Bertucci et al. 2013; Weis et al. 1989), we have only recently applied the stable isotope techniques used to determine CA activity to this system (Hopkinson et al. 2015; Tansik et al. 2015; Tansik et al. 2017). We determined that corals have high rates of CA activity both at the bottom of the diffusive boundary layer on the surface of the coral (Tansik et al. 2015; Tansik et al. 2017) and within their tissues (Hopkinson et al. 2015), rates high enough to support both photosynthesis and calcification (Hopkinson et al. 2015). We were also able to determine DIC related kinetics for photosynthesis for both coral and symbiont (Tansik et al. 2017), and how CO_2 and HCO_3^- were partitioned to support net photosynthesis (Tansik et al. 2015).

With this additional information, we constructed a more complete, quantified model of DIC flow through a coral. This study was focused on evaluating the impacts that OA had on gross photosynthesis, calcification and calcifying fluid pH. The detailed nature of it allowed for

examination of changes to DIC flux between the different compartments as well as proposed drivers behind OA's effects on calcification and calcifying fluid pH.

Methods

Model description

The flux and processing of inorganic carbon and calcium of a scleractinian coral was described using a box model. The model represented the transect from seawater through the coenosarc tissues to the calcifying space with a diffusive boundary layer, oral tissue, the coelenteron, aboral tissue and the calcifying space (Fig. 1). In each compartment, mass balance for CO_2, HCO_3^-, CO_3^{2-}, Ca^{2+}, and total alkalinity was expressed as:

$$\frac{dc}{dt} = \frac{(F_{in} - F_{out})}{V_i} + \sum R + \sum B$$

where F is the flux of the chemical (c), V_i is the volume of the compartment, Σ R represents the net reaction rate due to acid-base reactions and carbonic anhydrase (CA) mediated exchange, and Σ B indicates the net increase or decrease due to biological processes.

Photosynthesis by the symbionts was considered in the oral tissue layer, along with respiration by the coral animal and the symbionts (Fig. 4.1). Respiration was also accounted for in the aboral tissue layer (Fig. 4.1). While the importance of the organic matrix in stimulating calcification has been noted previously (Clode and Marshall 2003; Von Euw et al. 2017), there is not yet a way to properly parameterize it. As a result, calcification in the bottom layer of the model depended on the aragonite saturation state (Fig. 4.1). Fluxes between compartments were driven by the concentration gradients between them. There were additional fluxes of all chemicals from the bulk seawater to the calcifying fluid (Fig. 4.1), reflecting the transport of chemicals through the paracellular pathways of the coral (Furla et al. 2000). An alkalinity pump was included based on the proposed Ca^{2+}/H^+ exchange transporter (Tambutte et al. 1996) as a

way to maintain high alkalinity in the calcifying fluid (Fig. 4.1). Biologically modified seawater was imported to the coelenteron from surrounding polyps to account for the connectivity of coral colonies (Fig. 4.1).

Model parameters included seawater temperature, coral surface area and tissue thickness, diffusive boundary layer thickness, symbiont concentration, photosynthetic kinetic parameters for the holobiont and the symbionts, respiration rates for the holobiont and symbionts and CA activity rates of the coral. Fluxes and reactions were parameterized based on experimental data and peer-reviewed literature (Table 4.1). Parameters were primarily determined for *Orbicella faveolata*, an important Caribbean boulder coral. Only the CA activity in the calcifying fluid, and the efficiency of the proton pump were tuned to match measured rates of gross photosynthesis and calcification for *O. faveolata*, and yield a pH consistent with values proposed for the calcifying fluid (Cai et al. 2016; Holcomb et al. 2014); the initial estimate of the CA activity in the calcifying fluid was obtained from the total CA activity of the coral (Hopkinson et al. 2015) and activities observed in small volumes (Hopkinson et al. 2011; Tansik et al. 2017). The efficiency of the proton pump was estimated with consideration to what a reasonable investment energy investment on the part of the coral would be, balanced by the need to maintain a high pH in the compartment.

The model was implemented in MATLAB R2016a (MathWorks) and run to steady state. Initial conditions reflected equilibrium concentrations for given external seawater conditions (pH, DIC concentration and temperature). pH values for all internal layers of the coral except the calcifying fluid were imposed based on microelectrode measurements (Cai et al. 2016). A complete listing of the process rate and flux expressions is given in Appendix B (Appendix Table B1).

Model runs

The sensitivity of the model to the biological parameters was tested by varying the base value by either the reported standard error or 10%. The resulting outputs were then calculated as the percent change from the starting value (Appendix Table B2).

In order to evaluate the impact of ocean acidification on the DIC flow in a coral, starting parameters for external pH and DIC concentration were set to predicted values for mid- and end-century in accordance with the IPCC's RCP 8.5 scenario (IPCC 2014). The baseline run had values of 8.2 and 2000 μM DIC. The mid-century scenario was run with starting values of 8.0 and 2100 μM DIC. The most extreme run was conducted with a pH of 7.8 and a DIC concentration of 2225 μM. No changes were made to the biological parameters of the system.

Results

Model function

First, the base model was tuned to estimate values for the two critical, unconstrained parameters: proton pumping efficiency, CA activity in calcifying fluid. The rate of gross photosynthesis was insensitive to both the calcifying fluid CA activity and the proton pump efficiency (Fig. 4.2a; 4.3a, respectively), therefore their final values were determined based on the pH of the compartment and the calcification rate. The best fit of the model to the experimental data occurred when the calcifying fluid CA activity was 10,000 s^{-1}, and the proton pump efficiency was 0.5 (Fig. 4.2b,c; Fig. 4.3b,c). This CA activity was considered reasonable in light of the overall activity of the enzyme within the coral (Hopkinson et al. 2015) and the small volume of the calcifying space, which would lead to a concentration of the CA and a resulting high activity rate. The removal of protons from half the calcifying fluid was acceptable, as other activities within the compartment—such as exchange between the different DIC species—are

constantly adding new protons to the system, and removing them from a larger proportion of the space would require a much greater energy investment than seems practical for the organism.

Using quantified CA activity rates and photosynthetic kinetic parameters for *O. faveolata*, the model produces a gross photosynthetic rate that nearly matches that of experimental measurements (3.27E-7 mmol cm^{-2} s^{-1} vs. 3.54E-7 mmol cm^{-2} s^{-1}) (Tansik et al. 2017). CO_2 and HCO_3^- both enter the oral tissue layers to support this process, originating at the surface of the coral as well as in the coelenteron (Fig. 4.4). The fluxes from the surface of the coral dominate the DIC influx; they are each over one third the rate of gross photosynthesis (Fig. 4.4). It is notable, however, that the rate of CO_2 fluxing in from the coelenteron is mostly balanced by the flow of CO_2 from the aboral tissues to this central cavity (Fig. 4.4).

The model gives a calcifying fluid pH of 9.26, which is in the range of those reported using various methods of measurement (8.4 – 10) (Cai et al. 2016; Holcomb et al. 2014). The flux of CO_2 and HCO_3^- into the calcifying fluid from the aboral tissues and the bulk seawater and the removal of CO_3^{2-} via calcification and flux to the bulk seawater work to reduce the pH, while the proton pump maintains the elevated pH (Fig. 4.4). The simulated rate of calcification, however, is approximately half that of experimental measurements (6.65E-6 mmol cm^{-2} s^{-1} compared to 1.11E-7 mmol cm^{-2} s^{-1}). Such rates of calcification are only approached by the model with a proton pump efficiency of 0.8 or above, at which level the calcifying fluid pH reaches above 10 (Fig. 4.3b,c). With calcification defined by precipitation/dissolution dynamics, and missing possible biological catalyzation (Clode and Marshall 2003; Von Euw et al. 2017), this is considered a reasonable approximation of the process.

Effects of ocean acidification

Simulations including lower seawater pH and higher seawater DIC concentrations led to variable responses in gross photosynthesis, calcification and calcifying fluid pH. A very slight (< 1%) increase in gross photosynthetic rate occurred under ocean acidification conditions (Fig. 4.5a), showing the minimal impact of the external DIC and pH environment on this process in the model. As respiration rates are unchanged in the model, this specifically indicates a lack of response in photosynthetic production to an increase in available CO_2. The fluxes of CO_2 from both the surface of the coral and the coelenteron to the oral tissue layer increased (Fig. 4.6), resulting in a higher concentration in the compartment.

In contrast, both the rate of calcification and the calcifying fluid pH declined under simulated OA conditions, indicating a greater sensitivity to ocean acidification (Fig. 4.5b,c). The aragonite saturation state in both scenarios remained high; 13.25 for 2050, and 13.10 for end-century. Calcification rate had a small decrease from the baseline in both the mid-century (-1.69%) and end-century runs (-3.70%) (Fig. 4.5b). The mid-century 0.3 and end-century 0.5 reduction in calcifying fluid pH were more notable (-3.42% and -5.58%, respectively; Fig. 4.5c). These differences indicate that calcification rate is more resilient than calcifying fluid pH to the changes predicted under acidified conditions. Regardless of the scale of the changes seen, which are better determined by direct experimentation, we were interested in examining the drivers behind them.

To understand what may be driving these changes in the calcifying space, differences to the steady state fluxes of CO_2 and HCO_3^- into this compartment were examined in more detail. These included both fluxes from the aboral tissue layer and those directly from the bulk seawater. Overall, the total flux of HCO_3^- was still much greater than that of CO_2; however, the

former declined with lower seawater pH, while the latter increased (Fig. 4.7a). Additionally, the percent change in HCO_3^- fluxes were one to two orders of magnitude lower than those of CO_2 (Fig. 4.7b). However, while all fluxes of CO_2 into the calcifying fluid increased, HCO_3^- fluxes showed a mixed response, with decreasing flux from the seawater and elevated flux from the aboral tissues (Fig. 4.6). While there was an increase in transport of HCO_3^- from the aboral tissues of 16%, it was not enough to offset the 39% decline in flux from the bulk seawater, reflecting the reduced concentration gradient between the seawater and the calcifying fluid (Fig. 4.6). The combination of decreased HCO_3^- and increased CO_2 influx into the calcifying space pushes the pH toward a more acidic condition with consequent impacts on DIC speciation and aragonite saturation state.

Discussion

Experimental and natural settings reflecting projected ocean acidification conditions have returned variable results on coral photosynthesis and calcification (Anthony et al. 2008; Huang et al. 2014; Langdon and Atkinson 2005). While there are taxa-specific differences in these processes (Herfort et al. 2008; Huang et al. 2014; Tansik et al. 2017), all corals require DIC to be processed in a similar manner. As such, using models to investigate the impacts of OA on these vital processes can allow for a more detailed exploration, not only of any changes to the commonly measured rates, but also the potential drivers behind these alterations.

Previous models have examined this with varying degrees of detail, especially in relation to the biological processes ongoing within the coral tissues (Hohn and Merico 2012; Nakamura et al. 2013). A full understanding of a coral's response requires that these biological processes be parameterized in such a way as to accurately reflect how varying concentrations of DIC will affect the physiology. For example, defining photosynthesis based on its Michaelis-Menten

kinetics allows for the rate to be directly determined by the concentration of DIC in the system, as well as easy manipulation of only one or two parameters in the model to examine potential acclimation of the coral to an altered environment. Earlier models were hindered in this regard by a lack of quantitative data about the DIC processing of corals (Hohn and Merico 2012; Nakamura et al. 2013). Incorporation of recent work on the DIC-related kinetics of photosynthesis (Tansik et al. 2015; Tansik et al. 2017) and CA activity (Hopkinson et al. 2015; Tansik et al. 2017) into our model allows for improved understanding of DIC movement within and through a coral, as well as the potential effects of OA on photosynthesis and calcification.

Impact of reduced seawater pH – photosynthesis

Since photosynthetic production is dependent on having CO_2 to fix, one might expect that increasing the concentration of this DIC species leads to an increase in photosynthesis. However, model simulations showed less than 1% increase under even the most extreme projected OA conditions. This aligns with the fact that *O. faveolata* is DIC saturated for photosynthesis under current oceanic conditions (Tansik et al. 2017). Additionally, previous work has shown that DIC is scarce for the coral's photosynthetic symbionts, and they saturate net photosynthesis at low carbon concentrations (Tansik et al. 2017). Their regular rates of production are, therefore, unlikely to be impacted by increased concentrations of CO_2 in the oral tissues. Hence, reflecting these observations, the projected model response does not show an increase in photosynthesis for *O. faveolata* under OA conditions.

Photosynthetic productivity is an important consideration for corals, as most of their energy is derived from the translocation of fixed carbon from their *Symbiodinium* symbionts (Falkowski et al. 1984). Changing oceanic conditions, especially increasing sea surface temperatures, put stress on both host and symbiont; this can cause the disruption of

photosynthate transfer and negatively impact the energy budget of the coral (Anthony et al. 2009; Hughes et al. 2010; Tremblay et al. 2016). While heterotrophy can provide a source of stored carbon (Hughes et al. 2010) and promote recovery from stress (Connolly et al. 2012; Grottoli et al. 2006; Tremblay et al. 2016), corals are forced to use their energy reserves in times of stress (Hughes et al. 2010; Tremblay et al. 2016). There are also indications that some corals, including *O. faveolata*, cannot support their carbon needs via heterotrophy when exposed to annual bleaching events (Levas et al. 2016), reinforcing the importance that autotrophic carbon plays in the energy budgets of corals. However, with no indication that photosynthetic production will increase, and the likelihood of annual bleaching regularly reducing the number of symbionts and their photosynthates (IPCC 2014; Levas et al. 2016), it is probable that corals will be functioning with increasingly negative energy budgets.

However, not all corals are carbon saturated for photosynthesis; other taxa have been shown to increase their rates of net photosynthesis with additional DIC in the system (Herfort et al. 2008; Tansik et al. 2017). These species may show a more positive response to OA than was seen in this parameterization of the model. This could result in some taxa being able to mitigate the impacts of stress more easily than others.

Impact of reduced seawater pH – calcification

The impact of OA on coral calcification has been of greater interest than that of photosynthesis, due to the need for CO_3^{2-} and the predicted decrease in availability of this DIC species. The simulations run here showed a decline in calcification with decreasing seawater pH, in line with some experiments and one of the previous models (Hohn and Merico 2012; Langdon and Atkinson 2005; Okazaki et al. 2013). Our results, however, are far less extreme than other experimental data across the same pH range (Huang et al. 2014; Marubini et al. 2008). This

relatively small change could be related to the fact that the modeled calcification rates are only half of those measured experimentally. With less demand for CO_3^{2-}, the system is naturally more resilient to changes in pH. Therefore, with higher rates of calcification, the changes to the system could be larger. Though the impact modeled here is small, any reduction in calcification rate has the potential to be important, as growth must keep up with rates of erosion and sea level rise in order to maintain the reef structure in the surface waters (DeCarlo et al. 2015; Enochs et al. 2015; Silbiger et al. 2014). This small reduction in calcification rate modeled also implies that it is perhaps realistic for corals to make physiological changes which may allow for continued growth at normal rates, such as has been seen in naturally occurring, low pH systems (Barkley et al. 2017; Prada et al. 2017).

The decline in calcification in the model can be attributed to a reduction in the pH of the calcifying fluid. Of interest is the fact that the rate of calcification decreased less than the calcifying fluid pH. Although OA results in reduced calcifying fluid pH, the total concentration of DIC in the calcifying fluid increased, leading to only modest declines in carbonate concentrations in the calcifying fluid allowing calcification rates to remain relatively high. Even though the pH in the calcifying fluid dropped, it still remained alkaline enough to result in aragonite saturation states well above 1; calcification was, therefore, still favored, though less so than under non-OA conditions. Should the calcifying fluid pH decline farther, however, the ability of corals to continue laying down skeleton could be compromised as the speciation of DIC shifts away from CO_3^{2-} (Cohen and Holcomb 2009).

A topic of some debate is the driver behind the decline in calcifying fluid pH and skeletal growth. One suggestion, based on evidence for a mainly biological source of DIC for calcification (Allison et al. 2014; Furla et al. 2000; McCulloch et al. 2012), is that increases in

seawater CO_2 will result in a greater flux of this mild acid through the tissues into this compartment, reducing the pH and hence calcification. Others propose that bulk seawater is transported and used for calcification, so the resulting changes to its DIC chemistry, such as shifts in speciation and aragonite saturation state, will cause parallel changes in the calcifying fluid (Cohen and Holcomb 2009). Our model supports the first view; the flux of CO_2 from the tissues as well as the bulk seawater increased dramatically with decreasing external pH, to double and triple the original flux under the mid- and end-century scenarios. This may be partially an artifact of how the model was designed; there is a greater dependence on metabolic sources to supply the DIC needed for calcification, making it dependent on diffusion from the tissues, which depends on concentration gradients. However, there was also little change in the aragonite saturation state between the OA scenarios, suggesting that whatever alterations are happening in the overlying seawater are not being reflected in the calcifying fluid.

The two ideas are not necessarily mutually exclusive. Even if whole seawater is transported to the calcifying space, the increase in CO_2 diffusing into and through the tissues from the external seawater and the coelenteron would increase the flux into the calcifying fluid. This could result in even greater impacts on the calcifying fluid that the coral must deal with in order to continue precipitating $CaCO_3$. Both theories also result in the same outcome for the coral; it must find a way to maintain a pH in its calcifying fluid which is elevated in relation to the external seawater, as well as a high aragonite saturation state. Addressing this would require likely require increased energy availability (Cohen and Holcomb 2009), which have to come from somewhere other than photosynthetic production, as it does not increase.

Such environmental pressures can stimulate acclimation of the coral to altered conditions (Barkley et al. 2017), a factor that was not accounted for in the simulations. There is, for

example, evidence for the downregulation of the CA found in the calcifying fluid of *Stylophora pistillata* with decreasing external pH (Zoccola et al. 2016). It has also been proposed that increasing proton pumping from the calcifying fluid could be one way for corals to regulate this space (Cohen and Holcomb 2009). Changes to the photosynthetic DIC kinetics, such as a higher half-saturation constant (Shi et al. 2017; Wu et al. 2010), which have been seen in other marine primary producers but not yet experimentally determined in corals would also be worth examining.

Acknowledgements

This work was funded by a grant to B.M.H and C.M. from the National Science Foundation (NSF 1315944).

References

Al-Horani, F. A., S. M. Al-Moghrabi, and D. de Beer. 2003. Microsensor study of photosynthesis and calcification in the scleractinian coral, Galaxea fascicularis: active internal carbon cycle. Journal of Experimental Marine Biology and Ecology 288: 1-15. doi: 10.1016/s0022-0981(02)00578-6.

al-Moghrabi, S. M., C. Goiran, D. Allemand, N. Speziale, and J. Jaubert. 1996. Inorganic carbon uptake for photosynthesis by the symbiotic coral-dinoflagellate association II. Mechanisms for bicarbonate uptake. Journal of Experimental Marine Biology and Ecology 199: 227-248.

Albert, J. A., A. D. Olds, S. Albert, A. Cruz-Trinidad, and A. M. Schwarz. 2015. Reaping the reef: Provisioning services from coral reefs in Solomon Islands. Mar. Pol. 62: 244-251. doi: 10.1016/j.marpol.2015.09.023.

Allemand, D. and others 2004. Biomineralisation in reef-building corals: from molecular mechanisms to environmental control. C. R. Palevol 3: 453-467. doi: 10.1016/j.crpv.2004.07.011.

Allison, N., I. Cohen, A. A. Finch, J. Erez, A. W. Tudhope, and F. Edinburgh Ion Microprobe. 2014. Corals concentrate dissolved inorganic carbon to facilitate calcification. Nat. Commun. 5: 6. doi: 10.1038/ncomms6741.

Anthony, K. R. N., M. O. Hoogenboom, J. A. Maynard, A. G. Grottoli, and R. Middlebrook. 2009. Energetics approach to predicting mortality risk from environmental stress: a case study of coral bleaching. Funct. Ecol. 23: 539-550. doi: 10.1111/j.1365-2435.2008.01531.x.

Anthony, K. R. N., D. I. Kline, G. Diaz-Pullido, S. Dove, and O. Hoegh-Guldberg. 2008. Ocean acidification causes bleaching and productivity loss in coral reef builders. Proc Natl Acad Sci U S A 105: 17442-17446. doi: 10.1073/pnas.0804478105.

Arthur, R., T. J. Done, H. Marsh, and V. Harriott. 2006. Local processes strongly influence post-bleaching benthic recovery in the Lakshadweep Islands. Coral Reefs 25: 427-440. doi: 10.1007/s00338-006-0127-4.

Barkley, H. C., A. L. Cohen, Y. Golbuu, V. R. Starczak, T. M. DeCarlo, and K. E. F. Shamberger. 2015. Changes in coral reef communities across a natural gradient in seawater pH. Science Advances 1: e1500328. doi: 10.1126/sciadv.1500328.

Barkley, H. C., A. L. Cohen, D. C. McCorkle, and Y. Golbuu. 2017. Mechanisms and thresholds for pH tolerance in Palau corals. Journal of Experimental Marine Biology and Ecology 489: 7-14. doi: 10.1016/j.jembe.2017.01.003.

Barott, K. L., A. A. Venn, S. O. Perez, S. Tambutte, and M. Tresguerres. 2015. Coral host cells acidify symbiotic algal microenvironment to promote photosynthesis. Proc Natl Acad Sci U S A 112: 607-612. doi: 10.1073/pnas.1413483112.

Bénazet-Tambutté, S., D. Allemand, and J. Jaubert. 1996. Permeability of the oral epithelial layers in cnidarians. Marine Biology 126: 43-53. doi: 10.1007/bf00571376.

Bertucci, A., A. Moya, S. Tambutté, D. Allemand, C. T. Supuran, and D. Zoccola. 2013. Carbonic anhydrases in anthozoan corals—A review. Bioorganic & Medicinal Chemistry 21: 1437-1450. doi: 10.1016/j.bmc.2012.10.024.

Bertucci, A., S. Tambutte, C. T. Supuran, D. Allemand, and D. Zoccola. 2011. A new coral carbonic anhydrase in Stylophora pistillata. Mar Biotechnol (NY) 13: 992-1002. doi: 10.1007/s10126-011-9363-x.

Brading, P., M. E. Warner, D. J. Smith, and D. J. Suggett. 2013. Contrasting modes of inorganic carbon acquisition amongst Symbiodinium (Dinophyceae) phylotypes. New Phytol. 200: 432-442. doi: 10.1111/nph.12379.

Brown, B. E. 1997. Coral bleaching: causes and consequences. Coral Reefs 16: S129-S138.

Burton, E. A., and L. M. Walter. 1990. THE ROLE OF PH IN PHOSPHATE INHIBITION OF CALCITE AND ARAGONITE PRECIPITATION RATES IN SEAWATER. Geochimica Et Cosmochimica Acta 54: 797-808. doi: 10.1016/0016-7037(90)90374-t.

Buxton, L., M. Badger, and P. Ralph. 2009. Effects of Moderate Heat Stress and Dissolved Inorganic Carbon Concentration on Photosynthesis and Respiration of Symbiodinium Sp. (Dinophyceae) in Culture and in Symbiosis(1). J Phycol 45: 357-365. doi: 10.1111/j.1529-8817.2009.00659.x.

Cai, W. J. and others 2016. Microelectrode characterization of coral daytime interior pH and carbonate chemistry. Nat. Commun. 7: 8. doi: 10.1038/ncomms11144.

Castillo, K. D., J. B. Ries, J. F. Bruno, and I. T. Westfield. 2014. The reef-building coral Siderastrea siderea exhibits parabolic responses to ocean acidification and warming. Proc. R. Soc. B-Biol. Sci. 281: 9. doi: 10.1098/rspb.2014.1856.

Clode, P. L., and A. T. Marshall. 2002. Low temperature FESEM of the calcifying interface of a scleractinian coral. Tissue Cell 34: 187-198. doi: 10.1016/s0040.8166(02)00031-9.

Clode, P. L., and A. T. Marshall. 2003. Calcium associated with a fibrillar organic matrix in the scleractinian coral Galaxea fascicularis. Protoplasma 220: 153-161. doi: 10.1007/s00709-002-0046-3.

Cohen, A. L., and M. Holcomb. 2009. Why Corals Care About Ocean Acidification: Uncovering the Mechanism. Oceanography 22: 118-127.

Comeau, S. and others 2017. Coral calcifying fluid pH is modulated by seawater carbonate chemistry not solely seawater pH. Proc. R. Soc. B-Biol. Sci. 284: 10. doi: 10.1098/rspb.2016.1669.

Connolly, S. R., M. A. Lopez-Yglesias, and K. R. N. Anthony. 2012. Food availability promotes rapid recovery from thermal stress in a scleractinian coral. Coral Reefs 31: 951-960. doi: 10.1007/s00338-012-0925-9.

Crook, E. D., D. Potts, M. Rebolledo-Vieyra, L. Hernandez, and A. Paytan. 2012. Calcifying coral abundance near low-pH springs: implications for future ocean acidification. Coral Reefs 31: 239-245. doi: 10.1007/s00338-011-0839-y.

Davy, S. K., D. Allemand, and V. M. Weis. 2012. Cell Biology of Cnidarian-Dinoflagellate Symbiosis. Microbiol. Mol. Biol. Rev. 76: 229-261. doi: 10.1128/mmbr.05014-11.

de Putron, S. J., D. C. McCorkle, A. L. Cohen, and A. B. Dillon. 2010. The impact of seawater saturation state and bicarbonate ion concentration on calcification by new recruits of two Atlantic corals. Coral Reefs 30: 321-328. doi: 10.1007/s00338-010-0697-z.

DeCarlo, T. M. and others 2015. Coral macrobioerosion is accelerated by ocean acidification and nutrients. Geology 43: 7-10. doi: 10.1130/g36147.1.

Enochs, I. C., D. P. Manzello, R. D. Carlton, D. M. Graham, R. Ruzicka, and M. A. Colella. 2015. Ocean acidification enhances the bioerosion of a common coral reef sponge: implications for the persistence of the Florida Reef Tract. Bull. Mar. Sci. 91: 271-290. doi: 10.5343/bms.2014.1045.

Falkowski, P. G., Z. Dubinsky, L. Muscatine, and J. W. Porter. 1984. LIGHT AND THE BIOENERGETICS OF A SYMBIOTIC CORAL. Bioscience 34: 705-709. doi: 10.2307/1309663.

Feely, R. A. and others 2004. Impact of anthropogenic CO2 on the CaCO3 system in the oceans. Science 305: 362-366. doi: 10.1126/science.1097329.

Ferrario, F., M. W. Beck, C. D. Storlazzi, F. Micheli, C. C. Shepard, and L. Airoldi. 2014. The effectiveness of coral reefs for coastal hazard risk reduction and adaptation. Nat. Commun. 5: 9. doi: 10.1038/ncomms4794.

Furla, P., I. Galgani, I. Durand, and D. Allemand. 2000. Sources and mechanisms of inorganic carbon transport for coral calcification and photosynthesis. J. Exp. Biol. 203: 3445-3457.

Gagnon, A. C., J. F. Adkins, and J. Erez. 2012. Seawater transport during coral biomineralization. Earth Planet. Sci. Lett. 329: 150-161. doi: 10.1016/j.epsl.2012.03.005.

Gattuso, J.-P., D. Allemand, and M. Frankignoulle. 1999. Photosynthesis and Calcification at Cellular, Organismal and Community Levels in Coral Reefs: A Review of Interactions and Control by Carbonate Chemistry. American Zoologist 39: 160-183.

Gattuso, J.-P., M. Frankignoulle, I. Bourge, S. Romaine, and R. W. Buddemeier. 1998. Effect of calcium carbonate saturation of seawater on coral calcification. Global and Planetary Change 18: 37-46.

Goiran, C., S. M. Al-Moghrabi, D. Allemand, and J. Jaubert. 1996. Inorganic carbon uptake for photosynthesis by the symbiotic coral/dinoflagellate association I. Photosynthetic performances of symbionts and dependence on sea water bicarbonate. Journal of Experimental Marine Biology and Ecology 199: 207-225.

Grottoli, A. G., L. J. Rodrigues, and J. E. Palardy. 2006. Heterotrophic plasticity and resilience in bleached corals. Nature 440: 1186-1189. doi: 10.1038/nature04565.

Herfort, L., B. Thake, and I. Taubner. 2008. Bicarbonate Stimulation of Calcification and Photosynthesis in Two Hermatypic Corals(1). J Phycol 44: 91-98. doi: 10.1111/j.1529-8817.2007.00445.x.

Hoadley, K. D. and others 2015. Physiological response to elevated temperature and pCO(2) varies across four Pacific coral species: Understanding the unique host plus symbiont response. Sci Rep 5: 15. doi: 10.1038/srep18371.

Hohn, S., and A. Merico. 2012. Modelling coral polyp calcification in relation to ocean acidification. Biogeosciences 9: 4441-4454. doi: 10.5194/bg-9-4441-2012.

Holcomb, M. and others 2014. Coral calcifying fluid pH dictates response to ocean acidification. Sci Rep 4: 4. doi: 10.1038/srep05207.

Hopkinson, B. M., C. L. Dupont, A. E. Allen, and F. M. M. Morel. 2011. Efficiency of the CO_2-concentrating mechanism of diatoms. PNAS 108: 3830-3837. doi: 10.1073/pnas.1018062108.

Hopkinson, B. M., A. L. Tansik, and W. K. Fitt. 2015. Internal carbonic anhydrase activity in the tissue of scleractinian corals is sufficient to support proposed roles in photosynthesis and calcification. J. Exp. Biol. 218: 2039-2048. doi: 10.1242/jeb.118182.

Huang, H., X. C. Yuan, W. J. Cai, C. L. Zhang, X. B. Li, and S. Liu. 2014. Positive and negative responses of coral calcification to elevated pCO(2): case studies of two coral species and the implications of their responses. Marine Ecology Progress Series 502: 145-156. doi: 10.3354/meps10720.

Hughes, A. D., A. G. Grottoli, T. K. Pease, and Y. Matsui. 2010. Acquisition and assimilation of carbon in non-bleached and bleached corals. Marine Ecology Progress Series 420: 91-101. doi: 10.3354/meps08866.

Hughes, T. P. and others 2017. Coral reefs in the Anthropocene. Nature 546: 82-90. doi: 10.1038/nature22901

IPCC. 2014. Climate Change 2014: Synthesis Report. Contribution of Working Groups I, II and III to the Fifth Assessment Report of the Intergovernmental Panel on Climate Change, p. 151 pp. *In* R. K. P. a. L. A. M. Core Writing Team [ed.]. IPCC.

Kelly, M. W., and G. E. Hofmann. 2013. Adaptation and the physiology of ocean acidification. Funct. Ecol. 27: 980-990. doi: 10.1111/j.1365-2435.2012.02061.x.

Kuhl, M., Y. Cohen, T. Dalsgaard, B. B. Jorgensen, and N. P. Revsbech. 1995. MICROENVIRONMENT AND PHOTOSYNTHESIS OF ZOOXANTHELLAE IN SCLERACTINIAN CORALS STUDIED WITH MICROSENSORS FOR O-2, PH AND LIGHT. Marine Ecology Progress Series 117: 159-172. doi: 10.3354/meps117159.

Langdon, C., and M. J. Atkinson. 2005. Effect of elevated pCO(2) on photosynthesis and calcification of corals and interactions with seasonal change in temperature/irradiance and nutrient enrichment. J. Geophys. Res.-Oceans 110: 16. doi: 10.1029/2004jc002576.

Levas, S. and others 2016. Can heterotrophic uptake of dissolved organic carbon and zooplankton mitigate carbon budget deficits in annually bleached corals? Coral Reefs 35: 495-506. doi: 10.1007/s00338-015-1390-z.

Mackey, K. R. M., J. J. Morris, F. M. M. Morel, and S. A. Kranz. 2015. Response of Photosynthesis to Ocean Acidification. Oceanography 28: 74-91. doi: 10.5670/oceanog.2015.33.

Marubini, F., C. Ferrier-Pages, P. Furla, and D. Allemand. 2008. Coral calcification responds to seawater acidification: a working hypothesis towards a physiological mechanism. Coral Reefs 27: 491-499. doi: 10.1007/s00338-008-0375-6.

McCulloch, M., J. Falter, J. Trotter, and P. Montagna. 2012. Coral resilience to ocean acidification and global warming through pH up-regulation. Nat. Clim. Chang. 2: 623-633. doi: 10.1038/nclimate1473.

McCulloch, M. T., J. P. D'Olivo, J. Falter, M. Holcomb, and J. A. Trotter. 2017. Coral calcification in a changing World and the interactive dynamics of pH and DIC upregulation. Nat. Commun. 8: 8. doi: 10.1038/ncomms15686.

Moya, A. and others 2008. Carbonic anhydrase in the scleractinian coral Stylophora pistillata: characterization, localization, and role in biomineralization. J Biol Chem 283: 25475-25484. doi: 10.1074/jbc.M804726200.

Nakamura, T., K. Nadaoka, and A. Watanabe. 2013. A coral polyp model of photosynthesis, respiration and calcification incorporating a transcellular ion transport mechanism. Coral Reefs 32: 779-794. doi: 10.1007/s00338-013-1032-2.

Oakley, C. A., G. W. Schmidt, and B. M. Hopkinson. 2014. Thermal responses of Symbiodinium photosynthetic carbon assimilation. Coral Reefs 33: 501-512. doi: 10.1007/s00338-014-1130-9.

Okazaki, R. R., P. K. Swart, and C. Langdon. 2013. Stress-tolerant corals of Florida Bay are vulnerable to ocean acidification. Coral Reefs 32: 671-683. doi: 10.1007/s00338-013-1015-3.

Pandolfi, J. M. and others 2005. Are U.S. coral reefs on the slippery slope to slime? Science 307: 1725-1726. doi: 10.1126/science.1104258.

Prada, F. and others 2017. Ocean warming and acidification synergistically increase coral mortality. Sci Rep 7: 10. doi: 10.1038/srep40842.

Shi, Q., W. Q. Xiahou, and H. Y. Wu. 2017. Photosynthetic responses of the marine diatom Thalassiosira pseudonana to CO2-induced seawater acidification. Hydrobiologia 788: 361-369. doi: 10.1007/s10750-016-3014-1.

Silbiger, N. J., O. Guadayol, F. I. M. Thomas, and M. J. Donahue. 2014. Reefs shift from net accretion to net erosion along a natural environmental gradient. Marine Ecology Progress Series 515: 33-44. doi: 10.3354/meps10999.

Silverman, D. N., and C. K. Tu. 1976. CARBONIC-ANHYDRASE CATALYZED HYDRATION STUDIED BY C-13 AND O-18 LABELING OF CARBON-DIOXIDE. J. Am. Chem. Soc. 98: 978-984. doi: 10.1021/ja00420a019.

Tambutte, E., D. Allemand, E. Mueller, and J. Jaubert. 1996. A compartmental approach to the mechanism of calcification in hermatypic corals. J. Exp. Biol. 199: 1029-1041.

Tansik, A. L., W. K. Fitt, and B. M. Hopkinson. 2015. External carbonic anhydrase in three Caribbean corals: quantification of activity and role in CO2 uptake. Coral Reefs 34: 703-713. doi: 10.1007/s00338-015-1289-8.

Tansik, A. L., W. K. Fitt, and B. M. Hopkinson. 2017. Inorganic carbon is scarce for symbionts in scleractinian corals. Limnology and Oceanography: doi: 10.1002/lno.10550.

Tremblay, P., A. Gori, J. F. Maguer, M. Hoogenboom, and C. Ferrier-Pages. 2016. Heterotrophy promotes the re-establishment of photosynthate translocation in a symbiotic coral after heat stress. Sci Rep 6: 14. doi: 10.1038/srep38112.

Von Euw, S. and others 2017. Biological control of aragonite formation in stony corals. Science 356: 933-+. doi: 10.1126/science.aam6371.

Weis, V. M., G. J. Smith, and L. Muscatine. 1989. A "CO_2 supply" mechanism in zooxanthellate cnidarians: role of carbonic anhydrase. Marine Biology 100: 195-202. doi.

Wu, Y., K. Gao, and U. Riebesell. 2010. CO2-induced seawater acidification affects physiological performance of the marine diatom Phaeodactylum tricornutum. Biogeosciences 7: 2915-2923. doi: 10.5194/bg-7-2915-2010.

Zeebe, R. E., and D. Wolf-Gladrow. 2001. CO_2 in seawater: Equilibrium, Kinetics, Isotopes. Elsevier Science.

Zoccola, D., A. Innocenti, A. Bertucci, E. Tambutte, C. T. Supuran, and S. Tambutte. 2016. Coral Carbonic Anhydrases: Regulation by Ocean Acidification. Mar. Drugs 14: 11. doi: 10.3390/md14060109.

Table 4.1: Parameters of the model. Measured values come from experiments on *O. faveolata*. Where neither experimental measurements nor values from peer-reviewed literature were available, values were estimated.

Parameter	Value	Reference
external DIC (p.DIC)	2000 mmol cm^{-3}	measured
Temperature (p.T)	299.15 K	measured
external pH (p.pH)	8.2	measured
coral surface area (p.SA)	11.87 cm^2	measured
coral tissue thickness (p.tiss)	0.01 cm	Allemand et al. (2004); Gattuso et al. (1999)
diffusive boundary layer thickness (p.Ldbl)	0.02 cm	Kuhl et al. (1995)
symbiont density (p.zoox)	1e6 cells cm^{-2}	measured
Pmax of coral (p.Pmaxc)	9.94e-4 mmol cm^{-2} s^{-1}	measured
Pmax of symbiont (p.Pmaxf)	2.69e-14 mmol cell s^{-1}	Tansik et al. (2017)
DIC half saturation constant of coral photosynthesis (p.Kmdicc)	4.2e-4 mmol cm^{-3}	Tansik et al. (2017)
DIC half saturation constant of symbiont photosynthesis (p.Kmdicf)	1.24E-4 mmol cm^{-3}	Tansik et al. (2017)
respiration rate of coral (p.Rc)	1.61e-7 mmol cm^{-2} s^{-1}	measured
respiration rate of symbiont (p.Rz)	1e-14 mmol cm^{-2} s^{-1}	set of 0.5 holobiont R
external CA activity of coral (p.ksf)	1.21 cm s^{-1}	Tansik et al. (2017)
internal CA activity of coral (p.ktf)	82.7 s^{-1}	Hopkinson et al. (2015)
concentration of CO3 in coelenteron (p.co3coel)	3.554e-4 mmol cm^{-3}	Cai et al. (2016)
pH of coelenteron (p.pHcoel)	8.25	Cai et al. (2016)
Salinity (p.S)	35 psu	measured
diffusion coefficient for CO2 in water (p.Dco2)	1.9e-5 cm^2 s^{-1}	
diffusion coefficient for HCO3 in water (p.Dhco3)	1e-5 cm^2 s^{-1}	
diffusion coefficient for CO3 in water (p.Dco3)	8e-6 cm^2 s^{-1}	
membrane permeability of CO2 (p.mpco2)	5e-2 cm s^{-1}	Tansik et al. (2015)

Parameter	Value	Reference
tissue permeability of HCO3 (p.pdhco3)	3.5e-5 cm s^{-1}	Bénazet-Tambutté et al. (1996) (based on Cl)
tissue permeability of Ca (p.pdca)	1.6e-5 cm s^{-1}	Bénazet-Tambutté et al. (1996)
solubility product of aragonite (p.Ka)	$10^{-6.19}$ mol^2 kg^{-1}	Zeebe and Wolf-Gladrow (2001)
precipitation constant for aragonite (p.karag)	1.1e-9 mmol cm^{-2} s^{-1}	Burton and Walter (1990)
reaction order for aragonite precipitation (p.narag)	1.63	Burton and Walter (1990)
CA activity in the calcifying fluid (p.kcff)	10000	estimated
factor to partition CO2 and HCO3 for photosynthesis (p.pcorr)	0.5	Tansik et al. (2015)
DIC half saturation constant for calcification (p.Kmcalc)	1.25e-4 mmol cm^{-3}	de Putron et al. (2010); Gattuso et al. (1998)
factor to partition DIC from R and bulk for calcification (p.gcorr)	0.75	Furla et al. (2000)
volume of the coral surface layer (p.Vsurf)	0.01*volume of DBL	set at bottom 1% of DBL
factor to partition the coral tissue between oral and aboral (p.vcorr)	0.75	Allemand et al. (2004); Gattuso et al. (1999)
thickness of the calcifying space (p.Lcf)	2e-7 cm	Clode and Marshall (2002)
thickness of the coelenteron (p.Lcoel)	0.483 cm	Allemand et al. (2004); Gattuso et al. (1999)
proton pump efficiency	0.5	estimated

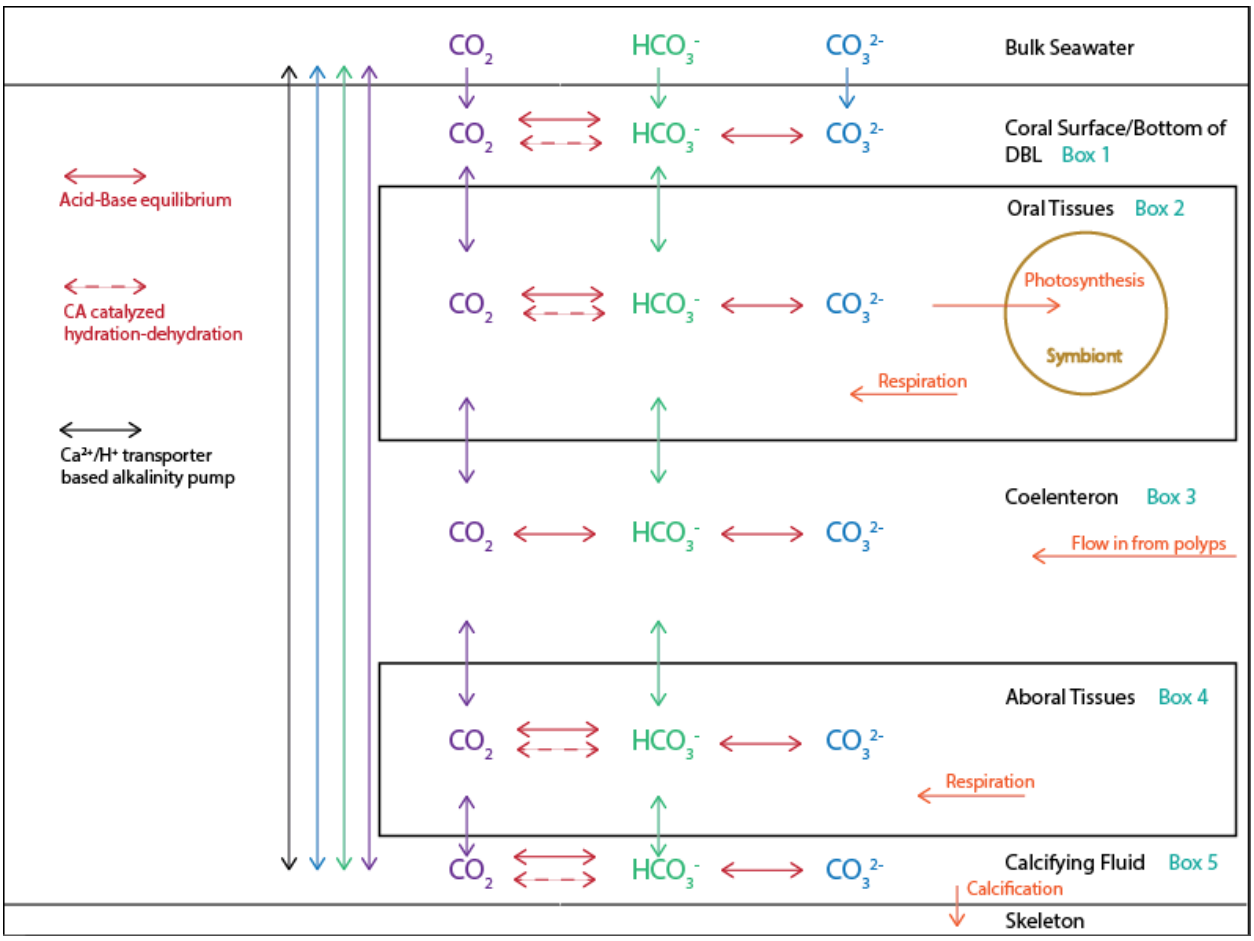

Figure 4.1. Overview of the five box model. The model represents the coenosarc area of a coral, between the polyps. All three DIC species diffuse across the boundary layer (DBL) to the surface of the coral from the bulk seawater. CO_2 and HCO_3^- move through the coral tissues according to concentration gradients, impacted by acid-base reactions, catalyzed exchange and biological processes. All the state variables move from the bulk seawater to the calcifying fluid. Arrowheads show the direction of potential movement of a chemical within the model.

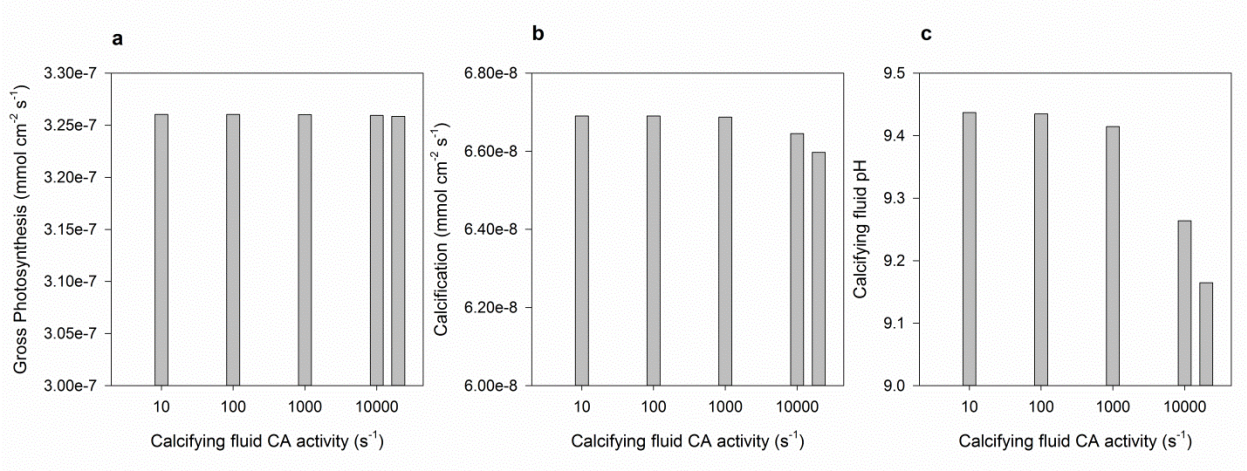

Figure 4.2. Effect of varying calcifying fluid CA activity. **a** Gross photosynthesis. **b** Calcification rate. **c** Calcifying fluid pH

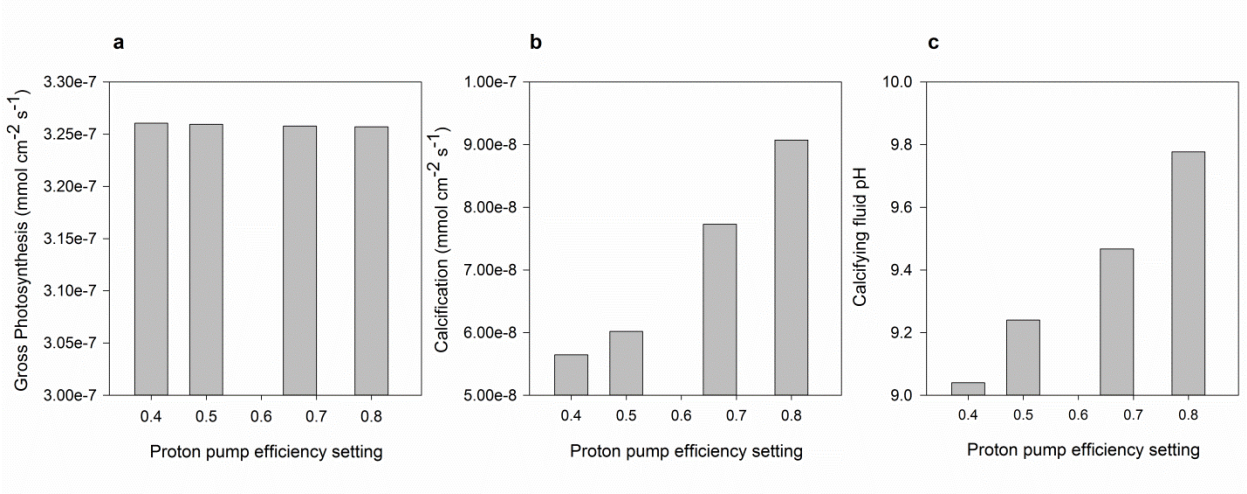

Figure 4.3. Effect of varying proton pump efficiency. **a** Gross photosynthesis. **b** Calcification rate. **c** Calcifying fluid pH

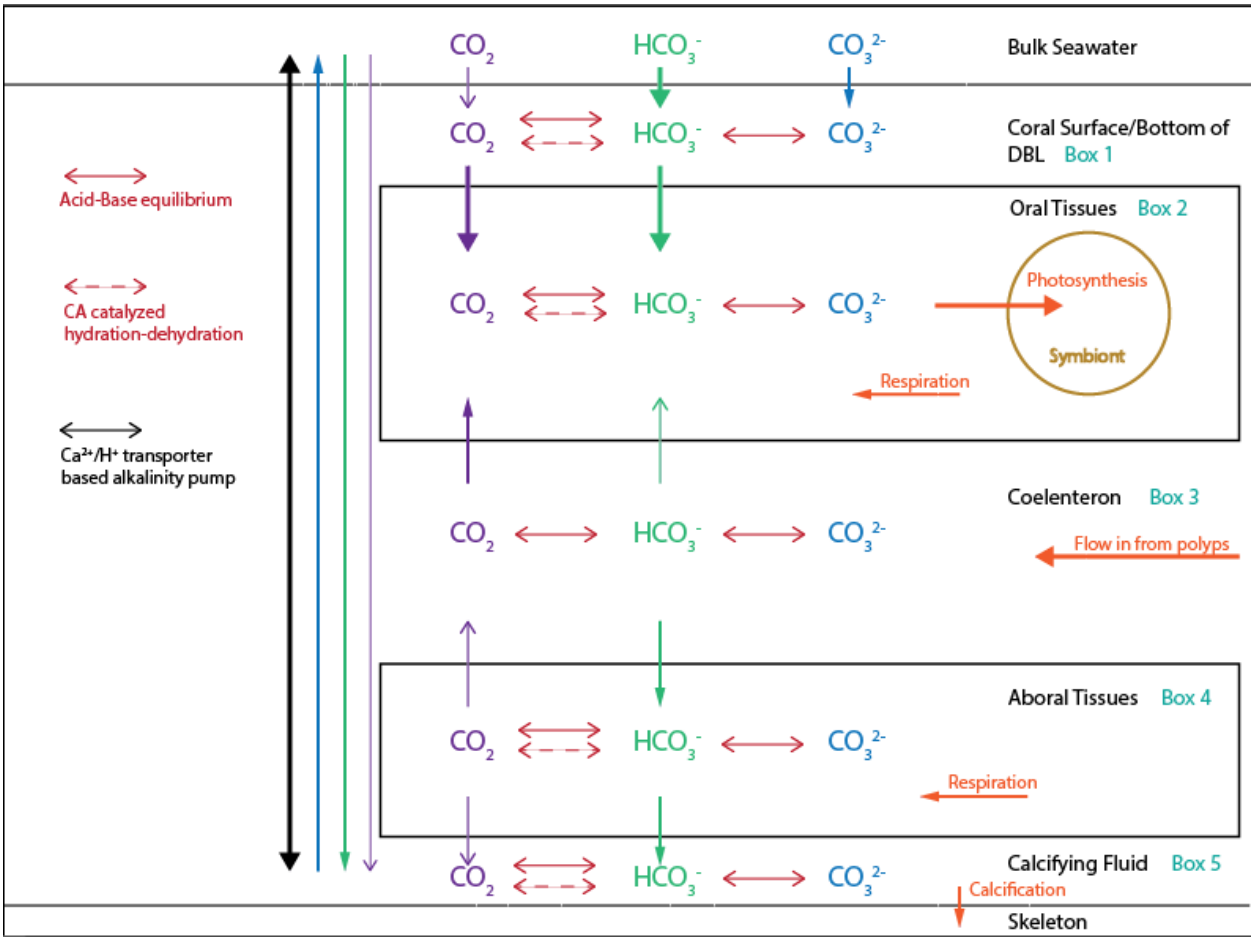

Figure 4.4. Steady state fluxes in the five box model under normal seawater conditions. The model outputs for the fluxes of all the state variables, photosynthesis, respiration, flow from polyps, and calcification. Arrowheads show the direction of the flow. The size of the arrows gives an indication of the order of magnitude of the flux. Largest arrow with large closed arrowhead = 1E-7 mmol cm^{-2} s^{-1}; mid-weight arrow with narrow closed arrowhead = 1E-8 mmol cm^{-2} s^{-1}; standard arrow with open arrowhead = 1E-9 mmol cm^{-2} s^{-1}; narrow arrow with small open arrowhead = 1E-10 mmol cm^{-2} s^{-1}.

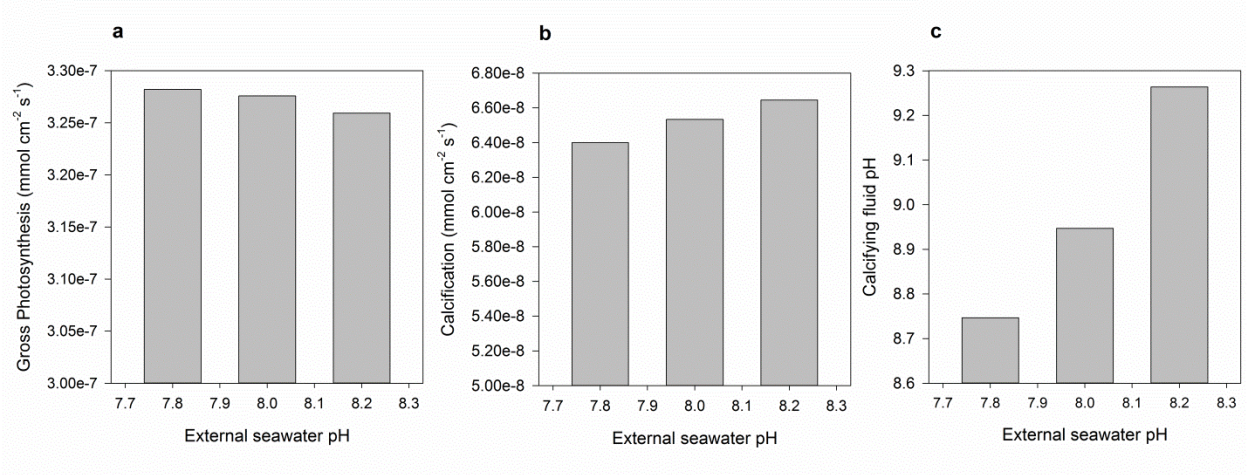

Figure 4.5. Effect of varying external seawater pH and DIC. **a** Gross photosynthesis. **b** Calcification rate. **c** Calcifying fluid pH

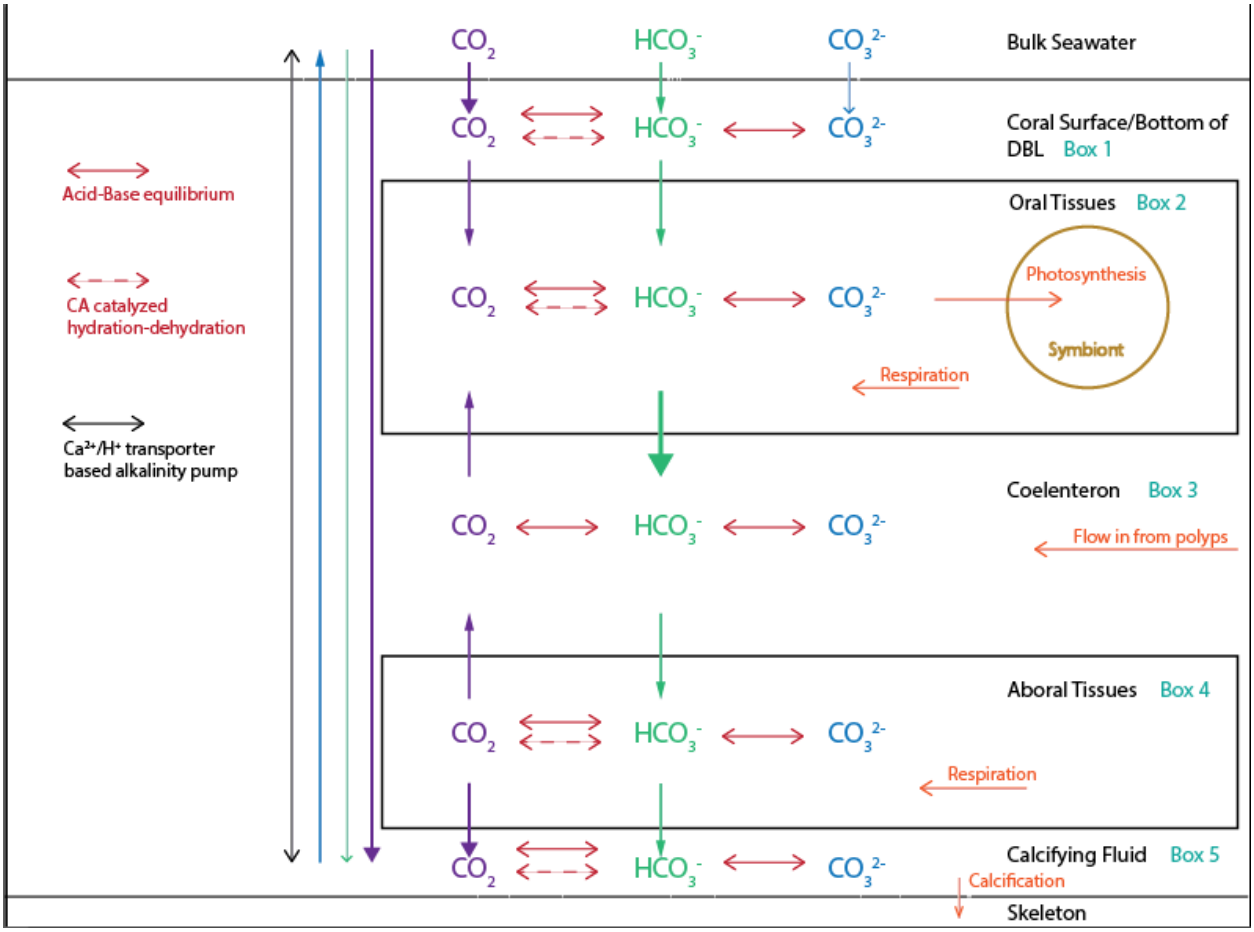

Figure 4.6. Changes to the steady state fluxes in the five box model from normal seawater conditions to end-century seawater conditions. Percent change to the model outputs for the fluxes of all the state variables, photosynthesis, respiration, flow from polyps, and calcification. Arrowheads show the direction of the flow under end-century conditions. The size of the arrows gives an indication of the order of magnitude of the change to the flux. Largest arrow with large closed arrowhead = 1E3 mmol cm^{-2} s^{-1} increase; mid-weight arrow with standard closed arrowhead = 1E2 mmol cm^{-2} s^{-1} increase; heavy standard arrow with narrow closed arrowhead = 1E1 mmol cm^{-2} s^{-1} increase; standard arrow with open arrowhead = no change; narrow arrow with narrow open arrowhead = 1E0 mmol cm^{-2} s^{-1} decrease; narrow arrow with small open arrowhead = 1E1 mmol cm^{-2} s^{-1} decrease.

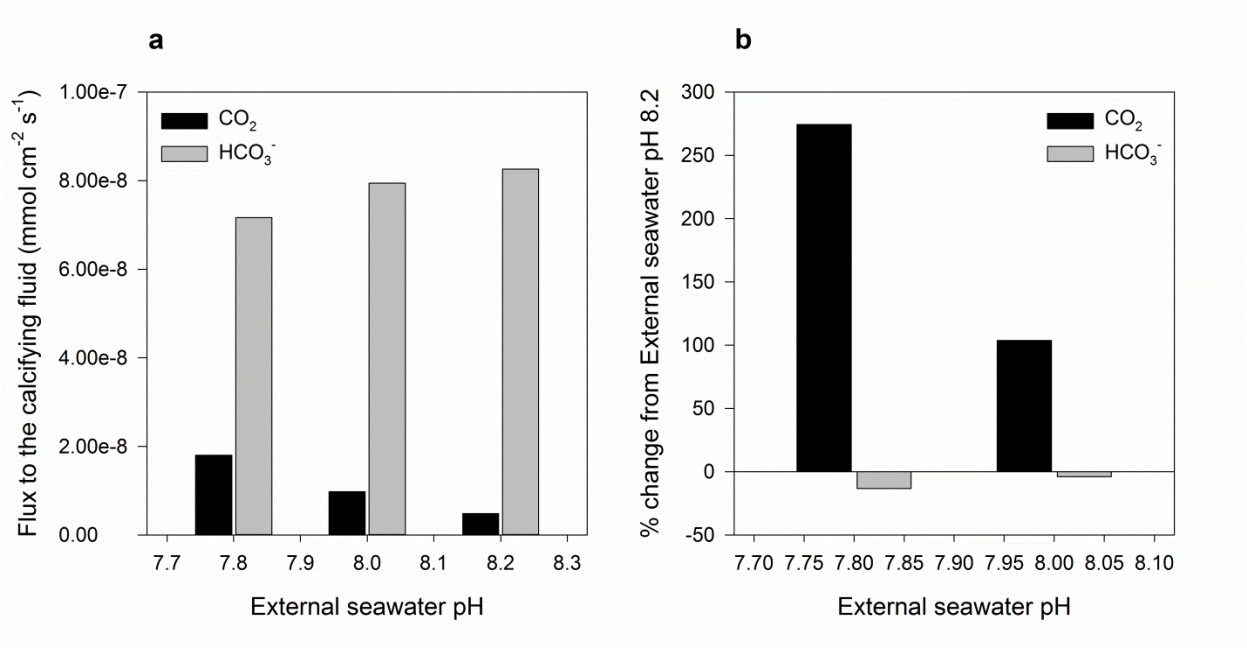

Figure 4.7 Impact of varying external seawater pH and DIC on CO_2 and HCO_3^- fluxes to the calcifying fluid. **a** Total flux to the calcifying fluid. **b** Percent change in the total flux from normal seawater conditions. Black bars represent CO_2, gray bars represent HCO_3^-.

CHAPTER 5

CONCLUSIONS

Throughout this dissertation, the work strives to create a clearer vision of inorganic carbon processing in tropical scleractinian corals. This is focused through the quantification of DIC cycling relating to photosynthesis, and the employment of some techniques for the first time on corals in order to characterize it as it had never been before. The model which resulted from the incorporation of this data is more detailed than those which came before, allowing for a more rigorous evaluation of changes to the system. This work creates a strong foundation to move forward in exploring the effects of OA on corals.

Inorganic carbon and coral photosynthesis

By applying methods used to characterize phytoplankton carbon concentrating mechanisms (Hopkinson et al. 2011), it was revealed that scleractinian corals have an active uptake and processing system to supply DIC to their symbionts. With high rates of eCA activity, internal CA activity (Hopkinson et al. 2015), and the need to supply half of the DIC for net photosynthesis with HCO_3^-, it is obviously an energy intensive process; a fact which was not entirely clear with the previous semi-quantitative and qualitative description (al-Moghrabi et al. 1996; Barott et al. 2015; Weis et al. 1989). It appears to be a fundamental process to scleractinian corals generally, as all three taxa had it, and they fill vastly different niches in the environment; diffusive limitation through the tissues would, in fact, severely limit photosynthesis without this system.

Even though a carbon concentrating process seems to be necessary for all scleractinian corals, there are still striking differences with regard to the Michaelis-Menten kinetics of the three studied taxa. Only *O. faveolata* is carbon saturated under current oceanic conditions, making it the only taxa to maximize its productivity at this time. This variation does reinforce the need to have as much data from as many different taxa as possible before making overly generalized statements. The variation in the corals also creates a stark contrast with the K_m values of their symbionts, which were all similar and very low. Such is indicative of living in carbon scarce conditions, a notion supported by the high internal CA activity rates of all three *Symbiodinium* types. The differences between host and symbiont could be a sign of host control over DIC delivery.

Applications of the model

Taking all the quantified information about DIC and photosynthesis, and adding in literature data as necessary, the model ended up requiring only two estimated parameters. This is a vast improvement over previous models (Hohn and Merico 2012; Nakamura et al. 2013). The model also incorporated DIC speciation as well as dynamic biological processes. It does well in reflecting gross photosynthetic rates and calcifying fluid pH, though it falls short in replicating measured calcification rates. This is likely due to unparameterized biological modification by the organic matrix (Von Euw et al. 2017), which could not be accounted for. Despite this, the model allows for the evaluation of OA impacts on photosynthesis, calcification and calcifying fluid pH. While photosynthesis was essentially unchanged, both calcification rate and calcifying fluid pH declined slightly as a result of OA. By examining the fluxes of the various DIC species, the drivers of the observed changes could be evaluated, showing that increasing fluxes of CO_2 into the calcifying fluid were causing the observed decreases.

Ocean acidification and the future of this work

Ocean acidification will continue to perturb the carbonate system of the ocean over the rest of the century (IPCC 2014). Therefore, corals will continue to be impacted by these changing conditions. The question is: to what extent? The work in this dissertation has laid a foundation for continued exploration of this topic, providing a baseline for comparison of experimental data. A logical next step would be to conduct OA experiments and run the same suite of assays to see if corals or their symbionts will acclimate to the new conditions. They could downregulate their carbon concentrating processes, or they might increase their K_m, both of which are responses seen in phytoplankton to increasing CO_2 concentrations (Mackey et al. 2015; Shi et al. 2017; Wu et al. 2010). With the possibility of some coral taxa being released from carbon limitation, it would be another opportunity to evaluate whether hosts do control DIC delivery to their symbionts. Eventually, additional stressors could be added and the interactions between them properly determined.

Another logical step would be to simulate these possible acclimation or multiple stressor scenarios in the model. It could then be evaluated against experimental data to decide how well it functions. Additionally, running the model with it parameterized to those taxa which are not carbon saturated could indicate if there is any kind of release from carbon limitation, and would provide insights into possible questions for experimentation. Similarly to the work done here, drivers for any observed changes can be explored in order to gain a greater understanding of coral physiology under OA conditions.

References

al-Moghrabi, S. M., C. Goiran, D. Allemand, N. Speziale, and J. Jaubert. 1996. Inorganic carbon uptake for photosynthesis by the symbiotic coral-dinoflagellate association II. Mechanisms for bicarbonate uptake. Journal of Experimental Marine Biology and Ecology 199: 227-248. doi.

Barott, K. L., A. A. Venn, S. O. Perez, S. Tambutte, and M. Tresguerres. 2015. Coral host cells acidify symbiotic algal microenvironment to promote photosynthesis. Proc Natl Acad Sci U S A 112: 607-612. doi: 10.1073/pnas.1413483112.

Hohn, S., and A. Merico. 2012. Modelling coral polyp calcification in relation to ocean acidification. Biogeosciences 9: 4441-4454. doi: 10.5194/bg-9-4441-2012.

Hopkinson, B. M., C. L. Dupont, A. E. Allen, and F. M. M. Morel. 2011. Efficiency of the CO_2-concentrating mechanism of diatoms. PNAS 108: 3830-3837. doi: 10.1073/pnas.1018062108.

Hopkinson, B. M., A. L. Tansik, and W. K. Fitt. 2015. Internal carbonic anhydrase activity in the tissue of scleractinian corals is sufficient to support proposed roles in photosynthesis and calcification. J. Exp. Biol. 218: 2039-2048. doi: 10.1242/jeb.118182.

IPCC. 2014. Climate Change 2014: Synthesis Report. Contribution of Working Groups I, II and III to the Fifth Assessment Report of the Intergovernmental Panel on Climate Change, p. 151 pp. *In* R. K. P. a. L. A. M. Core Writing Team [ed.]. IPCC.

Mackey, K. R. M., J. J. Morris, F. M. M. Morel, and S. A. Kranz. 2015. Response of Photosynthesis to Ocean Acidification. Oceanography 28: 74-91. doi: 10.5670/oceanog.2015.33.

Nakamura, T., K. Nadaoka, and A. Watanabe. 2013. A coral polyp model of photosynthesis, respiration and calcification incorporating a transcellular ion transport mechanism. Coral Reefs 32: 779-794. doi: 10.1007/s00338-013-1032-2.

Shi, Q., W. Q. Xiahou, and H. Y. Wu. 2017. Photosynthetic responses of the marine diatom Thalassiosira pseudonana to CO2-induced seawater acidification. Hydrobiologia 788: 361-369. doi: 10.1007/s10750-016-3014-1.

Von Euw, S. and others 2017. Biological control of aragonite formation in stony corals. Science 356: 933-+. doi: 10.1126/science.aam6371.

Weis, V. M., G. J. Smith, and L. Muscatine. 1989. A "CO_2 supply" mechanism in zooxanthellate cnidarians: role of carbonic anhydrase. Marine Biology 100: 195-202. doi.

Wu, Y., K. Gao, and U. Riebesell. 2010. CO2-induced seawater acidification affects physiological performance of the marine diatom Phaeodactylum tricornutum. Biogeosciences 7: 2915-2923. doi: 10.5194/bg-7-2915-2010.

APPENDIX A

EXTERNAL CARBONIC ANHYDRASE IN THREE CARIBBEAN CORALS: QUANTIFICATION OF ACTIVTY AND ROLE IN CO_2 UPTAKE ELECTRONIC SUPPLEMENTARY MATERIAL[4]

[4] Tansik, A. L., W. K. Fitt, and B. M. Hopkinson. 2015. External carbonic anhydrase in three Caribbean corals: quantification of activity and role in CO2 uptake. *Coral Reefs* 34:703-713. doi: 10.1007/s00338-015-1289-8 Reprinted here with permission of the publisher.

Supplemental Material

Text AI.I. ^{18}O-exchange in the presence of an eCA inhibitor

When eCA is inhibited or absent, ^{18}O-removal from CO_2 can typically be used to measure both CO_2 and HCO_3^- fluxes into biological samples such as red blood cells and microalgae (1). However, this requires resolution of two phases of ^{18}O-exchange dynamics: the first a rapid depletion of ^{18}O from CO_2 caused by the rapid influx of CO_2 into cells or other biological material containing CA, and the second a long term depletion of ^{18}O caused by the depletion of ^{18}O from HCO_3^-. In corals, the thickness of the diffusive boundary layer combined with low tissue surface area to solution volume ratio eliminate the rapid depletion phase. Consequently, CO_2 and HCO_3^- flux into the tissue cannot be rigorously discriminated, though the observation of ^{18}O depletion in the presence of an eCA inhibitor indicates there is passage of some C_i species into the coral tissue. Because biological membranes are generally much more permeable to CO_2, passage of CO_2 into coral tissue seems the most reasonable explanation for continued ^{18}O-depletion after DBAZ addition. However, in some instances this process is not able to account for the extent of ^{18}O-depletion observed (Fig. S2A) implying that either HCO_3^- passes through the membrane or eCA is incompletely inhibited. Either HCO_3^- flux alone (Fig. S1B) or a combination of CO_2 and HCO_3^- (Fig. S1C) are able to explain the data with no effect on the inferred eCA activity. Both CO_2 and HCO_3^- passage through the coral membrane are allowed in our model used to infer eCA activity: CO_2 flux because of the known properties of membranes, and HCO_3^- flux because it is required to explain the data. The particular choice of allowed fluxes does not significantly affect inferred eCA activities as long as they accurately account for ^{18}O-removal processes other than eCA. For example in the sample fit (Fig S1) the inferred eCA activities are indistinguishable when either HCO_3^- flux alone or CO_2 and HCO_3^- fluxes are allowed (2.1 ± 0.2 and 2.0 ± 0.2 respectively), but the inferred eCA activity rises in the CO_2 flux only case (4.0 ± 1.4) in an attempt to compensate for a reduction in intracellular ^{18}O removal.

Text AI.II. Model Details

The solution volume (V_e) and coral surface area (A) were measure directly. The length of the diffusive boundary layer (L_{DBL}) was taken to be 200 μm, on the low end of measured values (2, 3). The tissue thickness was estimated as 1 mm, which when multiplied by the surface area determines the effective internal volume (V_i). The value of V_i does not affect the inferred eCA

activities. Diffusivities of CO_2 (D_c) and HCO_3^- (D_b) were calculated based on temperature and salinity according to (4). The uncatalyzed CO_2 hydration/HCO_3^- dehydration rates in the bulk solution (k_{ef}, k_{er}) were determined from ^{18}O removal rates prior to the addition of the coral (5). The only remaining parameters in the model are CA hydration and dehydration rates (k_{sf}, k_{sr}, k_{if}, k_{ir}), which are related to each other via the CO_2/HCO_3^- equilibrium constant assuming microscopic reversibility, and the permeability of the coral outermembrane to CO_2 and HCO_3^- (P_c, P_b). Four unknowns that constrain the system (k_{sf}, k_{if}, P_c, P_b) were determined by fitting the model to the ^{18}O-CO_2 data. eCA activity (k_{sf}) was set to zero in the model after DBAZ was added.

References

1. Tu C, Wynns G, McMurray R, Silverman D (1978) CO_2 kinetics in red cell suspensions measured by 18O exchange. *J Biol Chem* 253:8178-8184.

2. Kuhl M, Cohen Y, Dalsgaard T, Jorgensen BB, Revsbech NP (1995) Microenvironment and photosynthesis of zooxanthellae in scleractinian corals studied with microsensors for O_2, pH, and light. *Mar Ecol Prog Ser* 117:159-172.

3. de Beer D, Kuhl M, Stambler N, Vaki L (2000) A microsensor study of light enhanced Ca^{2+} uptake and photosynthesis in the reef-building hermatypic coral *Favia* sp. *Mar Ecol Prog Ser* 194:75-85.

4. Boudreau BP (1997) *Diagenetic Models and Their Implemenation. Modelling Transport and Reactions in Aquatic Sediments* (Springer-Verlag, Berlin) p 414.

5. Hopkinson BM, Meile C, Shen C (2013) Quantification of extracellular carbonic anhydrase activity in two marine diatoms and investigation of its role. *Plant Physiol* 162:1142-1152.

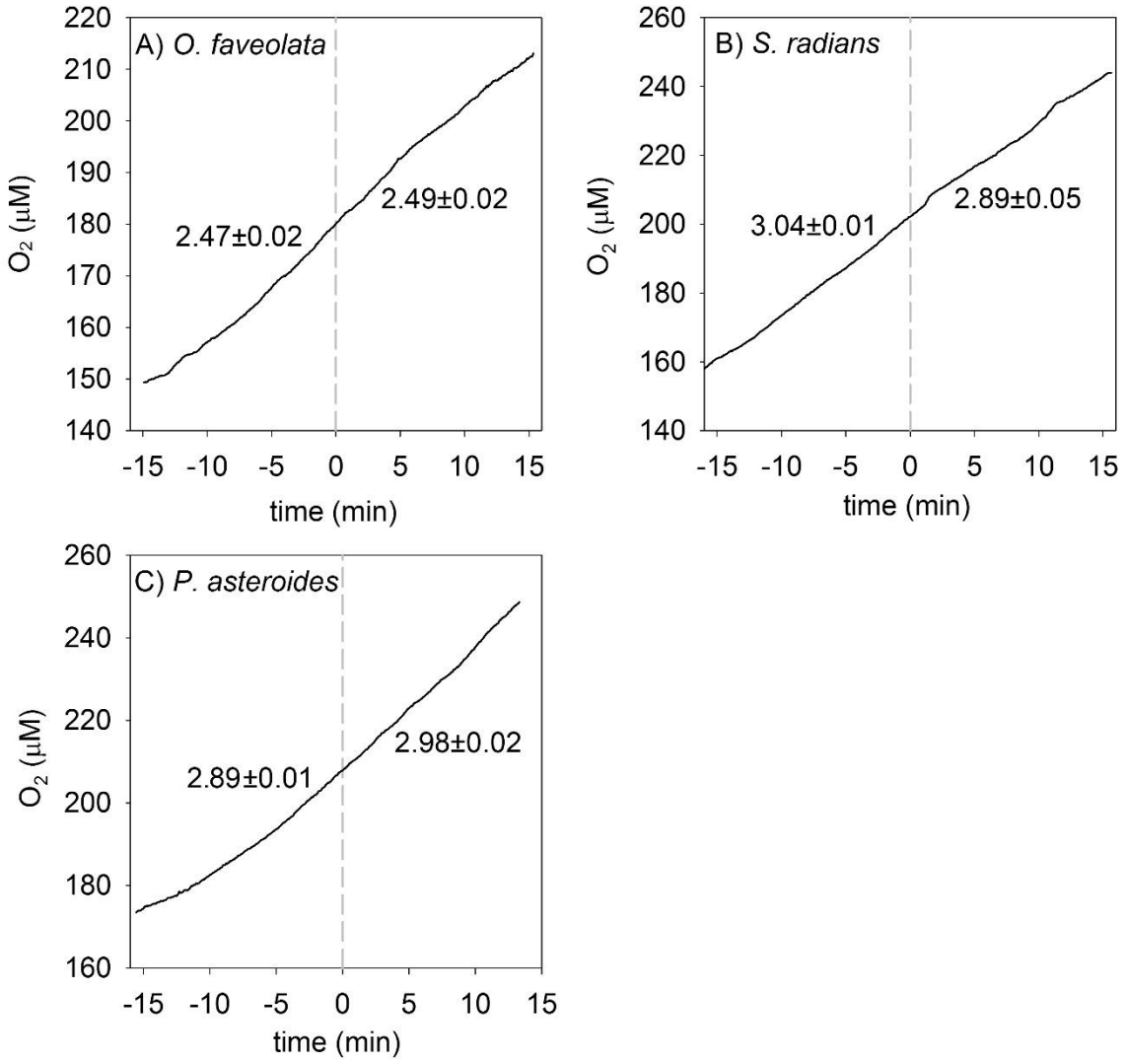

Figure A1. O_2 traces showing that photosynthesis in the three coral species was not inhibited by DMSO, the solvent in which DBAZ was dissolved. Photosynthetic rates (μM/min ± SE, indicated on graphs) were calculated 5 min before and 5 min after DMSO addition (final concentration 2 μL/mL, matching DBAZ additions) corresponding to the time periods used to determine the effect of DBAZ on photosynthesis.

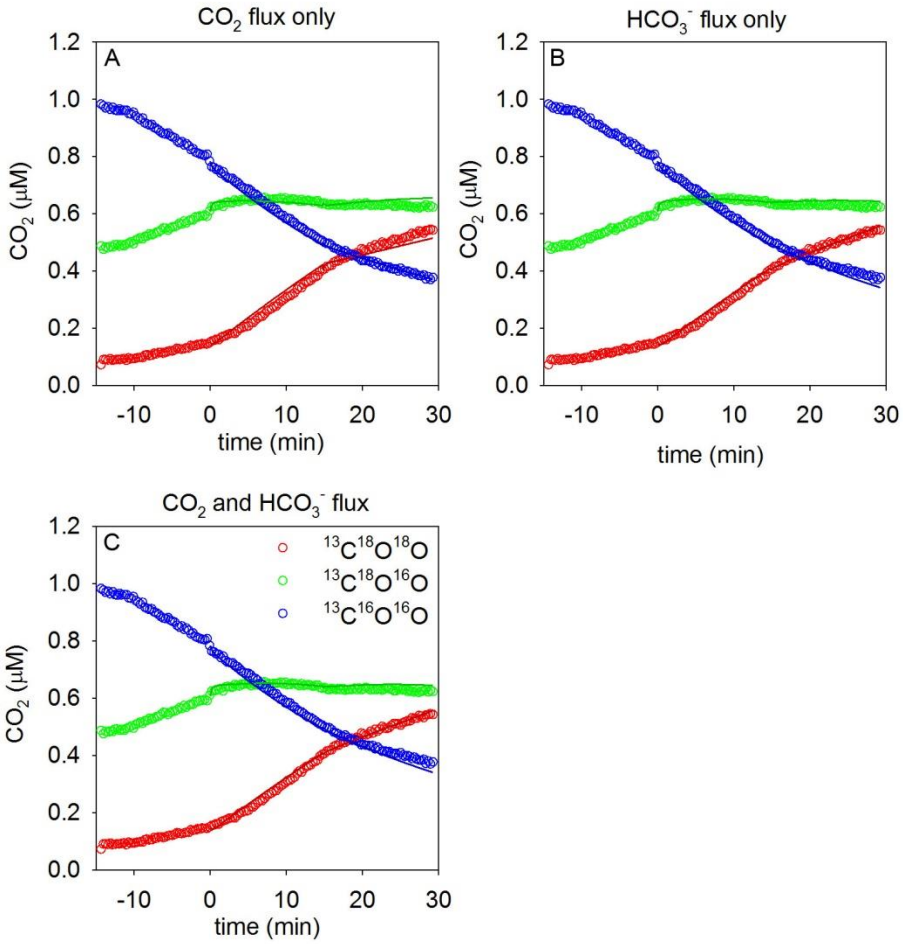

Figure A2. Model fits allowing various combinations of CO_2 and HCO_3^- flux through the surface layer. (A) CO_2 flux only, (B) HCO_3^- flux only, and (C) both CO_2 and HCO_3^- flux allowed.

APPENDIX B

INORGANIC CARBON FLUX MODEL SUPPLEMENTARY TABLES[5]

[5] Tansik, A.L., B.M. Hopkinson, and C. Meile. To be submitted to *Nature Climate Change*.

Table B1: Complete flux equations for the model. All fluxes are in mmol cm^{-3} s^{-1}. See Table 4.1 for parameter definitions. R1: acid-base equilibrium reaction HCO_3^- to CO_2; R2: acid-base equilibrium reaction CO_3^{2-} to HCO_3^-; Rcat: CA catalyzed equilibrium HCO_3^- to CO_2. Bulk: bulk seawater; surf: coral surface; oral: oral tissues; coel: coelenteron; aboral: aboral tissues; calc: calcifying fluid; Alk: alkalinity.

State Variable	Compartment	Equation
CO_2	Coral surface	$\frac{\left[\mathrm{p.SA} * \mathrm{p.Dco2} * \left(\frac{[CO_2]_{bulk} - [CO_2]_{surf}}{\mathrm{p.Ldbl}}\right)\right]}{\mathrm{p.Vsurf}} - \frac{[\mathrm{p.SA} * \mathrm{p.mpco2} * ([CO_2]_{surf} - [CO_2]_{oral})]}{\mathrm{p.Vsurf}} + \mathrm{R1} + \mathrm{Rcat}$
	Oral tissues	$\frac{[\mathrm{p.SA} * \mathrm{p.mpco2} * ([CO_2]_{surf} - [CO_2]_{oral})]}{\mathrm{p.Voral}} - \frac{[\mathrm{p.SA} * \mathrm{p.mpco2} * ([CO_2]_{oral} - [CO_2]_{coel})]}{\mathrm{p.Voral}} + \mathrm{R1} + \mathrm{Rcat} - \frac{\mathrm{P} * \mathrm{p.pcorr}}{\mathrm{p.Loral}} + \mathrm{R\_oral}$
	Coelenteron	$\frac{[\mathrm{p.SA} * \mathrm{p.mpco2} * ([CO_2]_{oral} - [CO_2]_{coel})]}{\mathrm{p.Vcoel}} - \frac{[\mathrm{p.SA} * \mathrm{p.mpco2} * ([CO_2]_{coel} - [CO_2]_{aboral})]}{\mathrm{p.Vcoel}} + \frac{\left[\mathrm{p.Qex} * \left([CO_2]_{polyp} - [CO_2]_{coel}\right)\right]}{\mathrm{p.Vcoel}} + \mathrm{R1} + \mathrm{Rcat}$
	Aboral tissues	$\frac{[\mathrm{p.SA} * \mathrm{p.mpco2} * ([CO_2]_{coel} - [CO_2]_{aboral})]}{\mathrm{p.Vaboral}} - \frac{[\mathrm{p.SA} * \mathrm{p.mpco2} * ([CO_2]_{aboral} - [CO_2]_{calc})]}{\mathrm{p.Vaboral}} + \mathrm{R1} + \mathrm{Rcat} + \mathrm{R\_aboral}$
	Calcifying fluid	$\frac{[\mathrm{p.SA} * \mathrm{p.mpco2} * ([CO_2]_{aboral} - [CO_2]_{calc})]}{\mathrm{p.Vcalc}} + \frac{[\mathrm{p.SA} * \mathrm{p.pdhco3} * ([CO_2]_{bulk} - [CO_2]_{calc})]}{\mathrm{p.Vcalc}} + \mathrm{R1} + \mathrm{Rcat}$
HCO_3^-	Coral surface	$\frac{\left[\mathrm{p.SA} * \mathrm{p.Dhco3} * \left(\frac{[HCO_3^-]_{bulk} - [HCO_3^-]_{surf}}{\mathrm{p.Ldbl}}\right)\right]}{\mathrm{p.Vsurf}} - \frac{[\mathrm{p.SA} * \mathrm{p.trhco3p} * ([HCO_3^-]_{surf} - [HCO_3^-]_{oral})]}{\mathrm{p.Vsurf}} - \mathrm{R1} + \mathrm{R2} - \mathrm{Rcat}$
	Oral tissues	$\frac{[\mathrm{p.SA} * \mathrm{p.mpco2} * ([HCO_3^-]_{surf} - [HCO_3^-]_{oral})]}{\mathrm{p.Voral}} - \frac{[\mathrm{p.SA} * \mathrm{p.mpco2} * ([HCO_3^-]_{oral} - [HCO_3^-]_{coel})]}{\mathrm{p.Voral}} - \mathrm{R1} + \mathrm{R2} - \mathrm{Rcat} - \frac{\mathrm{P} * (1 - \mathrm{p.pcorr})}{\mathrm{p.Loral}}$

State Variable	Compartment	Equation
HCO_3^-	Coelenteron	$\frac{\left[p.SA * \left(\frac{p.gcorr * G}{0.3 * 2E\text{-}3}\right) * \left([HCO_3^-]_{oral} - [HCO_3^-]_{coel}\right)\right]}{p.Vcoel} - \frac{\left[p.SA * \left(\frac{p.gcorr * G}{0.3 * 2E\text{-}3}\right) * \left([HCO_3^-]_{coel} - [HCO_3^-]_{aboral}\right)\right]}{p.Vcoel} + \frac{\left[p.Qex * \left([HCO_3^-]_{polyp} - [HCO_3^-]_{coel}\right)\right]}{p.Vcoel} - R1 + R2 - Rcat$
	Aboral tissues	$\frac{\left[p.SA * \left(\frac{p.gcorr * G}{0.3 * 2E\text{-}3}\right) * \left([HCO_3^-]_{coel} - [HCO_3^-]_{aboral}\right)\right]}{p.Vaboral} - \frac{\left[p.SA * (p.gcorr * G) * \left(\frac{[DIC]_{aboral}}{(p.Kmcalc + [DIC]_{aboral})}\right)\right]}{p.Vaboral} - R1 + R2 - Rcat$
	Calcifying fluid	$\frac{\left[p.SA * (p.gcorr * G) * \left(\frac{[DIC]_{aboral}}{(p.Kmcalc + [DIC]_{aboral})}\right)\right]}{p.Vcalc} + \frac{[p.SA * p.pdhco3 * \left([HCO_3^-]_{bulk} - [HCO_3^-]_{calc}\right)]}{p.Vcalc} - R1 + R2 - Rcat$
Ca^{2+}	Coelenteron	$\frac{\left[p.Qex * \left([Ca^{2+}]_{polyp} - [Ca^{2+}]_{coel}\right)\right]}{p.Vcoel}$
	Calcifying fluid	$\frac{[p.SA * p.pdca * \left([Ca^{2+}]_{bulk} - [Ca^{2+}]_{calc}\right)]}{p.Vcalc} + \frac{0.5 * (0.5 * p.Vcalc)}{p.Vcalc} - \frac{G}{p.Lcf}$
Alkalinity	Coelenteron	$\frac{\left[p.Qex * \left(Alk_{polyp} - Alk_{coel}\right)\right]}{p.Vcoel}$
	Calcifying fluid	$\frac{2 * [p.SA * p.pdca * \left([Ca^{2+}]_{bulk} - [Ca^{2+}]_{calc}\right)]}{p.Vcalc} + \frac{0.5 * (0.5 * p.Vcalc)}{p.Vcalc} - \frac{2 * G}{p.Lcf}$
CO_3^{2-}	Coral surface	$\frac{\left[p.SA * p.Dco3 * \left(\frac{[CO_3^{2-}]_{bulk} - [CO_3^{2-}]_{surf}}{p.Ldbl}\right)\right]}{p.Vsurf}$
	Coelenteron	$\frac{\left[p.Qex * \left([CO_3^{2-}]_{polyp} - [CO_3^{2-}]_{coel}\right)\right]}{p.Vcoel}$
	Calcifying fluid	$\frac{[p.SA * p.pdhco3 * \left([CO_3^{2-}]_{bulk} - [CO_3^{2-}]_{calc}\right)]}{p.Vcalc} - \frac{G}{p.Lcf} - R2$

Biological Process Equations

Photosynthesis (P)	$\left\{\left[\frac{\mathrm{p.Pmaxf} * \mathrm{p.zoox} * [\mathrm{DIC}]_{\mathrm{oral}}}{(\mathrm{p.Kmdicf} + [\mathrm{DIC}]_{\mathrm{oral}})}\right] + \left[2 * \frac{(\mathrm{p.Rc} - \mathrm{p.Rz} * \mathrm{p.zoox})}{\mathrm{p.tiss}} * \mathrm{p.tiss}\right]\right\}$
Respiration (R_oral; R_aboral)	$\left[\frac{(\mathrm{p.Rc} - \mathrm{p.Rz} * \mathrm{p.zoox})}{\mathrm{p.tiss}}\right]$
Calcification (G)	$\mathrm{p.kparag} * \left[\left([\mathrm{Ca}^{2+}] * \frac{[\mathrm{CO}_3^{2-}]}{\mathrm{p.Ka}}\right) - 1\right]^{\mathrm{p.nparag}}$

Table B2: Sensitivity to variation in parameters on modeled rates of photosynthesis (P) and calcification (G), and calcifying fluid (cf) pH. Values are given as percentage change from base value outputs; positive being above, and negative below base value. P_{max} = maximum rate of P; K_m = half-saturation constant; R = respiration rate; eCA = external carbonic anhydrase activity; iCA = internal carbonic anhydrase activity. High and low values were +/- SE for experimentally derived parameters, and +/- 10% for others.

Parameter	Base value	Low value	P	G	cf pH	High value	P	G	cf pH
coral surface area	11.87	10.683	2.18E-02	-1.10E-01	-1.87E-01	13.057	-2.00E-02	9.64E-02	1.76E-01
P_{max} of coral	2.76E-07	2.11E-07	-1.93E-01	3.97E-01	8.29E-01	3.41E-07	1.38E-01	-4.16E-01	-6.50E-01
P_{max} of symbiont	2.69E-14	1.87E-14	-2.20E+00	-1.65E-01	-2.76E-01	3.51E-14	2.16E+00	1.60E-01	2.99E-01
K_m for DIC of coral P	4.20E-04	3.05E-04	4.23E-02	-1.14E-01	-1.94E-01	5.35E-04	-4.07E-02	9.97E-02	1.82E-01
K_m for DIC of symbiont P	1.24E-04	6.89E-05	3.72E-01	2.77E-02	4.94E-02	1.79E-04	-3.31E-01	-2.47E-02	-4.32E-02
R of coral	1.61E-07	1.45E-07	-9.65E+00	-4.85E-01	-7.44E-01	1.771E-07	9.57E+00	4.55E-01	9.83E-01
R of symbionts	1.00E-14	9E-15	6.01E-01	3.00E-02	5.34E-02	1.1E-14	-6.01E-01	-3.01E-02	-5.25E-02
eCA of coral	1.21	1.041	-5.09E-03	1.47E-02	2.61E-02	1.379	3.80E-03	-1.12E-02	-1.96E-02
iCA of coral	82.7	65.8	-1.23E-02	9.71E-03	1.74E-02	99.6	8.13E-03	-6.32E-03	-1.13E-02
CO_2/HCO_3^- partition for P	0.5	0.45	-1.52E-02	7.46E-03	1.33E-02	0.55	1.47E-02	-7.51E-03	-1.32E-02
K_m for DIC of G	1.25E-04	1.13E-04	-4.60E-03	-1.43E-01	-2.44E-01	1.38E-04	4.69E-03	1.39E-01	2.62E-01
R/bulk DIC partition for G	0.75	0.675	1.90E-02	5.85E-01	1.43E+00	0.825	-1.89E-02	-7.52E-01	-1.10E+00